Computer simulation of epilepsy in discrete models of cortical neural networks

Inaugural-Dissertation
zur
Erlangung des Doktorgrades
der Mathematisch-Naturwissenschaftlichen Fakultät
der Universität zu Köln

vorgelegt von
Daniel Volk
aus Essen

Köln 2000

Contents

Contents

Introduction

Neurobiology is a field of science that has had its advances in the twentieth century: indeed the nerve cell had not been known before 1891 when the Spanish scientist Santiago Ramón y Cajal (1852-1934) found it. Before this finding thinkers like Plato and Descartes believed that the brain is tightly connected with the soul but its structure and physics was not analyzed in its elements, the neurons. Hence this field of science is rather young and we should not expect too much knowledge of the mechanisms underlying the population dynamics of such a large assembly of excitable cells as our brain is. Further, if our behavior, consciousness and free will are emergent phenomena of the nervous system, the complete understanding of the mechanisms of the brain would provide a logical paradox. So it is not surprising that, when we observe our inherent instrument of observation, we drown in a sea of complexity.

Nevertheless, progress has been made and eleven Nobel prices in physiology stress the attention that is paid to this field. Whereas physiological discoveries continue, another aspect has gained attention in the last decades. Driven also by the desire to build machines that can think, an understanding of the functional properties of the nervous system like memory, object recognition, classification of data, etc. is a very attractive research subject. Scientists try to capture these phenomena with computer simulations of mathematical models which are inspired by physiological findings.
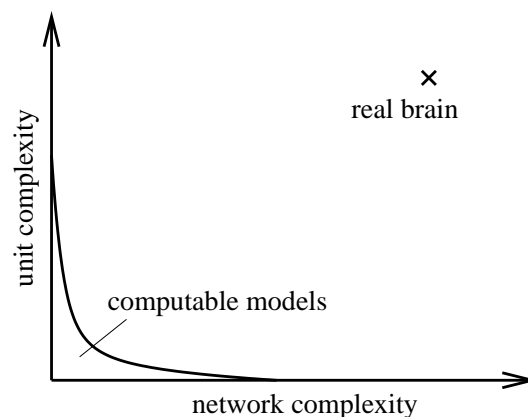
The figure should illustrate the problem that arises from limited computational facilities. Either a model includes many details of the single neurons and simulations are restricted to

small networks with a small number of synapses or the model uses a very reduced model of the single neuron and achieves the computability of more complicated networks. In that way the dynamics of real neural networks can be approached from two directions. One approach is based on the Hodgkin-Huxley model which was found in 1951 and which describes the dynamics of a neuronal membrane by a set of nonlinear differential equations. Models of this type are mainly used to analyze the *dynamics* of neural networks. The other approach, which is represented by e. g. the Hopfield model from 1982, tries to capture *cognitive aspects* like memory with very abstract models of the single neuron.

Epilepsy research in the past has mainly been carried out by using detailed differential equation models of single neurons which are interconnected to networks. This thesis tries to approach the phenomenon of epileptic seizures using a method that comes from the other side. Inspiring to this work was the previously started research at the mathematical institute here at the university of Cologne. In the group of Prof. Küpper the analysis of a differential equation model and computer simulations of small networks are employed in the investigation of epileptiform dynamics.

It is the crucial question of this work if the dynamics which underlie epileptic seizures can also be captured when we use a neuron model which is reduced as much as possible. The simplicity of the units should help to identify the part of the network in epileptogenesis. Starting with the very reduced Hopfield model which originates from theoretical physics, modifications and refinements will be made until eventually the model captures the characteristic features of epileptiform activity:

> A spontaneous onset of regularly oscillating activity, with an increased amplitude and a decreased frequency.

The first chapter will briefly summarize the physiological facts of neural networks as well as the phenomenology of brain waves and epilepsy. The second chapter will review some of the important network models which are applied to computer simulations of neural networks. This chapter shows the width of the spectrum of the current models of neural networks from the compartment models with up to 30 differential equations per neuron to the very reduced Hopfield model. Computer simulations of the latter were the starting point of my work. The quest for a simple epilepsy model converged to the model which is described in the third chapter. Simulation results of the newly developed model, the phenomenology and the parameter dependence are presented in chapter four. Chapter five concludes the thesis with a discussion of the new results presented in chapters 3 and 4.

1 Biological Neural Networks

1.1 Neurons

A neuron is one type of the variety of specialized cells animals are built of. Being a cell means that a couple of complex structures swimming within an electrolytic liquid is enclosed by a double lipid layer which is called membrane. The complex structures inside include those which are found in most cells and maintain the metabolism, i. e. nucleus, mitochondria, Golgi apparatus etc. The important specializing features of the nerve cell are its special shape and its excitability.

1.1.1 Structure

The shape of the neuron includes comparably long ramified tentacles which project from the cell body and reach a couple of millimeters or, in the case of motoneurons, even centimeters. This structure is usually divided into axonal tree, dendritic tree and soma. The general case is that a cell spreads its informational output via the axonal tree whereas it receives its input via the dendritic tree. In the middle of these branches is the soma where all the input comes together and the output is formed (cp. fig. 1.1). Information is passed in form of electrical potentials which propagate from the soma along the axon to the synapses thereby scattering the signal in various directions. The synapses transfer the signal to other neurons via chemical substances and thus induce electric potentials in the postsynaptic cell. Postsynaptic potentials (PSPs) in turn propagate along the dendrites and accumulate at the soma.

1.1.2 Membrane potential

An important feature which the neuron shares with e. g. the heart cell is that it is excitable. This means that the electrical potential difference at the membrane is used to communicate with other cells. There are many types of ions present in the fluid inside and outside the cells, the most important are Na^+, K^+, Ca^{++}, Cl^-. The ions are not equally distributed: K^+ is accumulated inside the cells whereas Na^+ is concentrated outside. Selective permeability of the membrane and active transport of the ions by ion pumps under consumption of ATP,
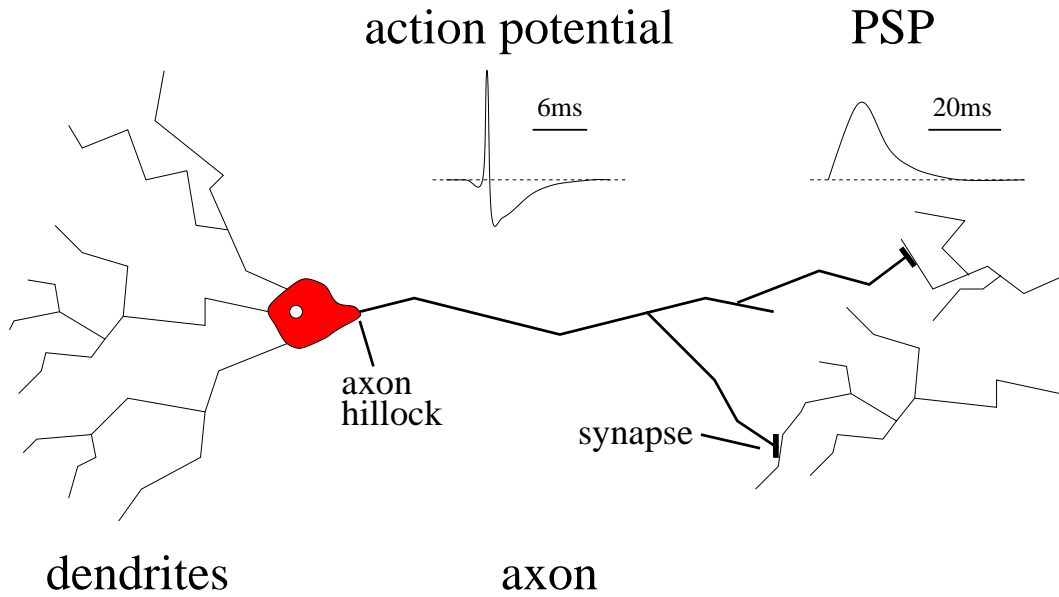
Figure 1.1: A schematical illustration of the neuron which consists of dendrites, soma and axon. The information flow is ideally from left to right: APs propagate along the axons to the synapses, at the synapses PSPs are induced in the dendrites.

maintain these concentration gradients against the equilibrating effect of leaks and functional membrane currents. The different concentrations of ions on both sides of the membrane bring along a gradient of the electric potential which also contributes to the energy balance of the system. The electrochemical potential with respect to a single type of ions is minimized at a certain potential difference E_i across the membrane, which is called the reversal potential of this kind of ion.

Thus, if by any reason a Na^+ channel opens, which selectively allows Na^+-ions to pass the membrane, the membrane potential will be attracted by E_{Na}, the reversal potential of Na^+. When the membrane potential, measured as inside minus outside, is below the reversal potential E_{Na}, the opening of the channel will result in an increase of the membrane potential. When the current membrane potential is higher than the reversal potential of Na^+, then the opening of a Na^+-channel will decrease the membrane potential. This is the mechanism by which transmembrane proteins which are selectively permeable for different kinds of ions can locally regulate the membrane potential. The capacity of the neural membrane is rather small so that even the ion currents of action potentials hardly affect the concentration gradient [36].

When the neuron is passive, the membrane potential is about -70mV whereas the reversal potentials for Na^+ and K^+ are +90mV and -90mV respectively [46]. As the resting potential of the membrane corresponds to a negative polarization of the membrane, ionic currents which increase the membrane potential are referred to a depolarizing currents whereas ionic currents that decrease the membrane potential are called repolarizing or hyperpolarizing respectively.

1.1.3 Action potential

The action potential (AP) is a sudden increase of the membrane potential to about +60mV which is then immediately repolarized. The process is triggered by a sufficient depolarization of the membrane to -60mV at the initial segment or axon hillock where the axon sprouts from the soma. In this region the membrane is especially excitable and thus a membrane depolarization of the soma effects first of all a conformational change of ion channels in this region. As the permeability of the ion channels in turn regulates the membrane potential, the AP is the result of a complex feedback process. The ion channels which react first to the depolarization are selectively permeable for sodium ions, thus a depolarizing current occurs and the membrane potential rises. With the increasing depolarization the sodium conductivity is further increased and thus the process is accelerating rapidly. With a certain delay, when the membrane is sufficiently depolarized, also the potassium channels open and effect a strong repolarizing current that decreases the membrane potential below the resting potential to -80mV. This hyperpolarization terminates the action potential which lasts one millisecond. After each AP it takes some time until the membrane potential regains its resting value. Immediately after the action potential the ion channel proteins can not switch into the conductive conformation and the membrane is inexcitable, thus another action potential can not be fired until about 2 to 5 milliseconds have passed. This period is called the refractory period and it limits the firing frequency of the neuron.

Due to the cable properties of the axon the depolarization of the membrane during the action potential spreads also to the membrane section next to the initial segment. This depolarization suffices to trigger the same sequence of ionic currents in the adjacent membrane section and this way the iteration of this process makes the AP propagate along the axon. The refractory period of the ion channels implies that the propagation is directed. The achieved propagation speed of APs in axons of cortical neurons is about 2m/s. In motoneurons the cable properties of the axons can be improved by a myelinic covering of the membrane which decreases the capacity and increases the resistance of the membrane. The myelinic cover is frequently interrupted at segments where the ion channel density is very high and thus an action potential can easily be triggered. Between these points the signal propagates via the electrotonic conduction mechanism of the axon. The combination of electrotonic conduction and active amplification by action potentials, which is called saltatory conduction, yields a maximized propagation speed of 10-120m/s.

Hodgkin and Huxley developed a detailed mathematical model describing the generation of action potentials which until today plays an important part in computer simulations of neural processes [43]. The model is thus briefly described in section 2.1.1.

1.1.4 Synapses

Synapses are the junctions between neurons, they can be divided into electrical and chemical synapses, further they are classified as axo-axonical, dendro-dendritical, axo-somatical, etc.

according to the tangent segments of the neurons. Among this variety the most common type is the chemical synapse where the axon of the presynaptic neuron and the dendrites of the postsynaptic neuron meet.

On the presynaptic side of the synapse small vesicles accumulate within the axon. The vesicles carry the neurotransmitters, chemical substances which affect transmembrane proteins in the postsynaptic dendrital membrane. Ca^{++}-influx associated with a passing or terminating action potential effects a fusion of the vesicles with the membrane of the presynaptic cell and a release of the neurotransmitter into the synaptic cleft. When the neurotransmitter arrives at receptor proteins in the postsynaptic membrane it effects the opening of ion channels which induces currents through the postsynaptic membrane. Depending on the sign of these postsynaptic currents (PSCs), i. e. whether they result in a depolarization or a hyperpolarization of the postsynaptic membrane, they are called excitatory or inhibitory. The induced alterations of the membrane potential are called excitatory postsynaptic potentials (EPSPs) or inhibitory postsynaptic potentials (IPSPs) respectively. The temporal structure of PSPs (if they are fast or slow) is important for the network dynamics as the input coming from the network to one neuron accumulates *spatially and temporally*: a volley of EPSPs which are induced by different neurons of the network is more likely to induce an action potential in the postsynaptic cell when the single EPSPs arrive in fast temporal sequence.

The variety of the chemical substances and the appropriate receptors make the synaptic transmission a very complex procedure. Different transmitter substances and receptors induce PSPs of different sign, i. e. excitatory or inhibitory and different kinetics, e. g. different duration, time to peak. The general case is that every transmitter substance affects only certain types of receptors and that every receptor regulates the permeability only for certain types of ions. Now Dale's principle states that through its metabolic unity a neuron has the same collection of transmitters at all its synapses [22], thus it comes out that in the majority of cases a neuron exclusively has either inhibitory synapses or excitatory synapses. However the truth is more complex: as the equilibrium potentials of ions depend on the extracellular concentrations which are subject to fluctuations and are even modulated it may occur that the postsynaptic potentials reverse in some cases. Recently the $GABA_A$ receptor which is usually believed to induce inhibitory PSPs has been hypothesized to induce depolarization with a slower characteristic time than most other excitatory PSPs [11].

Neurological disorders like e. g. epilepsy may be related to malfunctions of the transmitter production or the receptors. Most pharmaceuticals for the treatment of brain disorders, narcotics, toxins etc. work via influencing synaptic transmission. The principles are either mimicking a neurotransmitter by a substance which docks at the receptor protein and causes the opening of ion channels, these substances are called agonists, or blocking the receptor without an effect but making the receptor irreceptive to any agonist, these substances are called antagonists. Table 1.1 gives an overview of the most important neurotransmitters, receptor types, their agonists and antagonists. Further, one can not only block selected types of postsynaptic potentials but pharmacology also provides the possibility to change their shape. The application of barbiturates, e. g. pentobarbitone, prolongs the IPSPs effected by

receptor type	ions	agonist	antagonist
AMPA (exc., fast)	Na^+, K^+, Ca^{++}	AMPA	DNQX, NBQX
NMDA (exc., slow)	Na^+, K^+, Ca^{++}	ACPD, NMDA	D-AP5, CPP, NBQX
$GABA_A$ (inh., fast)	Cl^-	GABA, muscimol	bicuculline, picrotoxin
$GABA_B$ (inh., slow)	K^+	GABA, baclofen	phaclophen

Table 1.1: The most important receptors for synaptic transmission in the cortex.

f-band	name	correlated behavior
30-100Hz	gamma	alert, concentrated
15-30Hz	beta	
8-12Hz	alpha	awake, relaxed, eyes closed
3-7Hz	theta	sleep
0.5-2Hz	delta	deep sleep

Table 1.2: Brain waves

$GABA_A$ receptors. In the case of 40Hz oscillations (cp. section 1.2.1) this change of PSP duration can also have an effect apparent at the system level as lowering the frequency of population oscillations [30, 89].

1.2 Oscillations in Neural Networks

1.2.1 Brain waves, 40Hz Oscillations

Oscillations in the electrical activity of neural networks have been found in 1929 by the German physician Hans Berger [8]. He was one of the first who measured potential differences from the scalp of humans and is often called the inventor of electroencephalography. In particular he observed oscillations of the measured potential in a frequency range between 8 to 13 Hz which are called alpha waves. The discovery that alpha waves become apparent in the EEG when the measured person closes his eyes has been named "Berger effect". Similar oscillations of different frequencies are apparent in the EEG at any time, these oscillations are called "brain waves". The brain waves have been classified according to their frequencies, further it has been found that brain waves of different frequencies are roughly correlated with the behavioral state, (see table 1.2). Although there are some plausible hypotheses concerning the functions and mechanisms of the brain waves, research in this field is far from being complete.

Function: feature binding, scene segmentation and perception

From the beginning of electroencephalography until the end of the 1970ies it was believed that the EEG waves are nothing but noise corresponding to "idling of the brain" which has to be filtered out in order to get to the important data, i.e. the event related potentials [6]. Later oscillations have been observed to be in many cases correlated with certain stimuli. Since the early eighties several publications have been made suggesting that oscillations serve important functions in the cognitive processes. Especially in the olfactory bulb gamma waves appear as a reaction to stimulation with odorants [38]. Oscillations in this area have been hypothesized to rely on inhibitory feedback and the frequency of the oscillations to be determined by the time delay of the feedback loop.

In recent years gamma waves have been found to play a major roll in the synchronization of distributed parts of the brain which is important for the recognition of objects as ensembles of features and the distinction of features belonging to different objects [29]. It is thought that objects in the surrounding world are represented in the brain by ensembles of neurons. There are two competing theories of how this is organized. The "single cell hypothesis" claims that objects are generally represented by synaptically interconnected ensembles of neurons. Thus all memorized patterns are hard wired in the brain and can be recalled by synchronous mutual ignition of APs within the representing set of neurons (cp. section 2.2.1). Thus the problem arises that the number of thinkable objects is reduced: even if every single cell represents a single object then the combinatorial variety of objects that can be distinguished by far exceeds the number of neurons in our brain. If however various ensembles of neurons taken from the same basic set represent the objects, the combinatorial variety is also present inside the brain as a very large number of possible sets. But then the resolution of the different memories is gone as computer simulations with simple attractor neural networks show [86].

An alternative suggestion has been that only features of objects like green, round, soft, etc. are hard wired and that the combinatorial variety within the brain is achieved by temporal coding. This means that ensembles that represent features of the same object are in phase whereas ensembles that represent features of different objects are out of phase. It has been suggested that this phase relation is bound to different cycles in the gamma oscillation which is known to correlate with attention. Thus when we see a scene in which a red circle and a blue triangle appear the ensemble 'triangle' and the ensemble 'blue' fire within one gamma cycle whereas the ensembles 'circle' and 'red' fire in the next [55].

Final evidence of the correlation of 40Hz gamma oscillations and cognitive processes has been given in 1999 by Rodriguez et al. [77, 80]. Probands have been shown moony faces which could be either recognized as a face or discarded as meaningless, the test persons were asked to push a button when they saw a face. During the period from the beginning of the presentation up to 400ms after presentation increased gamma activity has shown up which has been significantly stronger when the proband perceived a face in the picture. The most convincing observation, however, has been that when perceiving a face, synchrony of the gamma oscillation over distant parts of the scalp could be seen whereas the oscillations were

not synchronous when no face was recognized. To summarize the idea: Perception of a face from this type of picture requires a lot of different features, i.e. angles, curves etc., which have to be put together to form a face. Assuming that the representing neuronal ensembles of the single features are spread over the scalp, long range synchrony may be the clue that these features have been identified as belonging to the same object and can be recognized as a face.

Later, this principle has been expanded such that 6Hz theta oscillations in the hippocampus bind objects together and form ensembles of objects [54, 55]. According to this latter hypothesis the period of the theta oscillation covers about seven cycles of the gamma oscillation each of which represents another object. This ratio of periods has been proposed to explain why one can have in mind only seven objects at the same time, a fact that has been found out in psychological experiments in 1956 [66]. The hypothesis is that a hierarchical order exists such that basic features are represented by synaptically interconnected neuronal ensembles, objects are represented by ensembles of features which are temporally bound together in gamma cycles and associations are represented by ensembles of objects which are temporally bound together in theta cycles.

Mechanisms of 40Hz oscillations

Not much is definitely known on the mechanisms which underlie brain waves whereas there are lots of different hypotheses. It is possible that brain waves of different frequency bands and in different regions of the brain depend on different mechanisms. Most theories agree that as the EEG measures a large population of neurons, thus the oscillation of the EEG signal indicates synchronous firing of the neurons as a collective phenomenon. Some possible mechanisms that have been proposed to underlie that synchronization are listed below.

- The oscillation could be initiated by pacemaker neurons which are intrinsically oscillating and drive the rest of the population [57]. In this case the conditions for synchronization of the neurons would be interesting, but the population serves as an amplification of the pacemaker and has no indispensable contribution to the mechanism of the oscillation.

- Second the oscillation can arise in a network where the interplay of inhibitory and excitatory neurons exhibits a temporal delay in between the two subpopulations which is due to finite times of signal propagation (feedback loops) [27]. This includes the hypothesis that there exists a phase lag between inhibitory and excitatory neurons [32].

- A third variant of the oscillating mechanism is that the different durations of excitatory and inhibitory synaptic potentials lead to a late superiority of the IPSPs such that the action potentials of all neurons are in phase whereas the cumulative inhibitory and excitatory postsynaptic potentials have a phase lag. The inhibitory neurons effect IPSPs in many other neurons. As the IPSPs last longer than the EPSPs they effect a resetting of all neurons and the simultaneous release from inhibition causes a synchronous onset of neural firing [18].

Blocking either excitation or $GABA_A$ mediated inhibition has been found to abolish 40Hz oscillations and so both are essential for 40Hz population oscillations [89, 30]. The first hypothesis however does not answer why inhibition is necessary for population oscillations. Computer simulations of neural networks with excitatory coupling only could produce synchronous population oscillations [72, 7]. In this case neurons had intrinsic oscillatory properties due to a refractory period and external stimulation. Thus if the first hypothesis applies to brain waves, excitatory connections should suffice for synchronization which disagrees with in vitro experiments.

The second hypothesis has been rejected at least for the case of gamma oscillations in the hippocampus where excitatory and inhibitory neurons have been found to fire in phase [12].

On the other hand there have been several indices pointing at the third hypothesis. Whereas a phase lag is not found between action potentials of excitatory and inhibitory neurons, experiments showed that there exists one between the excitatory and inhibitory postsynaptic potentials in this way that the IPSPs peak later [30]. The synchronizing effect of GABA mediated IPSPs in a population of cortical networks has experimentally been found by Cobb et al., further Whittington et al. found that the frequency of population oscillations can be regulated by changing the duration (time constant) of IPSPs [89].

Thus there are lots of indicators that the third hypothesis of the mechanism of population oscillations applies in a lot of cases. We anticipate here that mechanism three will also apply to oscillations in the newly developed model which is presented in this thesis (cp. section 4.2). Further a hypothetical mechanism of how this works when population IPSPs are considered will be outlined in section 4.2.1.

1.2.2 Epilepsy

Epilepsy is a chronic neurological disorder, its symptoms are seizures which spontaneously occur once in a while and are accompanied by loss of consciousness, rhythmic convulsions of the muscles, falling to the ground, temporary absence, etc. The duration of such seizures ranges from a couple of seconds to some minutes, most seizures end by themselves without treatment. About one percent of the world population is classified as having epilepsy, which means that seizures occur repeatedly whereby the frequency ranges from once within three months to many seizures every day. The origin of the disorder can be genetic as well as localized modifications of the tissue which are induced by a lesion, a tumor or developmental malfunction. Although patients with epilepsy do not sense their disease during the time between the seizures they are hindered in their every day life because the time point of the next seizure is not known: having a seizure while driving very fast in a car on a highway can be deadly. The medical treatment of the disease is usually pharmacological and prophylactic application of antiepileptic drugs (AEDs) in many cases helps to reduce the frequency of seizures significantly. About 20% of the cases can not be controlled with AEDs and require surgical treatment [24]. The necessity of a medical treatment is justified also because of the progress-

ive nature of some kinds of epilepsy, i.e. the seizures can induce secondary epileptogenesis in other, currently intact regions of the brain [52].

The detailed symptoms of the seizures and the possible origins are various and a classification of the epilepsies leads to numerous subtypes [28]. A principal distinction is made between focal seizures which are restricted to a small area of the brain and generalized seizures that affect the whole brain. The focal seizures arise from a localized area of epileptogenic tissue which lies often in the cortex and can be surgically removed in certain cases when pharmacological treatment of the disease does not apply. The extent of the removed brain tissue ranges from an area as large as a thumbnail to half of the brain.

Encephalography of epileptic brains

Epilepsy is closely related to brain oscillations. An important method for diagnosis and analysis of epilepsy is the EEG. The onset of an epileptic seizure is accompanied by a qualitative change which can be seen from figure 1.2. Characteristic for epileptic seizures is a significant increase of the EEG amplitude whereby the oscillations become very regular. In some cases as it is presented here the frequency decreases to 3Hz. Several patterns of EEG signals are
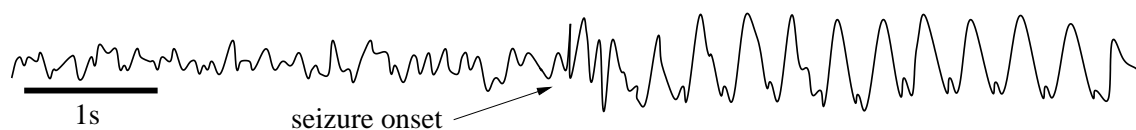
Figure 1.2: Example of the EEG at the onset of an epileptic seizure (modified from [48]).

called epileptiform as they are often observed during epileptic seizures [25]. The distinction is made as epileptiform activity may occur without a seizure. The common phenomenon which is thought to underlie all kinds of epileptiform patterns in the EEG is that many neurons fire synchronously. Whereas synchronous firing occurs also during the appearance of brain waves it is much more pronounced during epileptic seizures and thus called hypersynchronous. Epileptiform patterns of the EEG signal can be seen not only during seizures (ictal) but also between the seizures (interictal). An example of interictal activity is the occurrence of isolated high amplitude spikes, i.e. monophasic or biphasic potentials with a high amplitude (cp. section 4.8).

As the regularity of oscillations leaves it fingerprint in the kinetics of the EEG, since 1986 [5] it has been investigated if an epileptic seizure is the occurrence of low-dimensional chaos in the very complex dynamical system of the brain. Today the nonlinear time series analysis of the EEG has become an important method of seizure prognosis and detection of the epileptic focus [51, 52, 4] (cp. section 4.3).

Physiology of epileptic seizures

Characteristic of the behavior of single cells in a neural network during epileptic behavior is a prolonged depolarization of the membrane which results in burst discharges. A burst is a brief sequence of action potentials initiated by a slow depolarization of the membrane. While a burst may occur in an isolated cell as a response to a single stimulus due to special intrinsic properties in certain rare types of neurons [20], it might also be evoked by synaptic stimuli from many neurons. Thus the distinction between endogenous and network bursts has been made. Strong experimental support exists for the hypothesis that network bursts during epileptic seizures are evoked by a compound EPSP triggered by the firing of many neurons in the network [45]. Further, the bursts are thought to correspond with the interictal discharges in the EEG.

2 Mathematical Models of Neural Networks of the Brain

Besides animal models, slice preparations and single cell experiments, computer simulations of neural networks become more and more important in neuroscience. The appealing advantages of computational methods are the repeatability of experiments with exactly the same initial conditions, the opportunity to measure lots of details synchronously and - hopefully - a reduction of the number of animal experiments. The beginning of this development was the model of the dynamics of the giant squid axon published by Hodgkin and Huxley in 1952 [43]. Since then many refined models have been derived from this work and are applied in computer simulations of neuronal and neural network dynamics. On the other hand a second group of neural network models was initiated with the Hopfield model in 1982 [44]. These models concentrate on the function of the network as a whole whereas the complexity of physiological details of single neurons is substantially reduced. The two classes of the underlying mathematical models which have been employed in the computational analysis of brain function and neurological disorders are briefly reviewed in this chapter.

2.1   Continuous models

The Hodgkin-Huxley model [43] has been the first model of the dynamics of a single neuron. Its characteristics are that the different ionic currents are explicitly modeled and that the neuronal dynamics are nonlinear. The kinetics of an action potential are modeled with great accuracy but in many cases the details are too many and an easier model is wanted. Simplifications of the Hodgkin-Huxley model have been developed since then: the FitzHugh-Nagumo model [31, 70] or the Morris-Lecar model [68] have been applied in the computer simulation of epilepsy [76, 34, 35]. The complexity of the single neuron in these models limits the size of the population that can be simulated on the computer. One of the largest population of neurons which were modeled by a Hodgkin-Huxley derivative consisted of 6400 neurons and was simulated on a cluster of 19 Inmos T800 transputers in 1993 [90].

On the other hand also more complex derivatives of the Hodgkin-Huxley model have been developed by subdividing a neuron into compartments which interact via ionic currents or

by introducing additional ionic currents. These compartment models are the most complex models which have been used for the simulation of neural network dynamics [59, 85, 91].

2.1.1 Hodgkin-Huxley Model

The Hodgkin-Huxley model captures the dynamics of the action potential in a set of differential equations. The point is that the membrane potential is determined by the ionic currents belonging to various types of ions. On the other hand the transmembrane conductivities of the various types of ions are determined by the membrane potential. The latter dependence is due to conformational changes of the channel proteins according to the membrane potential. This feedback constellation leads to the action potential which can be mathematically described in the following equations.

The total current which determines the change of the membrane potential is given as the sum of the input from the synapses I_{syn}, the external input I_{ext}, which for example might be applied by the experimentalist through electrodes, and the ionic currents which generate the action potential. These are Na^+- and K^+- currents and a leak current gathering the contributions of the other ions.

$$C_{\mathrm{m}}\frac{dV}{dt} = I_{\mathrm{syn}} + I_{\mathrm{ext}} - g_{\mathrm{Na}}(V - E_{\mathrm{Na}}) - g_{\mathrm{K}}(V - E_{\mathrm{K}}) - g_{\mathrm{L}}(V - E_{\mathrm{L}}) \tag{2.1}$$

A stochastic model now assumes that the conductivities are related to the fraction of ion channels which are open. Thus if $\hat{g}_{\mathrm{K}}$ and $\hat{g}_{\mathrm{Na}}$ are the maximal conductivities which correspond to the situation that all channels are open, the present conductivities are given by this maximal conductivity multiplied by the probability that a channel permeable for the respective ion is open.

$$g_{\mathrm{K}} = \hat{g}_{\mathrm{K}} n^4 \tag{2.2}$$
$$g_{\mathrm{Na}} = \hat{g}_{\mathrm{Na}} m^3 h \tag{2.3}$$

Here n, m and h are probabilities of some permeability allowing states of certain substructures of the transmembrane channel protein. The K^+-channel is thought of requiring four equally probable events to occur in order to be permeable, whereas the Na^+-channel is more complex.

The probabilities n, m and h are modeled as first order reactions and the two reaction coefficients $\alpha(V_{\mathrm{m}})$ and $\beta(V_{\mathrm{m}})$ describe the opening rate and the closing rate respectively, which are both dependent on the membrane potential. Thus the gating equations are

$$\frac{dn}{dt} = \alpha_{\mathrm{n}}(V_{\mathrm{m}})(1 - n) - \beta_{\mathrm{n}}(V_{\mathrm{m}})n \tag{2.4}$$

$$\frac{dm}{dt} = \alpha_{\mathrm{m}}(V_{\mathrm{m}})(1 - m) - \beta_{\mathrm{m}}(V_{\mathrm{m}})m \tag{2.5}$$

$$\frac{dh}{dt} = \alpha_{\mathrm{h}}(V_{\mathrm{m}})(1 - h) - \beta_{\mathrm{h}}(V_{\mathrm{m}})h \tag{2.6}$$

The solutions of equations (2.4), (2.5) and (2.6), each regarded as isolated, are exponential time courses which are characterized by the time constants and equilibrium values given in equations (2.7) and (2.8).

$$\tau_n(V_m) = \frac{1}{\alpha_n(V_m) + \beta_n(V_m)} \tag{2.7}$$

$$n_\infty(V_m) = \frac{\alpha_n(V_m)}{\alpha_n(V_m) + \beta_n(V_m)} \tag{2.8}$$

Equations (2.7) and (2.8) can analogously be written for m and h.

Hodgkin and Huxley experimentally measured the time constants and equilibrium values and thus determined the reaction constants. Calculations of the whole model, i. e. equations (2.1) to (2.6), agree very well with the measured dynamics of the membrane potential when an action potential occurs.

2.1.2 Integrate and Fire Models of Neural Dynamics

Another class of simplified models consists of the so called integrate-and-fire models which are employed in many simulational studies of the dynamics of neural networks. Characteristic is that the dynamics of an action potential are reduced to a point like event in time whereas the postsynaptic mechanisms of temporal and spatial summation can be found more or less detailed in various subtypes.

The heart of the integrate-and-fire neuron is the membrane potential V_i which is charged by postsynaptic currents according to equation (2.9)

$$\tau_m \frac{dV_i}{dt} = -V_i + R_m I_i(t) \tag{2.9}$$

Here $\tau_m = R_m C_m$ is the time constant of the membrane which is modeled as an RC circuit. The synaptic current is generated by firing events of other neurons in the network, a general description is given by equation (2.10).

$$I_i(t) = \sum_{j=1}^{N} w_{ij} \sum_{\tau \in A_j} K(t - \tau) \tag{2.10}$$

Here w_{ij} is the coupling constant giving the strength of the synapse which neuron j projects onto neuron i, A_j is the set of time points when an action potential is fired by neuron j and the kernel function $K(t)$ gives the temporal course of a single PSP.

The various subtypes of the integrate-and-fire model use different shapes of the PSPs. According to how close the modeler wants to stick to the findings of the physiologists he can

choose the kernel function $K(t)$ among discontinuous onset with exponential decay, power law onset with exponential decay, sum of two exponentials with different time constants etc. (see e. g. [33]).

An action potential is triggered when V_i reaches a given firing threshold. Then the current time is joined to the set A_i and the membrane potential V_i is reset to zero.

2.2   Discrete Attractor Neural Networks

Twenty years ago discrete neural networks have been developed as a model of human memory. The inspiration came from the physics of spin glasses. Indeed not much was changed in order to make a neural network out of the spin glass model. The magnetic moments in the spin glasses of Edwards and Anderson [26] can orientate in two directions: either parallel to the exterior field or antiparallel. In contrast to ferromagnetic or antiferromagnetic Ising models the sign of the couplings between neighboring spins is not generally positive or generally negative, but randomly set for each pair of neighboring spins. The emergent difference to the ferromagnetic Ising model is that the spin glass has multiple ground states at zero temperature. Whereas the energy of the ferromagnetic Ising model at zero temperature is minimal for a completely parallel oriented array of spins, either all up or all down, the ground states of a spin glass are frustrated such that not all pairs of spins can simultaneously obtain the state of lowest energy and many couplings that yield a positive contribution to the energy remain when the energy of the system is minimal. Thus the ground state energy is higher than that of the ferromagnetic Ising model and further the number of ground states is much larger: many different conformations of the spin glass model have the same ground state energy.

In 1982 the physicist John Hopfield formulated a neural network model which is based on the spin glass dynamics [44]. The spins have been identified with neurons, the couplings have been extended to a complete graph and different ground states have been regarded as memorized patterns. This was the first model of the class of discrete attractor neural networks which are models of human memory. Since then a whole family of such discrete attractor neural networks arose [3] from the model which is described in the following section.

2.2.1   The Hopfield Model

The Hopfield model consists of N neurons each of which can take the values -1 or $+1$. Each neuron represents a pixel in a certain position of the stored patterns which are thus taken from the set $\{-1, 1\}^N$ of all possible states of the Hopfield-network. The neurons are connected in complete graph manner by $\binom{N}{2}$ couplings. A set of patterns $\{\xi^1, \ldots, \xi^P\} \subset \{-1, 1\}^N$ is stored

by fixing the coupling weights according to the Hebb-learning rule (cp. chapter 3)

$$w_{ij} = \sum_{\mu=1}^{P} \xi_i^\mu \xi_j^\mu, \quad w_{ii} = 0. \tag{2.11}$$

Here ξ_i^μ denotes the i-th pixel in pattern μ and the integer $w_{ij} \in \mathbb{Z}$ denotes the coupling-weight of neurons i and j for $i, j \in \{1, \ldots, N\}$. The couplings of the neurons are symmetric, i.e. $w_{ij} = w_{ji}$, and can be written as a symmetric weight-matrix W.

To retrieve the stored information the network is initialized with a pattern $S(0) \in \{-1, 1\}^N$ similar to one of the stored patterns and then iteratively updated according to the following update rule.

$$S(t+1)_i = \text{sign}\left(\sum_{j=1}^{N} w_{ij} S(t)_j\right) = \text{sign}\left((WS(t))_i\right) \tag{2.12}$$

The iteration is continued until a fixed point or a periodic cycle of length two is reached (cp. next section). The final state of the network S^{f} or respectively one of the two states in the cycle S_1^{f}, S_2^{f} is supposed to be the desired stored information or at least not to differ significantly from it. In terms of human memory the initial state $S(0)$ represents the stimulus and the final pattern S^{f} represents the association.

Thus the hypothesis that representations of objects in the human brain are ensembles of neurons and the principle of learning through synaptic plasticity which was formulated by the Canadian psychologist Donald Hebb elegantly entered the model. The information of all stored patterns is kept in the totality of the coupling weights of the neural network. On the other hand the Hopfield network is nothing but a dynamical system with several stable solutions, each of which has its basin of attraction.

If however too many patterns are loaded onto the network, the basins of attraction become blurred or even merge and simultaneously none of the stored patterns can be properly retrieved. It has been found that the number of patterns at which this phase transition from the retrieval phase to the spin glass phase occurs scales linearly with the system size N [2]. If one defines the capacity α of the network as the ratio of the number P of stored patterns to the number N of neurons, the estimates of the critical value scatter roughly around $\alpha_c \approx 0.14$. The controversy concerning the exact value of the critical threshold and a large scale simulational study were the very beginning of this work, the results are summarized separately [86].

Finally, there are some technical applications of the Hopfield model. The possibility to retrieve stored patterns when a distorted variant of the pattern is presented can be employed in optical character recognition, or speech recognition for instance. It can be assumed that the basic model is refined upon when it is employed for technical purposes.

Whereas this work concentrates on the oscillatory properties of neural networks, the Hopfield model does not have oscillatory properties. When asynchronous update is used the

Hopfield network does not oscillate but its dynamics always run into a fixed point. When synchronous update is employed also limit cycles of length two occur, which becomes more probable when the memory load of the network is increased [86]. One can imagine that the density of local minima in state space increases and that the network is switching between these minima when they are close enough. However, more complex oscillations are not possible. This fact can easily be proven by defining a Lyapunov function which can be thought of an energy of the system that monotonically decreases with time. Let us define

$$E(t) := -\sum_{i,j} w_{ij} S_i(t) S_j(t-1) = -S(t) W S(t-1) \tag{2.13}$$

If W is symmetric, which is the case in the Hopfield model,

$$E(t+1) - E(t) = -\sum_i (S_i(t+1) - S_i(t-1)) \sum_j w_{ij} S_j(t). \tag{2.14}$$

The definition of the systems dynamics, equation (2.12), shows that the second sum has the sign of $S_i(t+1)$ whereas the difference $S_i(t+1) - S_i(t-1)$ yields either zero or $2S_i(t+1)$. Thus all contributions to the sum in equation (2.14) are greater than or equal to zero. Thus $E(t+1) \leq E(t)$ holds for all $t \geq 1$ and $E(t)$ is a Lyapunov function of the dynamical system. If the system is caught in a periodic limit cycle of length p which is given by the states $S_1^l, S_2^l, \ldots, S_p^l$ then the energy of all these states must be equal. However, from the argumentation above it can easily be seen that $E(t+1) = E(t)$ iff $S(t+1) = S(t-1)$ and thus it holds that $p \leq 2$. This result is a special case of a more general mathematical theorem stating this "Period-Two-Property" holds for a larger class of discrete mathematical models [67].

2.2.2 Sompolinsky-Kanter Model

The oscillatory properties of the Hopfield model are rather poor but a minimal variation leads to a much richer behavior of the neural network. If the symmetry of the synaptic matrix is given up, then the theorem no longer holds and longer sequences can occur as limit cycles of the neural network. Aiming at a model of temporal associations between memories this modification of the Hopfield model has been introduced by Sompolinsky and Kanter in 1986 [82]. The modified network uses the same equation 2.12 for the time evolution, but the synaptic wiring has changed

$$w_{ij} = \sum_{\mu=1}^{P} \xi_i^\mu \xi_j^\mu + \lambda \sum_{\mu=1}^{P} \xi_i^{\mu+1} \xi_j^\mu, \quad w_{ii} = 0. \tag{2.15}$$

Here the synaptic couplings consist of two contributions: the first stabilizes the patterns whereas the second invokes the recalling of the next pattern when one of the stored patterns has been remembered. When the parameter λ is appropriately adjusted, the network fully remembers one state before it starts recalling the next state. Thus the model is capable

of subsequently recalling memorized patterns which is a model for association of different memories and temporal sequences. Further the system may now show complex oscillations and it has been employed in epilepsy models [63].

discrete time	Hopfield	Sompol.-Kanter		
continuous time			Integrate & Fire	Hodgkin-Huxley
network complexity	full symm.	full asymm.	arbitrary	arbitrary
PSP complexity	binary	binary	kernel function	kernel function
temporal summation	no	no	yes	yes
AP complexity	binary	binary	binary	dyn. membrane

3 A discrete model of cortical neural networks

In this chapter a description of a newly developed model of neural networks is given. The model has discrete time and state variables like the attractor neural networks described in the previous chapter and has been provided with additional features known from neurophysiology which appear important for the dynamics of real neural networks. Thus the discrete model should combine the essential features of earlier models that have been described in the previous sections. These are:

- Dale's principle: distinction between excitatory and inhibitory neurons

- Asymmetric synaptic connections

- Temporally extended synaptic action, i. e. temporal summation of PSPs

- Refractory period of single neurons

As we are targeting on the dynamical properties, in particular the oscillatory behavior, of the neural network rather than its cognitive functions such as the formation of memory and the recognition of memorized patterns, some of the features which do not appear essential for oscillatory dynamics are put back for later stages of the development of the model. Further, to keep the number of parameters manageable, some known interactions and dynamical aspects of biological neural networks which are unlikely to play a major part in the population dynamics are also put back. Introducing additional features of the brain to the discrete model can be done with respect to particular questions. The addition of a second slow IPSP for example will be discussed in section 4.8. First of all we want to investigate the dynamics of a network which is built of very simple neurons. The basic model will thus not take into account the following mechanisms which are inherent in neural networks of the brain:

- Morphological and dynamical diversity of neurons

- Diversity of receptors transmitters and ionic currents

- Long term potentiation (Hebbian learning)

- Neuromodulation

- Electric synapses (gap junctions)

- Ephaptic interactions (interactions between neighboring axons via the electro-magnetic field)

It has recently been published that inhibitory neurons could be classified into 14 different types according to the choice of their targets and to their postsynaptic effects [65, 39]. Thus, if a rapid of sequence of IPSPs is released, the amplitude of the IPSPs within the sequence will increase in one type whereas it will decrease in the other. Moreover there are different shapes of inhibitory neurons and correlations between the shapes and the kinetic behavior exist. Although it has been hypothesized since that these differences are related with different functions of the neurons [15], these findings will be neglected in our model. The introduction of a variety of neurons will dramatically increase the number of parameters and the simplicity of our model would be destroyed.

Also the variety of neurotransmitters and their corresponding receptors is large. For our basic model we will assume that all EPSPs and all IPSPs are equal respectively. In section 4.8 the introduction of a second inhibitory receptor will be discussed.

Long term synaptic potentiation (LTP) is the mechanism which is thought to underlie memory. The Canadian psychologist Donald Hebb postulated in 1949 that the development of memory in our brain is due to changes of the synaptic connections [41]. He suggested that a synapse by the use of which a neuron repeatedly excites another neuron above the firing threshold will increase its efficiency. This idea has been the fundamental principle for associative memory in attractor neural networks (cp. section 2.2). Meanwhile there have been lots of physiological experiments which give strong support to this principle (see [10] for a review). A quantitative analysis of the time scale of this process and the extent to which synapses can be changed has been done by Markram et al. [60]. Repeated dual stimulation of nearby neurons in vitro has lead to either increased or decreased EPSP amplitudes depending on the precise timing of the two stimuli. It is believed that the action potential in the postsynaptic neuron is propagating antidromically along the dendrites to the synapses where it meets an EPSP which has almost ceased and that this constellation effects the synaptic efficacy. Thus if the presynaptic cell is stimulated (and fires thereupon) 10ms before the postsynaptic cell, the EPSP amplitude of synapses between this neurons increased by 20%. Synapses that are pointing in the other direction "sense" the back-propagating action potential before the EPSP, this leads to a reduction of efficacy, also by 20%. However, it takes about five minutes of repeated stimulation until the effect becomes apparent. Thus the time scale of LTP is larger than that of our simulations. Nevertheless it would be interesting to investigate whether the synaptic connections in a neural network self-organize, via LTP, to a state which facilitates regular oscillations.

Neuromodulation means tuning the parameters of single neuron dynamics simultaneously in a large neural population on a time scale of more than a minute. This can be done

in vitro by adding neuromodulators to the artificial cerebrospinal fluid (ACSP) where the slice preparation is bathed in. Neuromodulators are neurotransmitters in most cases, the deviant terminology indicates that the substance is not locally present at a single synapse but rather in the surrounding fluid. Neuromodulators change the dynamics of the neural tissue and might thereby activate certain functions. Adding ACh (Acetylcholin) for example facilitates oscillations of the local field potential in the olfactory cortex [53]. Acetylcholin as well as Norepinephrine are known to support LTP in the hippocampus [71]. In vivo the concentration of neuromodulating substances varies with the arousal or mood of the individual. The transition from sleep to arousal for instance is accompanied by a widespread release of the neurotransmitters Acetylcholin (ACh), Norepinephrine (NE), Serotonin (5-HT), Histamine and Glutamate in the cortex and thalamus [83]. With respect to epilepsy this could be the clue to why some patients always have seizures at the same hour, e. g. in the morning. These neurotransmitters effect that firing rates of the neurons increase and low frequency rhythms (delta waves) are replaced by more rapid activity (gamma waves). However, as neuromodulators change large populations of neurons on a comparatively large time scale we can realize neuromodulation in our model by simply changing the parameters. The duration of our simulations will be too short to sense neuromodulation as a dynamical feature.

Gap junctions (electrical synapses) are channels which permanently connect the interior of two cell bodies and allow the exchange of molecules and electrical signals. The low resistance of gap junctions allow a very fast transmission of electrical signals between adjacent cells which is important in the propagation of action potentials among heart cells [81]. Although gap junctions are relatively rare in neural networks of the mammalian brain [79], they have been found to play a crucial part in the generation of high frequency (200Hz) population oscillations in the hippocampus [23], but the influence of gap junctions on the slower brain waves of the gamma band or lower frequencies is assumed to be negligible, these oscillations have been shown to be constituted by chemical synapses [18, 89](cp. also section 4.2). However the interaction through gap junctions may be added to the model at any time when the basic model has been analyzed.

Adjacent cells can also interact via their electromagnetic field. If one cell has for instance a strong Na^+ influx as in the case of an action potential then the extracellular current may evoke an electric potential in the neighboring cell. Ephaptic interactions are rather weak and do not contribute noticeable when the strong potentials of chemical synapses are present. Ephaptic interactions become important when bundles of unmyelinated axons are tightly packed as in the olfactory nerve fibers and recently even those weak interactions have been found to play a role in the synchronization of neuronal firing [11].

As we make a lot of simplifications the dynamics of a single neuron of our model are explicitly different than those of a real neuron. On the network level however, if the number of neurons is at least 1 000, the dynamics of the model network will be comparable with reality. The additional benefits of our simple model in comparison with differential equation models are that the number of parameters is smaller and that computer simulations are about a hundred times faster.

3.1 Description of the model

Modeling the neuron

After the simplifications mentioned above have been made a single neuron remains with two important types of electric potentials, action potentials (APs) and postsynaptic potentials (PSPs). The information carried by action potentials is rather binary, whereas the PSPs differ in strength and duration. The characteristic duration of the PSPs is much larger than the duration of an action potential which is about one millisecond. Events of a shorter characteristic time are not known. As a basic time unit of our model we therefore choose one discrete time step to correspond to one millisecond. Each neuron has further a limited spike frequency which is due to a refractory period or afterhyperpolarization (AHP) which lasts about six milliseconds and follows each action potential. During the refractory period a neuron cannot fire another AP.

Let N denote the number of neurons in our network and let p_{inh} be the fraction of the inhibitory units. In the following indices $1, \ldots, Np_{\mathrm{inh}}$ refer to the inhibitory neurons whereas indices $Np_{\mathrm{inh}} + 1, \ldots, N$ denote excitatory units. Throughout all our simulations p_{inh} has been set to 0.15 which is in agreement with physiological data [1]. We use one (binary) variable x_i to flag an action potential in neuron i and another integer variable r_i to count the remaining time steps, i.e. milliseconds, of the refractory period. The duration of the refractory period in milliseconds is denoted by r. Thus the pair $(x_i(t), r_i(t)) \in \{0, 1\} \times \{0, 1, \ldots, r\}$ describes the state of neuron i. How the two variables correspond with the action potential is shown in figure 3.1.

Modeling the network

Simulating a microscopic model of the human neocortex on a computer is rather impossible: The computer is too slow. If we compare the 40Hz cycle of the binding relevant gamma oscillations with the clock pulse of the computer then it appears as if the brain computes rather slowly. Of course the brain has no clock pulse on the single neuron level but the firing frequency of a single neuron is limited, due to the refractory period, to 200Hz which is still not much faster when compared with the clock rate of today's computers. On the other hand the 10^{10} neurons in the brain are working simultaneously and the emulation of such a large network is beyond today's computer power. If we assume that each neuron has 10^4 synapses which have to be updated with the state of the neuron one could guess that the update of a single neuron takes about 10^6 clock cycles on the computer under the additional assumption that a very elementary model of a synapse is employed. In this case today's typical computer with a clock rate of 10^9Hz would still be a billion times too slow. There is no need to talk about the required amount of memory to conclude that one has to restrict a microscopic model to a small part of the brain.
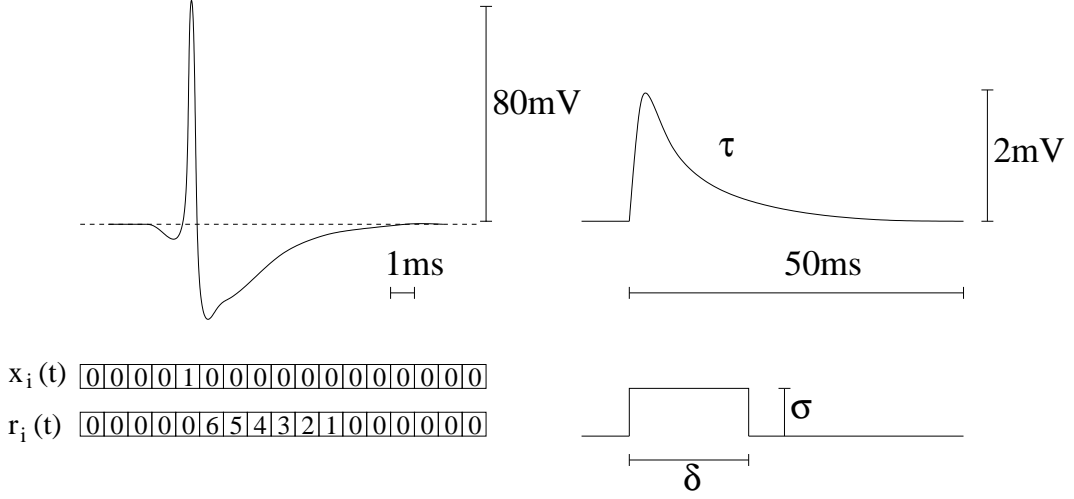
Figure 3.1: Discretization of an action potential (left) and a postsynaptic potential (right). The scale bars give the time scale for the real (upper) and model (lower) dynamics. The two variables x_i and r_i correspond to the presence of an AP and the remaining duration of the refractory period respectively. A PSP which is characterized in reality by a peak amplitude and a decay time constant is simplified to a square pulse with duration δ and amplitude σ.

With respect to epilepsy this makes sense as in the case of focal epilepsy seizures originate in a very restricted part of the brain. Due to a head trauma, a brain tumor, infections (encephalitis) or stroke the neuronal tissue of this epileptic focus could have slightly different structure or different neuronal properties. From this piece the epileptiform activity spreads through the brain tissue finally affecting the whole organism. If patients have pharmacologically intractable focal epilepsy the excision of the epileptic focus, a small piece of brain tissue, may cure the patient from epilepsy. Thus the alterations of neuron and network properties which are crucial for hyper-excitability and the generation of epileptiform activity can be found in a small region of neural tissue [75].

Concerning our computer simulation we desire the simulation of a cubic millimeter of cortex tissue. This tiny bit may contain about 90 000 neurons which is still too much to perform simulations within a reasonable time on a single processor workstation. This value of neuronal density corresponds to a mouse [14], whereas the human brain is different. Among mammals brain weight and body weight are related sublinear by a power law with exponent 0.7 and the density of neurons is the smaller the larger the whole brain is [1, 78]. Further, the density of neurons varies among the different areas of the human cortex: The density in the visual cortex is about 106 000 neurons per cubic millimeter whereas it is only 30 000 in the motor cortex [9]. Finally, the neuronal density varies between gyri and sulci within the same cortical region. Epilepsy may occur in mice as well as in humans and an epileptic focus might be located anywhere on the cortex, thus we will only keep in mind that the order of magnitude of neuronal density is between 10^4 and 10^5 neurons per cubic millimeter.
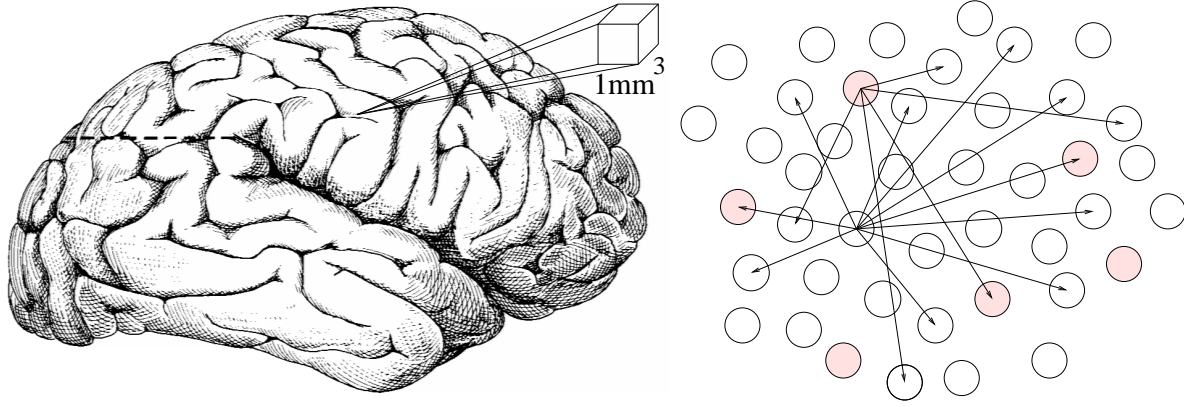
Figure 3.2: A cubic millimeter of cortex tissue contains approximately 90 000 neurons. As the reach of a neural axon is about one millimeter, such "small" networks are accurately modeled by a directed random graph. The right picture shows directed synaptic connections of two neurons as an example. The connections are set randomly according to a given density parameter. Shaded circles represent the inhibitory neurons which are about 15% of the neural population.

The reach of an axon is about one millimeter and so any neuron within this small box can in principle reach any other neuron in this box. Thus as long as we want to capture the structure of the cortex and we have neuron numbers below 30 000 we should construct the neural network as a random graph rather than placing the neurons on a lattice and assuming nearest neighbor interactions only. The latter would rather suit an assembly of heart cells among which action potentials affect the neighboring cells via electrical synapses, so called gap junctions [81]. The synaptic connections are determined randomly. Thereby we allow excitatory neurons to have a connectivity, i. e. a probability to have a synapse onto any arbitrary other neuron, which is different from inhibitory neurons. The probabilities are given by the network parameters κ_e and κ_i. The strength of the synaptic coupling will be the same for all inhibitory synapses and for all excitatory synapses respectively and will be given by the parameters σ_e and σ_i. The synaptic connections (where w_{ij} denotes the influence of neuron j on neuron i) are initialized according to equation (3.1) and kept constant throughout the simulation.

$$
\begin{aligned}
w_{ij}^{e} &= \begin{cases} +\sigma_e & \text{with probability } \kappa_e, \text{ if } j > Np_{\text{inh}} \\ 0 & \text{else} \end{cases} \\
w_{ij}^{i} &= \begin{cases} -\sigma_i & \text{with probability } \kappa_i, \text{ if } j \leq Np_{\text{inh}} \\ 0 & \text{else} \end{cases}
\end{aligned}
\tag{3.1}
$$

Calculation of the membrane potential and update rules

In each time step the membrane potential of the individual neurons is calculated. Thereby the spatial convergence of synaptic input from different neurons in the network and the temporal summation of the temporally extended PSPs are considered. Further the action potential flag

and refractory counter are updated corresponding to the following rules:

- temporal summation of PSPs:[1]

$$x_i^e(t) \;=\; x_i(t) + x_i(t-1) + \ldots + x_i(t - \delta_e - 1) \tag{3.2}$$

$$x_i^i(t) \;=\; x_i(t) + x_i(t-1) + \ldots + x_i(t - \delta_i - 1) \tag{3.3}$$

- spatial summation of PSPs:

$$V_i(t) = \sum_{j=1}^{N} \left(w_{ij}^e x_j^e(t) + w_{ij}^i x_j^i(t) \right) \qquad \text{(membrane potential)} \tag{3.4}$$

- flag action potential if firing threshold θ is reached:

$$x_i(t+1) = \begin{cases} 1 & \text{if} \quad V_i(t) \geq \theta \text{ and } r_i(t) = 0 \\ 0 & \phantom{\text{if}} \quad \text{else} \end{cases} \tag{3.5}$$

- updating refractory status:

$$r_i(t+1) = \begin{cases} r & x_i(t+1) = 1 \\ r_i(t) - 1 & \text{if} \quad r_i(t) > 0 \text{ and } x_i(t+1) = 0 \\ 0 & \text{else} \end{cases} \tag{3.6}$$

Random sequential update is applied in order to prevent the system from falling into unnatural limit cycles which is typical for synchronous updating. Random sequential update means that N times in each time step a neuron is randomly chosen and equation 3.5 is applied. Thereafter equation 3.6 will be applied. Whereas the application of equation 3.5 underlies chance, equation 3.6 is rigorously applied to any neuron in any time step such that the actual duration of the refractory period exactly equals the prescribed value r. Further will x_i be initialized to zero for each neuron at the beginning of each new time step.

In this way approximately a fourth of the neurons is chosen more than once in one time step. In this case a neuron which has already been set to fire an AP in the same time step will not be updated again, the effect is as if it was chosen just once. On the other hand in every time step there is some other group of neurons, approximately 37%, which is not updated at all. This causes some temporal jitter in the dynamics of every neuron as it may happen that a neuron is not updated for a couple of time steps. This is a source of noise which represents individual time delays occurring e. g. because of the release of neurotransmitter vesicles at the synapses or the electrotonic spread of PSPs along the dendrites [46]. The time that a neuron is waiting for being updated follows a geometric distribution, the expectation of the required number of trials is about 1.6 time steps (milliseconds) instead of one which would be

---

[1]The actual implementation does not execute this calculation explicitly. To save time the algorithm performs an event-related switching "on" or "off" a permanent contribution to the membrane potential.

the case for sequential update. The difference of 0.6 milliseconds corresponds very well to the synaptic time delay between the arrival of the action potential at the synapse and the release of neurotransmitter [46] and is therefore not problematic but rather welcome. The standard deviation of the waiting time is 0.97ms and will be referred to as jitter in the following.

There are three alterations when we use random sequential update instead of synchronous update:

- When a neuron fires an action potential, this affects the connected neurons that are subsequently updated *within the same time step.*

- As the sub-steps influence the results of further sub-steps within the same time step, also the order of the successive sub-steps becomes important.

- 37% of the neural population are not updated in every time step.

Whereas the first two points are negligible the major difference with respect to our model is the third one of this list. A comparison of synchronous update, sequential update with fixed order and sequential update with random order which has been newly determined in each time step showed no significant difference in the resulting network dynamics as long as all neurons have been regarded in each time step. The problem of all these variants of updating is that the activity is always attracted by some limit cycle. The resulting activity is what the EEG might look like if the brain had a clock pulse like a computer CPU.

On the cellular level the brain has no clock pulse, but delays of the molecular processes, fluctuations of ion-concentrations and other various kinds of noise are present. The conduction times of the axons as well as the exact time point of spike generation in sufficiently excited neurons are subject to jitter. There are four sources of jitter in the neural transmission process:

- Different lengths of axonal distance that has to be covered by the action potential, about 0.2ms (estimation by the author)

- Varying time of transmitter release in the synapse, about $50\mu s$ [1, 21]

- Different dendrital distance from synapse to soma, about 1ms [46]

- Fluctuations of the membrane potential lead to jitter in the time point of AP generation which is about 0.43ms (estimation by Abeles [1])

The summation of the jitter given above (Gaussian distributions granted) yields approximately 1.1ms which is roughly in agreement with the random sequential response jitter of 0.97ms in this model. In a continuous model with nonlinear dynamics, for example a network of Hodgkin-Huxley model neurons, those fluctuations may be hidden in the chaotic dynamics of the system. Tiny deviations of the state variables may have any order of magnitude and can develop now and then to a noticeable extent and cause the jitter which jeopardizes synchrony.

In a model with discrete time and discrete state variables there is a lower bound for the size of fluctuations which are explained by the systems dynamic equations. So random sequential update is an elegant way to introduce those features which cause small fluctuations into the model.

Also noise of a very low level has been added to the membrane potential in some simulations but this did not change the dynamics of the system substantially.

3.2 Which values should be chosen for the parameters?

Fraction of inhibitory neurons: p_{inh}

The percentage of inhibitory neurons in the cortex varies between 10 and 15 percent. In the simulations we always use $p_{\text{inh}} = 0.15$, this value has not been changed throughout the simulations.

Connection probabilities: κ_{e} **and** κ_{i}

Our model implies that between one pair of neurons there is only one synapse or none. Of course the possibility of multiple synapses between two neurons exists in principle but the probability under certain assumptions is low.

In our model a neuron establishes $N\kappa$ synapses onto targets randomly selected from the N neurons within the "cube". Thus, given that $N > 1\,000$ and $\kappa < 0.2$, the probability that a neuron receives k synapses from one distinct other neuron follows a Poisson distribution, i. e. $p(k, \kappa) = e^{-\kappa}\kappa^k/k!$. Thus the probability that a neuron has more than one synapse from one other neuron is given by

$$P_{\text{mult}} = 1 - e^{-\kappa} - \kappa e^{-\kappa} \tag{3.7}$$

Equation (3.7) yields that as long as $\kappa < 0.2$ the fraction of multiple synaptic connections between neurons is below 2% and if $\kappa < 0.1$ the fraction is even less than 0.5%. Thus the effect of multiple synapses appears negligible. The number of synapses per neuron is about $8\,000$ in the mouse cortex [14], thus with respect to the $90\,000$ neurons within the 1mm^3-cube of mouse brain one gets an order of magnitude for the relative connectivity of $\kappa \approx 0.1$. The important inhibitory synapses are located on the somata of the target cells and thus dominate the synapses targeting on the dendrites of cortical cells. Further, the reach of the axons of stellate cells, which are mainly inhibitory, is smaller [14]. Thus the connectivity of inhibitory neurons is assumed to be lower than the excitatory connectivity. A study of pyramidal cells in the motorcortex of the cat yielded connectivity values for the number of terminating inhibitory synapses around 60 per neuron [17]. Variations of the connectivities are discussed in the next chapter.

PSP amplitudes: σ_e **and** σ_i

The inhibitory synapses are supposed to have a higher amplitude than excitatory synapses for two reasons. First the IPSP measured directly at the location of the synapse in the postsynaptic cell is more pronounced than the EPSP. Second the inhibitory synapses to a large part terminate directly on the soma [1, 59, 17] whereas excitatory synapses terminate on spines which are located somewhere on the dendritic tree further away from the cell body. As the dendrites have the properties of leaky cables the impulse of the EPSP is more than the IPSP attenuated during its propagation from the synapse to the soma [46]. That inhibitory synapses are situated close to the soma is however again a simplification and not true in general. In the hippocampus inhibitory synapses have been shown to have qualitatively different functions whether they are targeting on the dendrites or the soma of a pyramidal cell [64]. We want to keep the model simple and therefore decide not to differentiate between somatic and dendritic inhibition rather than approximate the real situation by a mean IPSP which is stronger than the EPSP. In most simulations we set $\sigma_e{=}20$ and $\sigma_i{=}120$ whereby the firing threshold $\theta{=}180$. The threshold value of 180 was thought to correspond to 18mV of depolarization which is necessary to evoke the firing of an action potential. However, an interpretation of these values in mV is problematic as the summation of PSPs is nonlinear in reality whereas it is linear in the model. The dependence of the population dynamics on PSP strengths will be investigated in detail in the next chapter.

The value of the firing threshold will not be varied as this would be redundant. From equations (3.1) to (3.6) it follows that the ratios σ_e/θ and σ_i/θ are crucial.

PSP durations: δ_e **and** δ_i

The durations of inhibitory PSPs have a longer duration than the EPSPs. The most common excitatory neurotransmitter is NMDA, the duration of NMDA-mediated EPSPs is about 10ms. The prevalent inhibitory neurotransmitter is γ-amino-butyric acid (GABA). In contrast to the EPSPs the IPSPs appear in two markedly different variations which are initiated by two different variants of the GABA receptor. The early IPSP is mediated by the GABA$_A$ receptor, it has a time to peak of 28ms and a duration of about 80ms. The late IPSP which is mediated by the GABA$_B$ receptor, has a duration of 150-200ms and a time to peak of 135ms [61, 19]. In spite of this fact the basic model will include only one type of inhibitory PSP which corresponds to the GABA$_A$-mediated potential, this has been shown to be essential for 40Hz oscillations in the cortex (cp. sections 1.2.1 and 4.2). The influence of GABA$_B$ mediated IPSPs on the network dynamics has a special importance with respect to epilepsy and will be discussed in section 4.8.

parameter	suitable range	natural unit
κ_e	0.0-0.2	1
κ_i	0.0-0.1	1
δ_e	0-30	ms
δ_i	0-150	ms
σ_e	0-40	mV
σ_i	0-240	mV
r	2-5	ms
N	0-100 000	1
θ (fixed)	180	mV
p_{inh} (fixed)	0.15	1

Table 3.1: Suitable values for the model parameters

4 Simulation of the discrete neural network model

Now that a simple neural network model has been established we wish to employ it in answering the following questions:

- Which properties of a neural network support the synchronized firing of action potentials among the neural population?

- Does an order parameter exist, which characterizes the dynamics of the neural network?

- How can a spontaneous change of network activity from disordered firing to synchronized activity occur?

- Which parameters of the model network yield spontaneous oscillations?

- How do noise and stimulation contribute to (spontaneous) synchronization in the neural network?

With respect to these questions the newly constructed model offers appropriate requisites. As neural networks are complex systems which can hardly be treated analytically, information concerning the parameter dependent behavior is mainly obtained by means of (computer) experiments. The comparably small number of parameters and the high simulation speed of the simple discrete model are excellent preconditions for the investigation of parameter dependencies. We now can scan the parameter space point by point with thousands of test runs of different neural networks. Nevertheless, the analysis of the parameter dependencies will remain difficult as the parameter space is eight-dimensional[1] whereas one is used to two-dimensional graphs. The employment of three-dimensional graphs and greyscale images helps a little whereas the use of movies (with the time as third abscissae) could enable four-dimensional demonstrations which is not possible in this written document. Thus our phase-diagram of a neural network has to be pasted together from different projections of the parameter space.

---

[1]The firing threshold Θ can be easily canceled out as only the ratios σ_e/Θ and σ_i/Θ are relevant. p_{inh} will be kept fixed.

activity	$a(t)$	$:=$	$\sum_{i=1}^{N} x_i(t)$
mean activity	$\langle a(t) \rangle$		
amplitude	$D(a(t))$	$:=$	$\sqrt{\langle a(t)^2 \rangle - \langle a(t) \rangle^2}$
autocorrelation	$C(\tau)$	$:=$	$\langle a(t)a(t+\tau) \rangle - \langle a(t) \rangle \langle a(t+\tau) \rangle$
period	T	$:=$	1st Maximum of $C(\tau)$

Table 4.1: Observed quantities

For sure our model contains some rude simplifications which might render it worthless when we want to describe the neural tissue of real brains. We will thus compare the results of our computer simulations with physiological experiments and we will check if they agree. However, the brain is not homogeneous, it has different compartments which are all differently built with various types of neurons. A precise model of the cortex cannot be a model of the hippocampus. Our model just captures the essential features which are common in all types of neurons. It therefore can only describe the behavior of a general neural network. Diverging results indicate that the simulation of a certain part of the brain requires special improvements or upgrades of the basic model. Such results can also be regarded as important because we can learn which microscopic features of a neural network are essential to yield a certain phenomenon.

Moreover, although it is physiologically not correct we will also investigate the dynamics of a model without refractory period, i.e. $r = 0$. This will momentarily reduce the number of parameters of the model and gives us a chance to understand the role of the refractory period by observing the change of the dynamics with its introduction.

Table 4.1 gives definitions of some useful quantities which we will refer to in the subsequent investigations. The angular brackets denote a temporal average calculated in a time window of appropriate length, which is chosen to be 1 500 (in some case also 4 096) time steps (milliseconds).

4.1 Definition of different regimes of network activity

If we vary a single network parameter we can observe that the behavior of the simulated network changes. Let us have a quick view on what happens if we vary κ_i, the outward connectivity of the inhibitory neurons, when all other parameters are kept fixed. Figure 4.1 shows epochs of simulated network activity, i.e. $a(t)$ is plotted versus time. The different epochs, each of length 500 time steps, correspond to different values of κ_i. In all cases the network has been initialized with half of the neurons firing. After initialization it takes the system about 200 time steps to equilibrate to its final mean activity. The epochs have been recorded between time steps 1 000 and 1 500. We do not see synchronized firing when κ_i is

small. Synchrony means that the action potentials accumulate around certain time points whereas they are rare in between these time points, thus we would expect large fluctuations of the activity. If we raise κ_i, we observe that the mean activity is reduced. We would intuitively expect this because more inhibitory synapses lead to a lower average membrane potential and thus to a smaller number of neurons reaching the firing threshold. Further we see that more and more regular oscillations become apparent, the amplitude of which increases rapidly. If we further raise κ_i above some critical value κ_i^*, the network is not able to maintain any network activity autonomously and the firing of action potentials ceases. Thus the next epoch to the right which has not been plotted in figure 4.1 would show nothing but a straight line telling us that $a(t)$ constantly remains zero. We will call a network with such conditions over-inhibited.
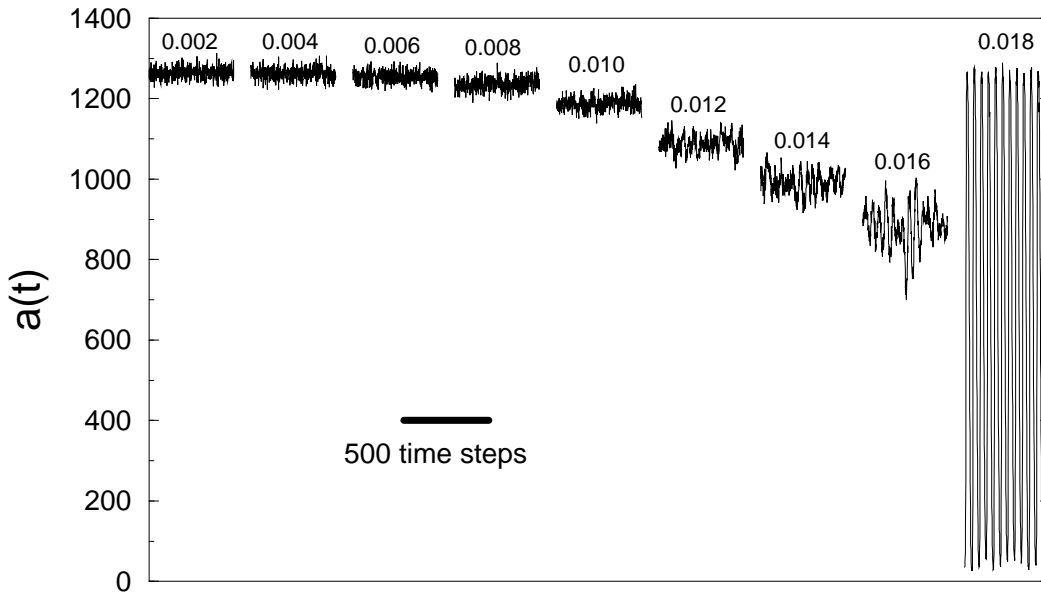
Figure 4.1: Epochs of 500 ms of the network activity corresponding to different values of κ_i, the efferent (outward) connectivity of the inhibitory neurons. κ_i is raised in steps of 0.002 from 0.002 to 0.018 (left to right). The other parameters are κ_e=0.060, (δ_e, δ_i)=(7,20), (σ_e, σ_i)=(20,120), r=0, N=2 000. For $\kappa_i \geq 0.012$ population oscillations with a frequency of 25Hz become apparent. When $\kappa_i \geq 0.02$ the network can not autonomously maintain activity.

We will now face the following questions:

- Is the transition from fluctuating dynamics to synchronous population firing smooth or a sharp first-order phase transition of the dynamical system?

- Where are the borders of the different regimes in the parameter space?

- Is there a bistable domain in the parameter space where the system spontaneously switches between fluctuating and oscillating dynamics?

Some points can be answered right away. Figure 4.2 shows the dependence of the amplitude $D(a(t))$ and the mean activity $\langle a(t) \rangle$ on κ_i which has been altered in small steps. The sudden increase of the amplitude at $\kappa_i^c \approx 0.017$ strongly suggests that a sudden qualitative change of the dynamics from fluctuating to oscillating dynamics takes place. It is yet not clear whether the graph is discontinuous or not and the value of κ_i at which the transition occurs varies with different arrangements of the synapses. Simulations of larger systems do not show that the increase of the amplitude becomes steeper with increasing system size (cp. section 4.4.2). However, the abrupt change of the dynamics within one simulation run, as it may occur in systems that are right at the critical point (cp. section 4.3), indicates that the attractor changes fundamentally. A clear discontinuity appears when the dynamics change from the oscillating to the flat regime.

However, the simulation results, particularly the values of κ_i^c and κ_i^*, depend not only on the parameters but also on the initialization of the random number generator which determines the details of synaptic wiring. Thus simulation results obtained using the same parameters but different random number generator seeds (RNGSs) are scattered. In the following sections the measured quantities will be averaged among a couple of simulations with different RNGSs. As we will show in section 4.4, the dispersion of simulation results decreases when the system size N is raised.

We have shown that there are three different regimes:

- The fluctuating regime is characterized by a low amplitude. Even in this regime population oscillations may appear in form of transitory waves with a characteristic duration of about 300 ms and a low amplitude. These waves occur the more pronounced the closer the system is located in the parameter space to the border of the oscillating regime. Characteristic for the fluctuating regime is a low value of $D(a(t))$, an example is given in the lower graph in figure 4.3.

- The oscillating regime in which the activity $a(t)$ follows a steady regular oscillation with a high amplitude, an example is given in the upper graph in figure 4.3.

- The flat regime in which the network activity will cease very soon after external stimulation because the inhibitory potentials are too strong.

If the network parameters are very close to the boundary of the oscillating and the flat regime transition the system may also be bistable. It then switches between the fluctuating and the oscillatig regimes (cp. section 4.3).
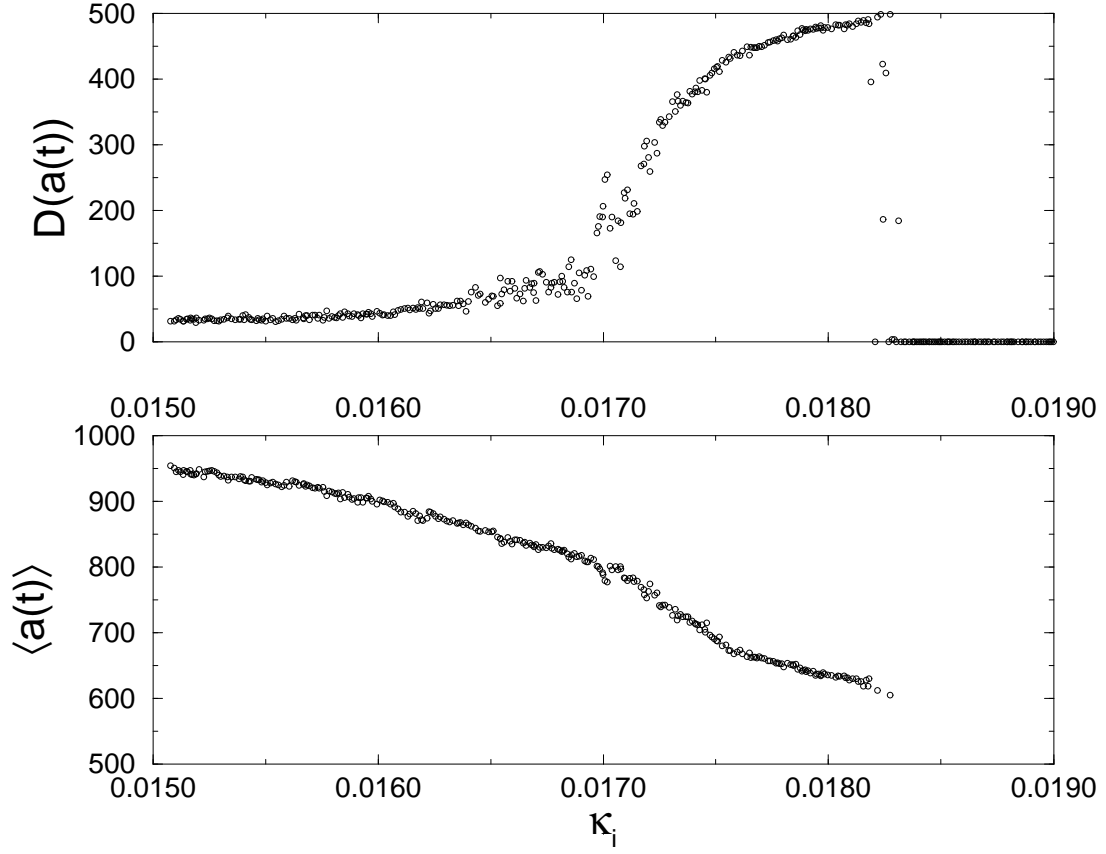
Figure 4.2: $D(a(t))$ and $\langle a(t) \rangle$ vs. κ_i. At $\kappa_i^c \approx 0.017$ the amplitude of the network activity jumps to a higher value. At $\kappa_i^* \approx 0.01825$ autonomous activity is not longer possible. The other parameters are κ_e=0.060, (δ_e, δ_i)=(7,20), (σ_e, σ_i)=(20,120), r=0, N=2 000, RNGS fixed.

4.2   The mechanism of population oscillations

It has been found that synchronization of neural firing is a collective network phenomenon in which inhibitory neurons are pivotal. Cobb et al. suggested that "synchronization of principal cell activity may be a fundamental role for these interneurons" [18]. They observed that in slice preparations of the rat hippocampus single action potentials of inhibitory neurons were able to reset the phase of excitatory pyramidal neurons. Shortly after the IPSPs have ceased, pyramidal neurons in the vicinity began firing synchronous volleys of action potentials which dispersed after a few cycles. In vitro experiments showed that the blockade of GABA$_A$-mediated inhibition with bicuculline stopped the 40Hz population oscillations whereas a slight stimulation of inhibitory neurons entrained the firing of action potentials in the pyramidal neurons of the slice preparation [16, 30]. In comparison with isolated IPSPs evoked by single synapses, the compound IPSPs measured during the oscillation have an amplitude which is
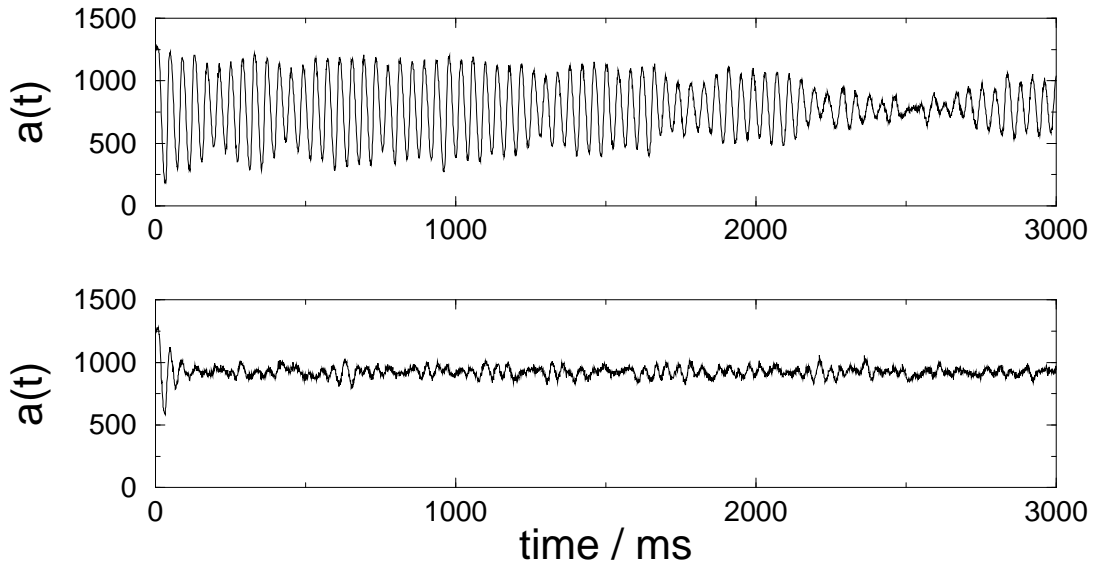
Figure 4.3: Examples of network activity in different regimes: The upper graph corresponds to κ_i=0.01698 and shows a steady regular oscillation. In the lower graph, when κ_i=0.01550, we see small oscillations which are coherent only for a few cycles. All other parameters are as in figure 4.2.

ten times higher and of a different shape [89]. Additionally, the frequency of the population oscillations can be lowered by addition of pentobarbitone, which increases the duration of $GABA_A$-mediated IPSPs [89, 16] (cp. also section 4.6).

These findings support the point of view that synchronization of action potentials is achieved rather by the inhibitory action in the network than by phase resetting of excitatory coupled neuronal oscillators. Further, the experiments cited above also showed that excitatory coupling is essential for synchronized firing: population oscillations can be induced by adding glutamatergic agonists whereas glutamate receptor antagonists do abolish oscillations. Thus excitatory *and* inhibitory couplings play a part in the synchronization of real neural networks.

We now have a look at the mechanism of population oscillations in our simulations. One major advantage of computer simulations is that one can easily observe all quantities of the system at the same time. This helps very much in understanding the mechanism of population oscillations in neural networks, which is rather difficult from experimental observations in real neural tissue. We record the time course of the activity $a(t)$ and further the globally accumulated excitatory and inhibitory postsynaptic potentials in simulations of our model. These two quantities which we call $E(t)$ and $I(t)$ are defined by equations (4.1) and (4.2).

$$E(t) \quad := \quad \sum_{i=Np_i+1}^{N} \sum_{\tau=0}^{\delta_e-1} x_i(t-\tau) \sum_{j=1}^{N} w_{ji} \qquad \text{(excitatory)} \qquad (4.1)$$

$$I(t) \quad := \quad \sum_{i=1}^{Np_i} \sum_{\tau=0}^{\delta_i-1} x_i(t-\tau) \sum_{j=1}^{N} w_{ji} \qquad \text{(inhibitory)} \qquad (4.2)$$

Based on the information given in figure 4.4 we hypothesize that the following mechanism in three steps underlies the population oscillations in our neural networks:
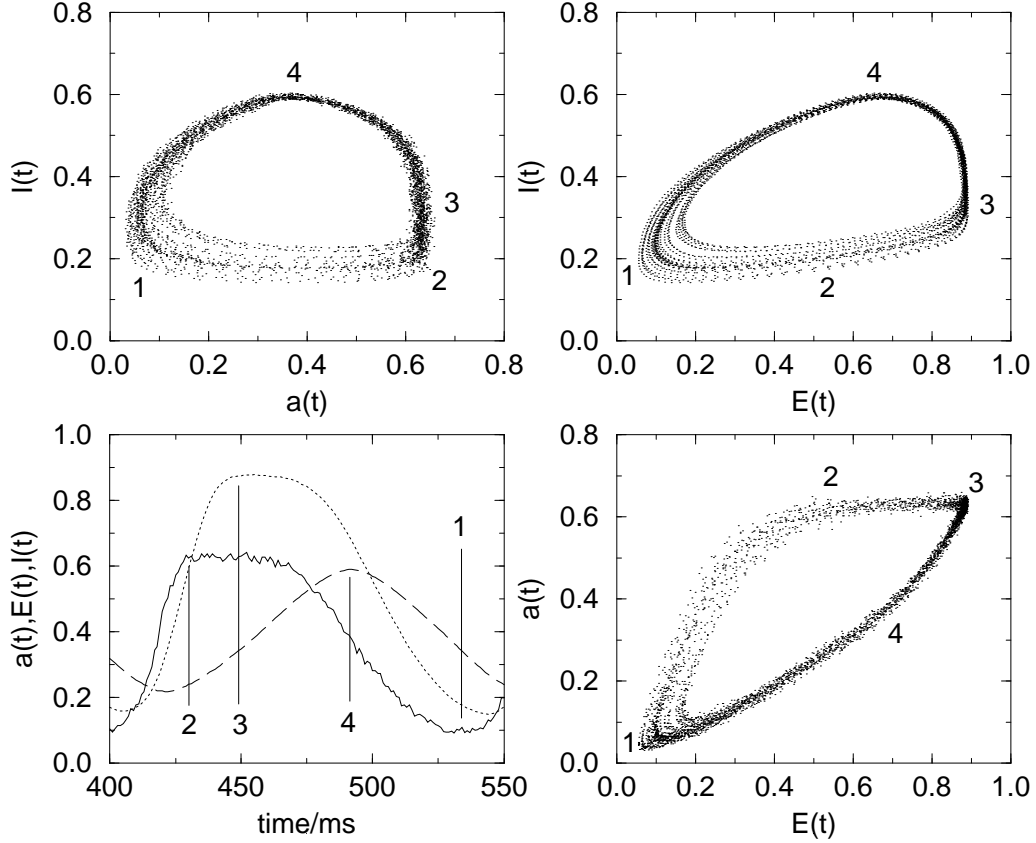

Figure 4.4: Projections of the attractor of a steady population oscillation in three-dimensional "phase space". The coordinates refer to $a(t)$(solid line), $E(t)$(dotted line) and $I(t)$(dashed line). The values have been divided by N, $N^2(1 - p_{inh})\kappa_e \sigma_e \delta_e$ and $N^2 p_{inh} \kappa_i \sigma_i \delta_i$ respectively. Label 1 marks to the minimum of the activity, labels 2, 3 and 4 indicate the maxima of $a(t)$, $E(t)$ and $I(t)$ respectively. The parameters are $(\kappa_e, \kappa_i)=(0.160, 0.032)$, $(\delta_e, \delta_i)=(20,73)$, $(\sigma_e, \sigma_i)=(20,120)$, $r=0$, $N=1\,000$.

- Chain reaction of AP firing:
  Let the cycle begin when the network activity is low and no significant IPSPs are present. This situation corresponds to label 1 in figure 4.4. In this example the number ratio of excitatory and inhibitory neurons is $(1 - p_{inh})/p_{inh} \approx 5.7$ and the ratio of the number of

synapses per neuron is $\kappa_e/\kappa_i{=}5$, on the other hand the ratio of synaptic strength σ_e/σ_i equals 1:6. Thus at the moment the firing of action potentials statistically increases the membrane potential of the neurons and more neurons are excited above the firing threshold. A sufficiently high initial activity thus triggers a chain reaction of neural firing. The increase of the network activity is limited only by the size of the total population, not by the inhibition in the network. Due to random sequential update it therefore saturates at $0.63N$ (label 2 in figure 4.4).

- Accumulation of the PSPs:
  The power of the inhibitory neurons lies to a great extent in the longer duration of the IPSPs. When the activity has saturated, $I(t)$ further increases for a longer time than $E(t)$. Thus $E(t)$ peaks significantly earlier than $I(t)$ (labels 3 and 4). As in this example δ_i is long enough, $I(t)$ grows until the neural population gets so much inhibition that the activity decreases.

- Ceasing of the accumulated IPSPs:
  When δ_i is not too high $I(t)$ ceases before the activity is completely extinguished. This activity is needed to ignite the chain reaction of action potentials at the beginning of the next cycle. After the IPSPs have ceased the state of the first step is reached again (label 1) and the sequence repeats.

It should be stressed that the excitatory and inhibitory subpopulation are in phase. This is not surprising as during the initial process of synaptic wiring the targets are not distinguished. The mechanism is therefore not the alternated firing of the excitatory and inhibitory subpopulation but the delayed power of the inhibitory neurons. This temporal sequence of the peak of action potential probability, the peak of the excitatory postsynaptic action and the peak of the inhibitory postsynaptic action within an oscillation cycle has also been observed in experiments with slice preparations in vitro [16, 30]. In those experiments a spike histogram in time bins of one ms has been created in order to measure the action potential probability. This quantity corresponds to $a(t)$ in our model and during population oscillations it is never zero but always in phase with the membrane potential in our model as well as in the in vitro experiments. Thus our assumption on the underlying mechanism is well supported by these experimental results.

In this case, where $r{=}0$, the neurons of our model do not have oscillatory properties. Thus obviously the synchronizing mechanism must be the inhibitory action in the network and phase resetting through excitatory coupling does not apply here. The contribution of the excitatory couplings to synchronized firing of the population is rather that they increase the speed of the chain reaction in the network and thus increase the synchrony of the neurons.

The oscillatory dynamics described above lacks two characteristic features of epileptiform activity. Further we would like to see the following phenomena (cp. section 1.2.2).

- A lower frequency of the regular population oscillations.

- A spontaneous onset of the hypersynchronous activity out of otherwise fluctuating network activity.

- So called "bursts", these are sequences of multiple action potentials rapidly fired by a single neuron with a frequency of about 200Hz.

Spontaneous synchronization and the frequency shift will be investigated in sections 4.3, 4.6.3 and 4.8. The high frequency oscillations of burst discharges are a consequence of a long lasting compound network EPSP and the reduced spiking frequency due to the refractory period, which will be shown in the next section.

The role of the refractory period

The refractory period in a real neuron is part of the complex mechanisms of an action potential (cp. section 1.1.3). These intrinsic mechanisms appear implicitly in the Hodgkin-Huxley model and its derivatives (cp. section 2.1.1). Whereas many continuous models include a detailed description of the exact dynamics of the recovery process, in our discrete model the refractory period is nothing but some idle time of each neuron after it has fired an AP. We assume that on the network level this will be all that counts and we remark here again that the reduction of action potential dynamics is one of the essential simplifications of our model.

On the single neuron level the effect of the refractory period is a decrease of the maximal frequency of action potential firing. Below we enlist the implications on the dynamics of the neural population.

- The introduction of the refractory period results in a noticeable decrease of the average activity and the amplitude of the oscillations. This is intuitively clear, as the neurons can only fire once in $r + 1$ time steps. Thus the average activity is lowered to a more realistic level around $0.1N$ whereas it is unnaturally high without a refractory period.

- The mechanism of the slow population oscillations is not changed, nevertheless another oscillation of a higher frequency is superimposed (see figure 4.5).

- In the oscillating regime population oscillations of a second frequency $f \approx 1/(r + 1)$ are apparent in the dynamics of $a(t)$. Looking at the time course of $a(t)$ in figure 4.5 we see that population spikes are situated on top of a slow wave of activity. The rapid increase of $a(t)$ after the suppression of the network initiates synchronous firing of the neurons with the frequency $f = 1/(r + 1)$ which is determined by the duration of the refractory period. The amplitude of this fast oscillation decays quickly.

These population bursts are believed to underlie epileptiform sharp waves in the EEG and fast ripples in local field potentials which are measured in slice preparations in the intercellular

space. Fast ripples are intermittently occurring high frequency oscillations (200-500Hz) which occur in epileptic patients and rat models of epilepsy [13].

On the single neuron level a paroxysmal depolarization shift, i. e. a long lasting depolarization composed of many EPSP from different source neurons which induces a burst of several action potentials can be observed (cp. figure 4.10 in section 4.3).
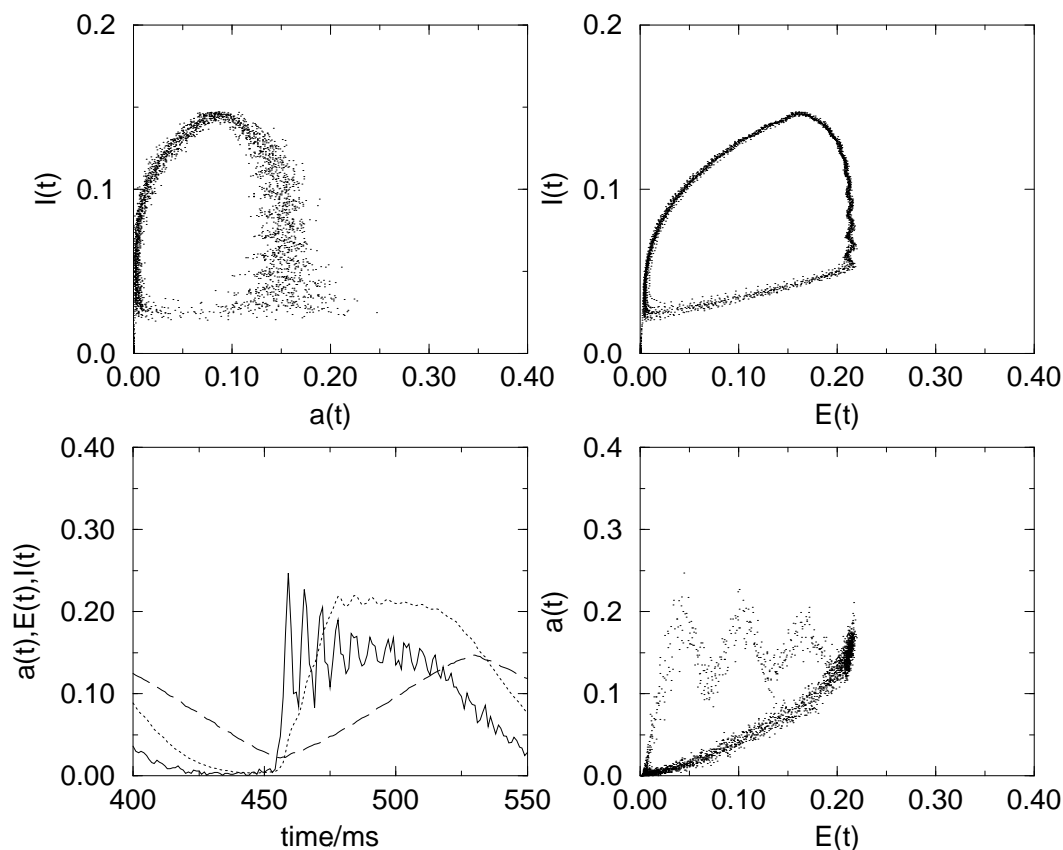

Figure 4.5: The sequence of spikes and postsynaptic potentials are presented in the same way as in figure 4.4. Except for $r=5$ the parameters are not changed. Due to the refractory period the activity $a(t)$ is apparently lower, further another type of oscillation with a high frequency is superimposed.

4.2.1   Why inhibition leads to synchronization

This section wants to give a qualitative explanation why the transition to synchronous network activity occurs when the inhibition in the network is strengthened. The basic idea is that a long duration of single IPSPs, a high inhibitory connectivity and also a high amplitude of single IPSPs sharpen the onset and decay of the cumulative inhibition $I(t)$ and thus contribute to the synchronization among the neural population.

Our model is complex and for that reason an accurate analysis is not possible. Thus this will be rather a demonstrative explanation with crude simplifications than a mathematical analysis.

We assume that the chain reaction of action potential firing within an oscillation cycle is a stochastic process which depends in some subtle manner on $E(t)$ and $I(t)$ which we do not know. For this consideration we will just use that $E(t)$ accelerates the increase of $a(t)$ whereas $I(t)$ decelerates the increase of $a(t)$. Thus we want to assume the following hypothetic refinements of the mechanism of the population oscillations from the last section:

- The trigger for the chain reaction of AP-firing within an oscillation cycle is that $I(t)$ ceases below some threshold $I_{\min}$. When $I(t)$ exceeds this threshold the activity in the network will be suppressed.

- The rapidness of the chain reaction which is represented by the slope $\Delta a(t)/\Delta t$ in cycle j is decreased by any remaining network inhibition from the preceding cycle, i. e. when $I(t)$ is decaying slowly.

The first hypothesis is supported by our observations from figures 4.4 and 4.5. The second hypothesis is supported by comparative measuring of the slopes $\Delta I(t)/\Delta t$ and $\Delta a(t)/\Delta t$ in the subsequent cycle in simulations which yielded varying oscillations. The measurements showed that the slope of $I(t)$ and the slope of $a(t)$ in the subsequent cycle are related by a power law with exponent 1.5. Figure 4.6 shows an epoch of an unsteady oscillation in which it can be seen that a slow decay of $I(t)$ and thereafter a slow increase of $a(t)$ precede a desynchronous period.

In the following we will argue that a fast increase of activity in the neural network at stage one will induce a fast decay of $I(t)$. Together with our assumptions this constitutes a feedback mechanism: A fast decrease of $I(t)$ leads to a fast increase of $a(t)$ and vice versa.

We constitute a very simplified mathematical model which describes the transition from fluctuating to oscillating behavior due to increasing values of δ_i.

Let us have a look at a single volley of action potentials and define the synchrony within the volley via the dispersion of the time steps at which action potentials are fired. We assume that the time points of firing events follow a Gaussian distribution with standard deviation
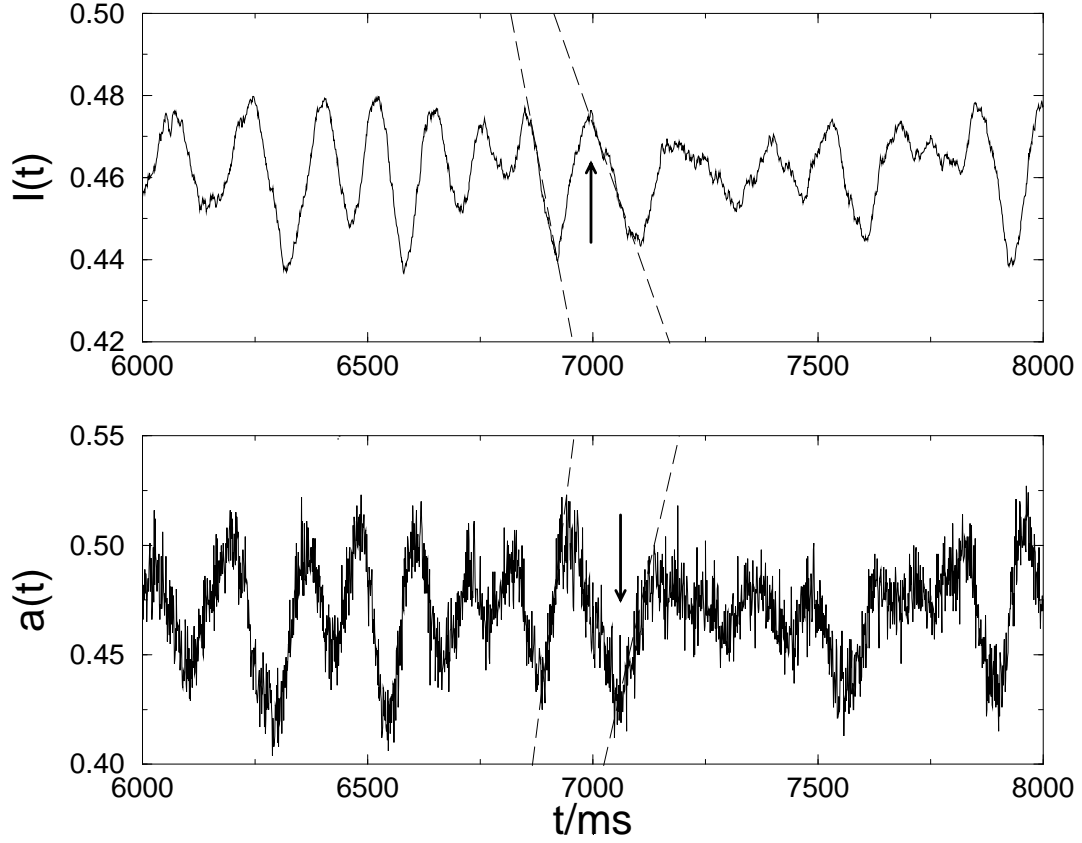
Figure 4.6: The slow decay of $I(t)$ (arrow in the upper frame) in turn decelerates the subsequent rising edge of the activity (arrow in the lower frame). A short desynchronous period follows. Again $a(t)$ and $I(t)$ have been normalized as described in the caption of figure 4.4.

ϕ which represents the jitter (temporal scattering) of the action potentials of the volley. The time course of the accumulated inhibition in the network is then given as the convolution of the time course of a single IPSP and the temporal distribution function of firing events.

In our model the IPSPs have the shape of a square pulse of height σ_i and duration δ_i, a single IPSP triggered at $t=0$ is thus described by the following function.

$$\sigma_i \chi_{[0,\delta_i]} \tag{4.3}$$

The temporal distribution of action potential firing events is given by the following probability density whereby ϕ has the dimension time.

$$f(t) = \frac{1}{\sqrt{2\pi}\phi} e^{-t^2/2\phi^2} \tag{4.4}$$

The number of synapses $N\kappa_i$ and σ_i which will enter the network inhibitory postsynaptic potential $I(t)$ as a multiplicative constant will be omitted in the following. Of course, a

discrete calculation would be appropriate as in this context the model underlies discrete time. Nevertheless we will use continuous time in the following calculation. Then $I(t)$ is given by the convolution of (4.3) and (4.4).

$$I(t) = \int_{t-\delta_i}^{t} f(\tau)d\tau \qquad (4.5)$$

The slope of the rising edge of $I(t)$ can be approximated by $I'(0)$

$$I'(0) = \frac{1}{\sqrt{2\pi}\phi}(1 - e^{-\delta_i^2/2\phi^2}) \qquad (4.6)$$

The shape of such a cumulative IPSP depends on δ_i and ϕ, examples are shown in figure 4.7. An increase of ϕ decreases the slope of the rising edge whereas an increase of δ_i increases the slope. Raising δ_i thus might stabilize synchronous firing which will otherwise be destroyed by sources of jitter in the neural network.
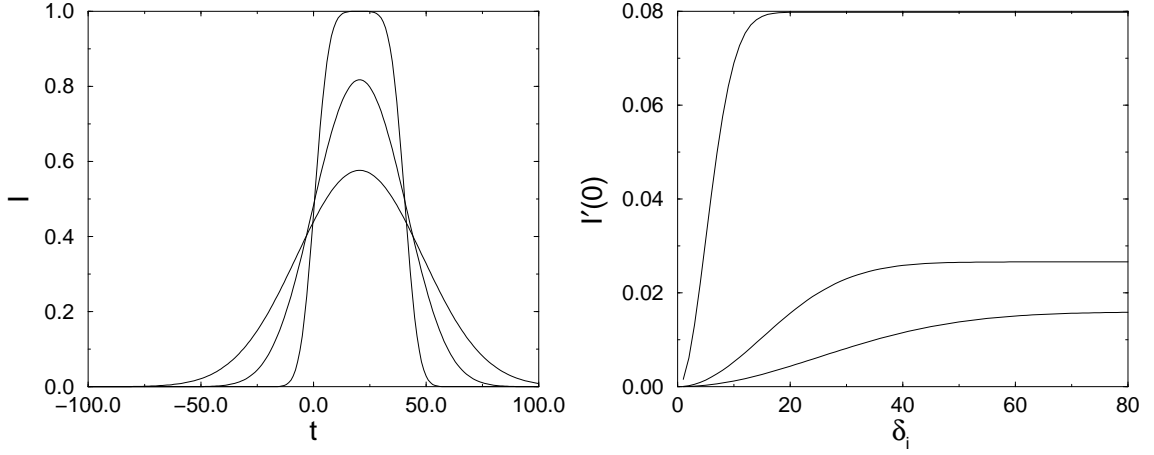
Figure 4.7: Left: examples of $I(t)$ for different values of jitter $\phi = 5, 15, 25$ and $\delta_i = 40$. Right: maximal slope vs. δ_i for $\phi = 5, 15, 25$ (from top to bottom).

A simplified model shows indeed a transition at some value of δ_i: Let s_j denote the maximal slope of the rising edge of $I(t)$ in the jth cycle of an oscillation. We now assume that the jitter which is induced in the subsequent volley of action potentials is reciprocally coupled to that slope. Further we add some constant ϕ_{int} which represents the jitter which is caused by the random sequential update (cp. section 3.1). Then equation (4.7) holds.

$$\phi_j = 1/s_j + \phi_{\text{int}} \qquad (4.7)$$

Now the maximal slope of the rising edge of $I(t)$ in the next cycle s_{j+1} can be approximated by equation (4.8) where the slope given by equation (4.6) is multiplied by some constant

α which represents the influence of the number of inhibitory synapses per neuron and the amplitude of a single IPSP.

$$s_{j+1} = \alpha \frac{1}{\sqrt{2\pi}\phi_j}(1 - e^{-\delta_i^2/2\phi_j^2}) \qquad (4.8)$$

For $\alpha = 3.5$ and $\phi_{\text{int}} = 2.0$ we can see that for small values of δ_i only $s^*=0$ is a stable fixed point whereas for larger values of δ_i another stable fixed point appears which corresponds to a synchronous population oscillation, see figure 4.8.
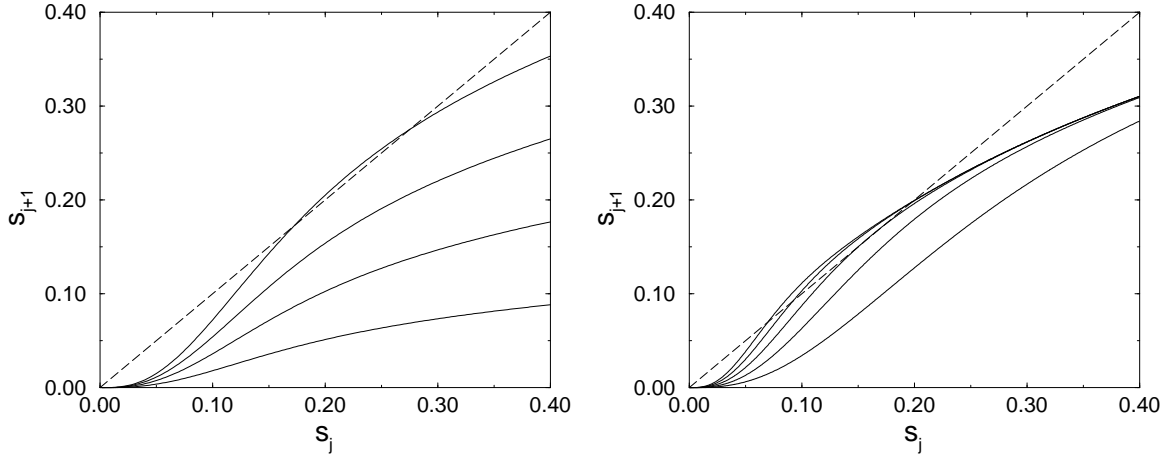
Figure 4.8: Left: Increasing α leads to nonzero stable fixed points when δ_i is kept fixed, this corresponds to increasing κ_i or σ_i. Here α=1,2,3,4 and δ_i=15. Right: Also increasing δ_i can induce oscillations (cp. section 4.5). Here δ_i=10,15,20,25,30 and α=3.5, in all graphs ϕ_{int}=2.

4.3   Spontaneous synchronization

In most in vitro experiments with slice preparations the transition from normal to epileptic behavior is induced by the addition of neuromodulators. An interesting question is whether we can find spontaneous switching of the dynamics of a model neural network from fluctuating to oscillating behavior which is a sign for bistability. The term "spontaneous" means that the change of the dynamics occurs without a stimulus and without changing any parameter. We expect to find such a behavior close to the border between the fluctuating and the oscillating regime.

In real brains as well as in our model random fluctuations can trigger the change of the dynamics from fluctuating to oscillating and back. A long time computer simulation of seven hours simulated network activity yielded that the system spent half of the time in each of the two dynamical attractors. Figure 4.11 shows that the durations of the seizures and that of the

normal periods follow exponential distributions which indicates that the transition between the two regimes is triggered with a constant rate.

A mechanism which might be responsible for the end of the seizure in real brains is that with some time delay the ongoing oscillating dynamics themselves change the circumstances which initiated the oscillations. One can think of exhaustion of transmitter reservoirs in certain types of synapses or that on a longer time scale of e. g. a minute the concentration gradients of various ions are altered due to the rhythmic firing.

Figure 4.9 shows the spontaneous change to synchronous population activity. Looking at a single neuron does not tell us that a dominant oscillation of 26Hz is present, a particular neuron may fire as well in the valleys of population activity. Rather the action potentials are stochastically concentrated at the periodic maxima of field potential oscillations. The fact that population oscillations can not be observed when one is looking at a single neuron is also known from computer simulations of continuous models of neural networks [84]. Interestingly, with the onset of the seizure epoch even a single neuron may exhibit a change of its firing behavior from firing isolated spikes to burst discharges which is characteristic for epileptiform behavior of the network (see figure 4.10). The phenomenon of intermittently occurring synchronization can be found in many simulations where parameters are right at the transition border between the oscillating and the fluctuating regimes.

Nonlinear time series analysis of simulation data

As in recent years the methods of nonlinear time series analysis applied to EEG data of epilepsy patients continuously gained attention, we applied the estimation of the autocorrelation dimension to epochs of the "seizure" and the low amplitude activity. The method has been introduced to measure the dimension of strange attractors [37] and has later been applied to EEG time series of epilepsy patients before and during seizures [5]. The estimated autocorrelation dimension has been found to significantly decrease with the onset of an epileptic seizure, which suggests that the brain activity becomes "less chaotic". A detailed description of the methods will be omitted here.

Figure 4.12 shows reconstructed attractors of the dynamical system obtained by embedding a seizure epoch and a normal epoch into two-dimensional space using delay coordinates, i. e. plotting $a(t)$ vs. $a(t + \tau)$. The hole in the middle of the plot of the seizure epoch suggests that the dynamical system might show low-dimensional chaos. Here the attractor is close to a limit cycle.

The D_2-values shown in figure 4.12 were obtained using the TISEAN software package [42]. Similar to the analysis of true epilepsy EEG time series [73] the plateau at $r \approx 160$ indicates an effective D_2-value between 1.5 and 2 for the seizure epoch whereas the value can not be estimated for the normal epoch where the dimension of the attractor is assumed to be higher.
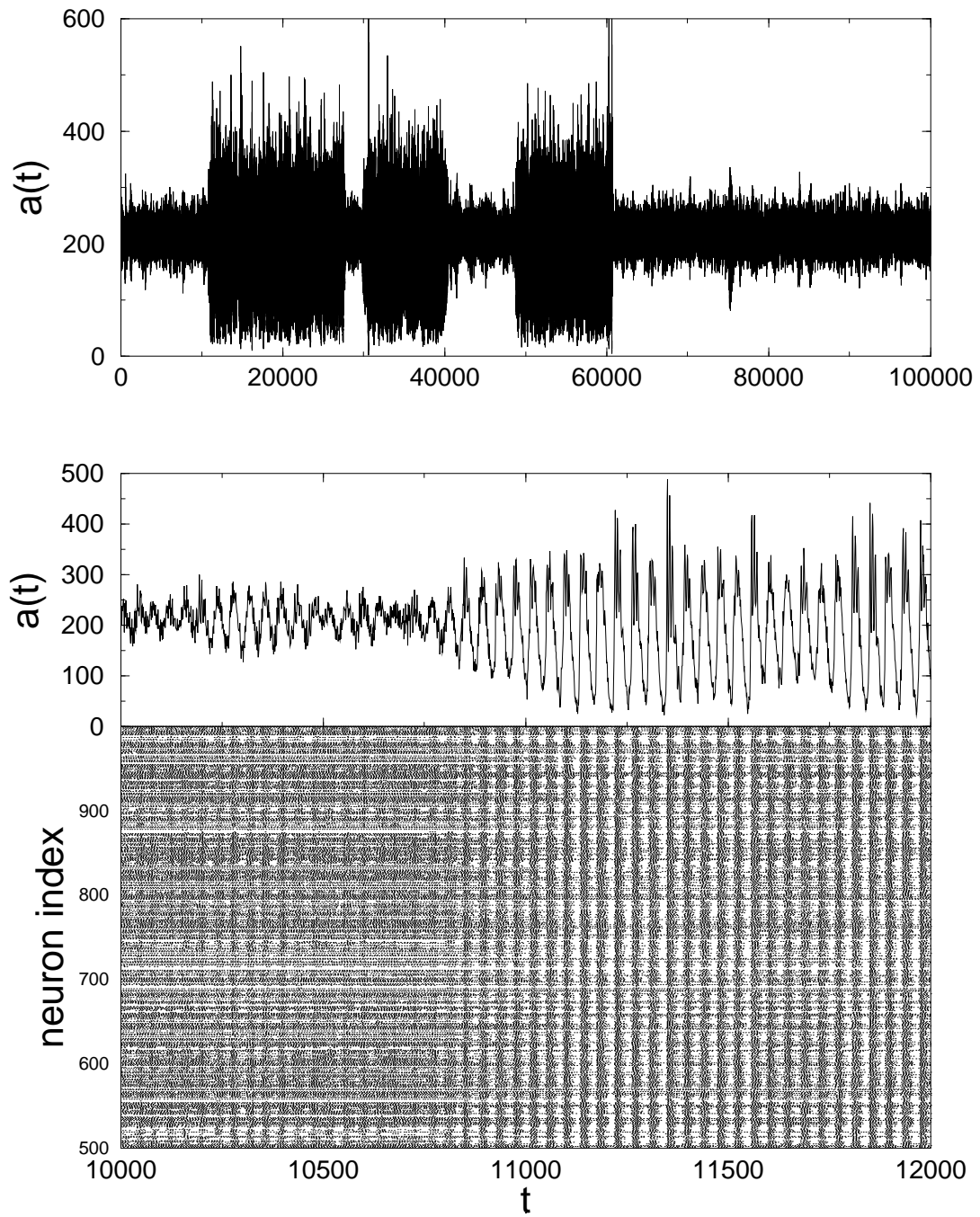
Figure 4.9: Top: The system switches between oscillating and fluctuating dynamics. Bottom: A raster plot of the onset of the first "seizure" shows the time steps at which action potentials are fired for 500 neurons of the network. The synchronization and the transition to the firing of burst discharges can be seen. The number of spikes per burst varies among the population and different cycles. Parameters are $(\kappa_e, \kappa_i) = (80,32)$, $(\delta_e, \delta_i) = (10,20)$, $(\sigma_e, \sigma_i) = (20,120)$, $r = 5$, $N = 2\,000$.
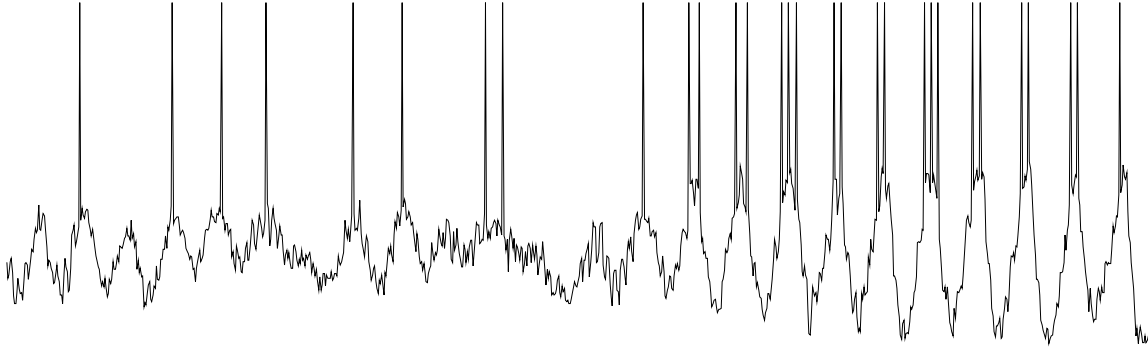
Figure 4.10: Here the oscillations of the membrane potential are shown, a spike is pasted on top when an action potential is fired. During normal activity APs are fired irregularly. With the onset of the synchronized firing the slope of the membrane potential increases and the neuron is entrained in the population oscillations and fires burst discharges which are characteristic for epileptic seizures. Data from the simulation shown in figure 4.9.
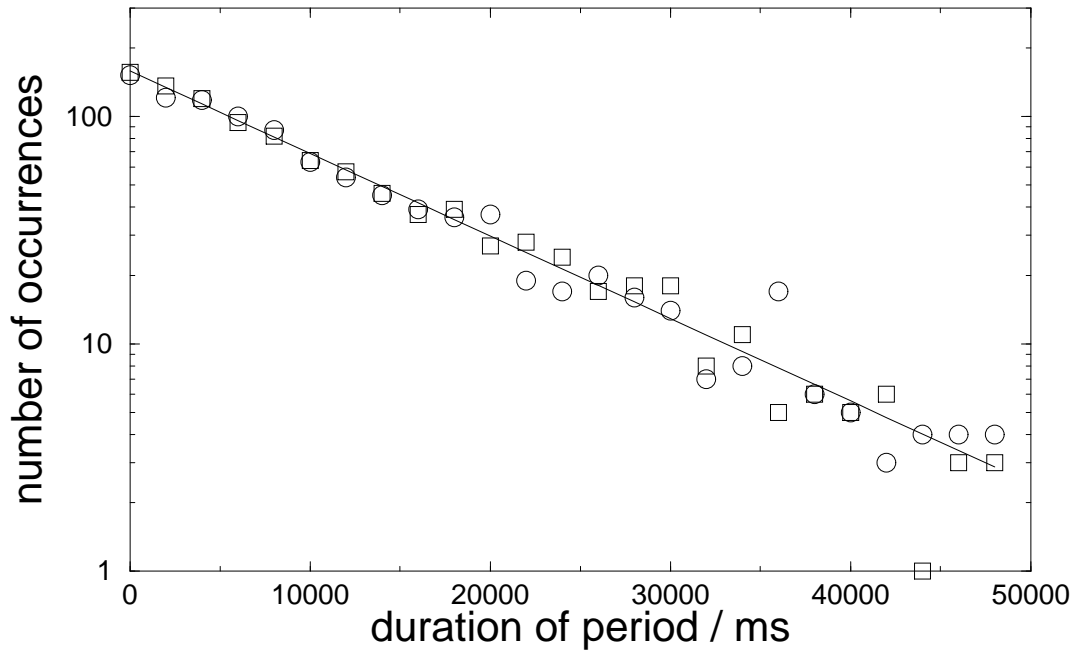
Figure 4.11: The durations of normal periods (circles) and seizures (squares) follow exponential distributions.
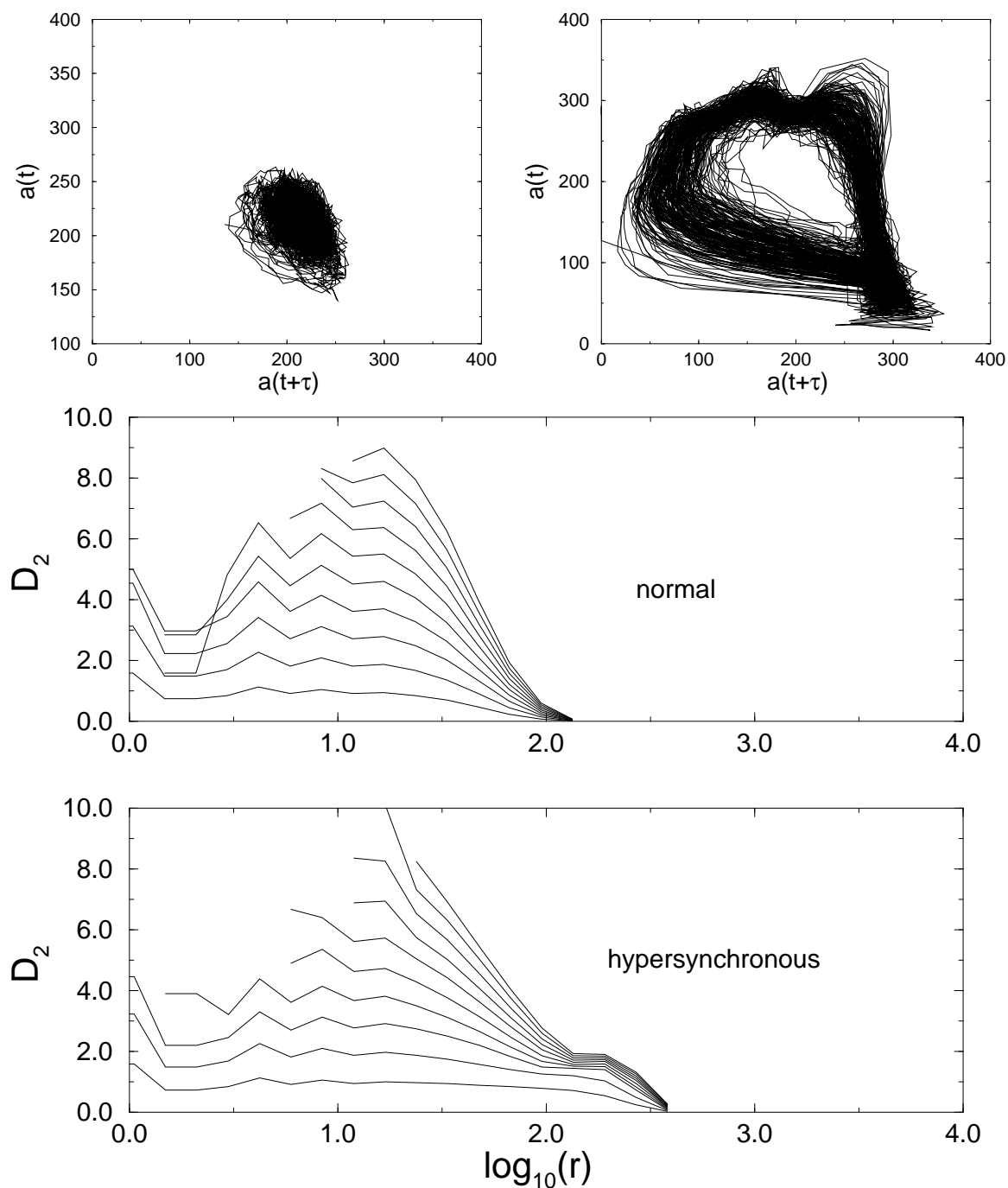
Figure 4.12: Top: Epochs of normal activity (left) and hypersynchronous activity (right) have been embedded into two-dimensional space using delay coordinates with $\tau=14$. The "epileptic" epoch exhibits the conjectural fingerprint of low-dimensional chaos. Bottom: An estimation of the autocorrelation dimension yields $D_2^{\text{eff}} \approx 2$ in the synchronous epoch whereas D_2^{eff} is higher in the normal epoch. The data correspond to figure 4.9.

4.4 The dependence on network parameters

This section illustrates how alterations of the connectivities and the network size change the systems dynamics. The main results are listed below:

- An increasing number of inhibitory synapses leads to the transition from the fluctuating to the oscillating regime.

- The absolute number of synapses originating from a single neuron determines the regime, not the relative fractions κ_e and κ_i.

- When the number of excitatory synapses per neuron is low only a smaller subnetwork is active in which the network parameters are different from those of the whole network.

- With increasing system size the sensitivity of the network dynamics to the details of synaptic wiring decreases.

- In large systems with sufficiently many synapses the border of the oscillating regime in the κ_e-κ_i-plane is roughly characterized by a linear equation $\kappa_i^c \approx \alpha \kappa_e + \beta$.

4.4.1 The dependence on connectivities

Figure 4.13 shows where the regimes are located in the κ_e-κ_i-plane. In this context the contents of the previous section is a closer look at an intersection through the graphs in figure 4.13. Now we can also see the influence of the κ_e-parameter. Remarkable in figure 4.13 are the following observations:

- The shape of the borders between the regimes in the κ_e-κ_i-plane remain the same if we alter the system size. Note that the κ-values scale reciprocally with the system size. Thus the underlying regime of the network dynamics appears to be dependent on absolute numbers of synapses rather than on the relative connectivity parameters.

- The oscillating regime, where $D(a(t))$ is large, i.e. the neurons fire synchronously, is situated between the flat regime and the fluctuating regime.

- In the domain where the number of excitatory/inhibitory synapses is below 50/75 we see a strange bump. This means that in this region of parameter space the transition from the oscillating to the flat regime is counterintuitively achieved by increasing the number of excitatory synapses. This effect is explained in section 4.4.3.

We will now determine the critical value $\kappa_i^*(N, \kappa_e)$ at which the transition between the oscillating and the flat regime occurs. Of course this value also depends on the other model parameters, but we will keep δ, σ and r fixed. To estimate this critical value of inhibitory
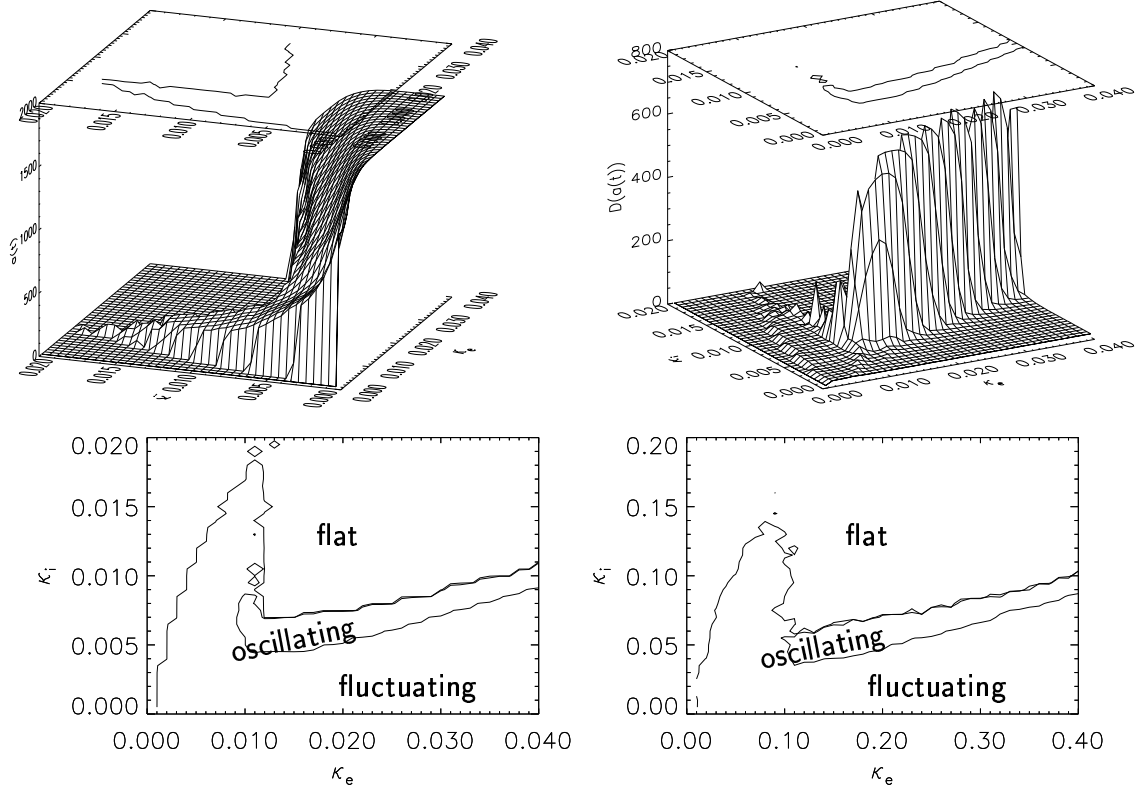
Figure 4.13: The upper graphs show $\langle a(t) \rangle$ (left) and $D(a(t))$ (right) vs. κ_e and κ_i. The other parameters are $(\delta_e, \delta_i) = (15,46)$, $(\sigma_e, \sigma_i) = (20,120)$, $r=0$ and $N=5000$. Results have been averaged among four initializations with different RNGSs. The lower graphs show phase diagrams for $N=5000$ (left) and $N=500$ (right).

connectivity, for each pair (N, κ_e) we run several simulations, where κ_i starts at a small value and is then successively raised until inhibition is too strong that any autonomous firing activity could be autonomously maintained by the network. The first value of κ_i for which network activity has ceased 50 time steps after initialization is the first step into the domain of the flat regime and thus an upper estimation of the critical value. This procedure is repeated 20 times with different RNGSs and we calculate the mean value which we denote by $\overline{\kappa_i^*}$.

A network was classified as "over-inhibited" if $a(t = 50) < 3$. Usually after 30 time steps the activity in an over-inhibited network had ceased although a small rest of a few neurons still blinking for some longer period occasionally occurred. In order to test if the above criterion is suitable, the tracing was also done in reversed order. Starting with high values of κ_i the parameter was decreased until $a(t = 50) \geq 0.02N$ to determine $\underline{\kappa_i^*}$. The difference of $\underline{\kappa_i^*}$ and $\overline{\kappa_i^*}$ was below 3% when using a κ_i-step of 0.001. In the following we only estimated $\underline{\kappa_i^*}$ for
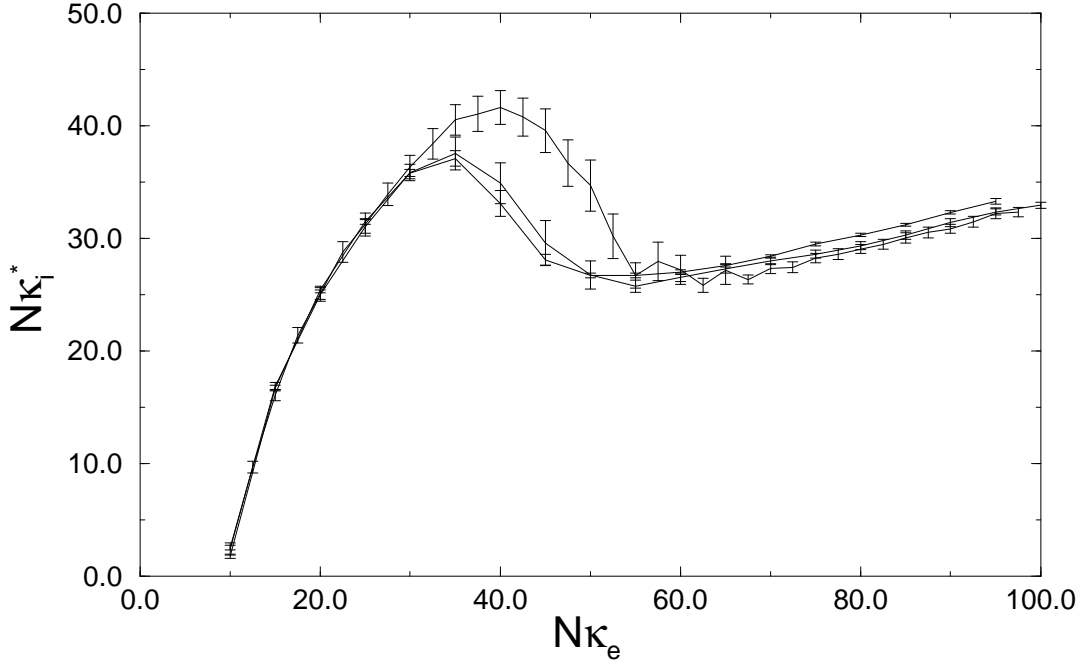
Figure 4.14: The dependency of κ_i^* on κ_e shows a bump in the range of low connectivities. The connectivity values have been scaled with the system size N, thus the values on the axes correspond to the average number of synapses per excitatory/inhibitory neuron. The number of neurons is N=500, 1 000, 10 000 (from top to bottom). The other parameters are (σ_e, σ_i)=(20,120), (δ_e, δ_i)=(7,20), r=0.

larger networks in order to save computing time[2] .

Figures 4.14 and 4.15 show the results from a couple of such trace runs. The bump in the region of low connectivities will be explained in the following section. Further we observe that with increasing N as well as with increasing r a linear relationship $\kappa_i^*(\kappa_e) \approx \alpha \kappa_e$ is approximated. Thus in the case of large systems ($N \geq 5\,000$) with a realistic refractory period of five or six milliseconds the ratio κ_e/κ_i is a suitable value to distinguish between the flat and the active regimes.

4.4.2 The dependence on system size

The following list summarizes the effects that occur with an increasing number of neurons:

- The transitions between the regimes are bound to *absolute* numbers of excitatory and

---

[2]The computing time for simulations of our model with an event related implementation increases linearly with the activity $a(t)$. Thus simulation runs of over-inhibited networks are very fast.
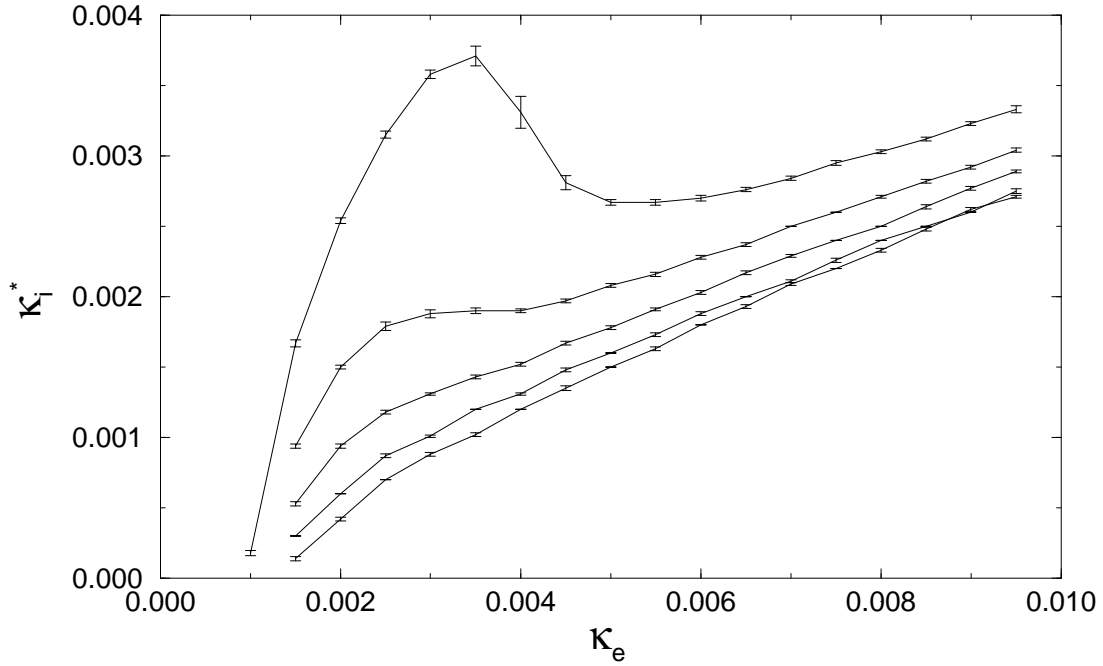
Figure 4.15: With increasing duration of the refractory period the bump vanishes and the linear approximation becomes more accurate. $N{=}10\,000$, $r{=}0,1,2,3,4$ (from top to bottom). All other parameters are as in figure 4.14.

inhibitory synapses. Thus, to stay in the same regime when N is altered, one has to adjust the connectivities accordingly: $\kappa_e \sim 1/N$ and $\kappa_i \sim 1/N$

- When the numbers of synapses and other parameters are kept fixed $\langle a(t) \rangle$ is proportional to N, whereas $D(a(t))$ is roughly proportional to $\sqrt{N}$ (see figure 4.17).

- The dispersion of values obtained from different random initializations with the same parameters slightly decreases with larger numbers of neurons (see figure 4.18).

Simulations of a few individual networks of different sizes whereby inhibitory synapses have been successively added failed to show an increasing slope of $D(a(t))$ in the region of the transition which would be characteristic for a sharp first-order phase transition (see figure 4.18).

4.4.3   Percolation effects in neural networks: The bump

When the number of couplings in the networks is small, the counterintuitive effect may occur that the addition of excitatory couplings can extinguish the autonomous activity in the
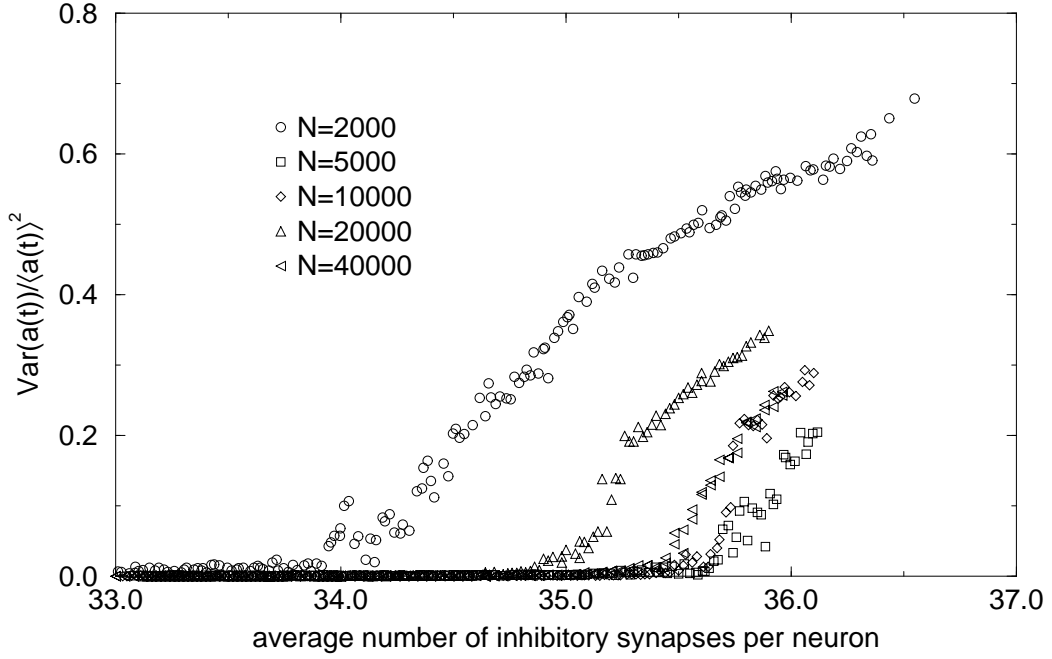
Figure 4.16: For better comparability of differently large systems we plot $D^2(a(t))/\langle a(t)\rangle$ vs. the average number of synapses per neuron. The critical number of inhibitory synapses per neuron scatters for differently wired networks. Here the transition is sharpest for N=20 000.

network. This can be seen in the previous section where the border between the regimes in the κ_e-κ_i-plane has a bump. Actually, this bump gives us an example of possible anomalies due to fluctuations in the synaptic connectivity. This finding could apply to experiments with slice preparations in vitro where the connectivity within the neural tissue is reduced as many neurites are cut off: the thickness of a slice preparation is approximately 400μm. However, the effect does not show up when the refractory period is sufficiently high and thus it is questionable whether it has an analogy in reality. Anyway, this effect represents an interesting occurrence of self-organization, a principle which is observed in many complex systems and moreover thought to be an essential ingredient in the emergence of life [47].

The position of the bump in the κ_e-κ_i-plane also scales reciprocally with the number of neurons as we already know from section 4.4.1. Figure 4.19 shows a detailed map of the bump in a system of $N = 500$ neurons. The figure does not contain any information on the average activity, we just recorded the instantaneous activity 50 time steps after initialization. This time suffices to let activity cease in an over-inhibited network. We regard an activity of eight action potentials fired in time step 50 as threshold to distinguish between the network being still active and the other case that activity has ceased. As the bump appears in many different synaptic wirings, it is not a casual phenomenon due to some very exotic set of synaptic connections, but a true feature of the model. We can guess that the bump is due
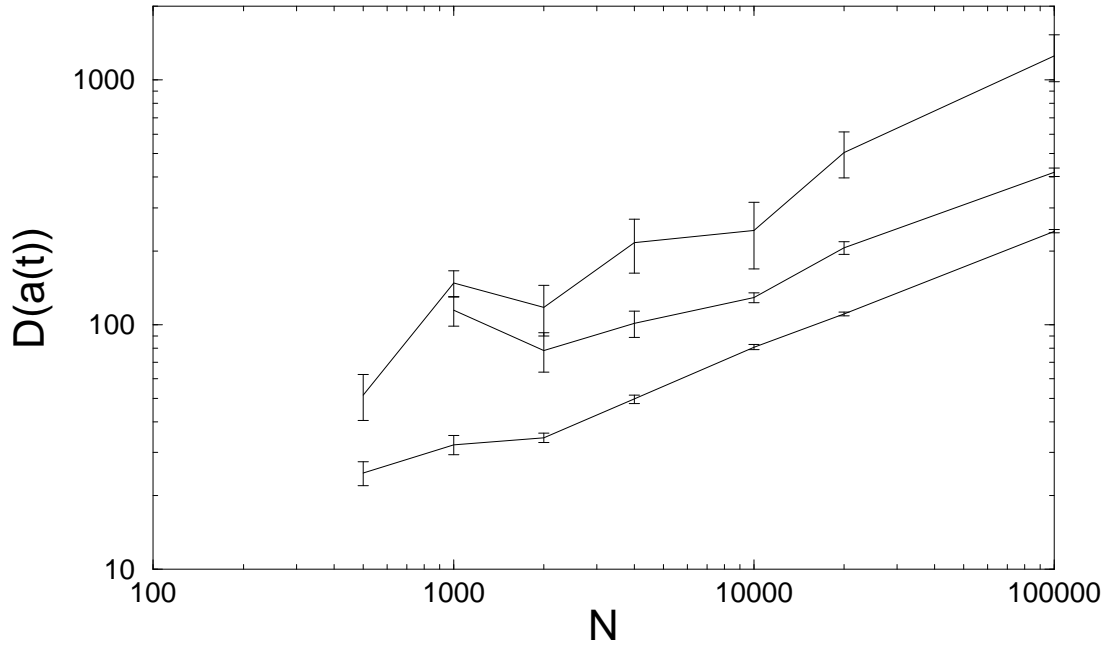
Figure 4.17: The amplitude $D(a(t))$ is roughly proportional to $\sqrt{N}$. The different graphs correspond to the different regimes shown in figure 4.3 (from top to bottom respectively). κ_i and κ_e were reciprocally scaled with N in order to stay in the same regime.

to certain properties of the organization of synaptic connections, e.g. the establishment of certain subnetworks which are decoupled (in some sense that applies here). In fact the bump does not show up, when we investigate a fully interconnected network and alter the synaptic strength as we can see in the right graph of figure 4.19, thus it is a phenomenon which is due to fluctuations in the synaptic connections.

This effect which may appear puzzling at first sight is indeed counterintuitive. The initialization of the synaptic matrix is done by comparing random numbers with the appropriate κ-value for each entry. If we use the same RNGS in each simulation, raising κ_e thus will result in the addition of extra excitatory synapses but not in the removal of any synapse which has been established in a simulation with a lower κ_e-value. Following a horizontal cross-section (κ_i fixed, κ_e increasing) which intersects the bump leads to a sequence flat-active-flat-active whereby each step corresponds to an enlargement of the set of excitatory synapses (cp. figure 4.20).

The explanation is that some percolation phenomenon is occuring here. We can imagine that in the case of low connectivity some neurons do not participate in the network activity at all. When we keep κ_i fixed at 0.3 and follow the trace which is indicated by the line in figure 4.20, the number of neurons which have fired within the first 50 time steps increases. The
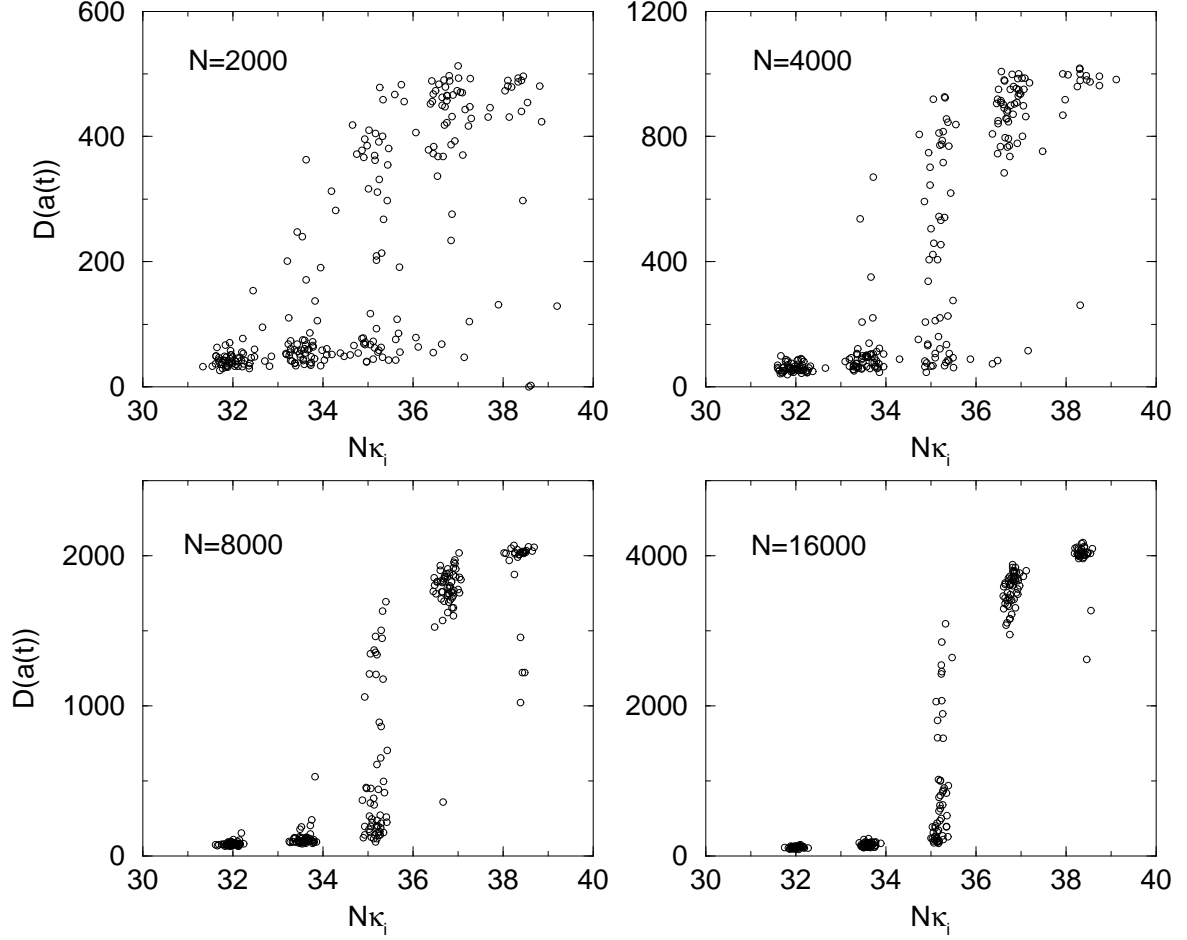
Figure 4.18: Amplitude $D(a(t))$ vs. average number of inhibitory synapses per neuron in systems with $N=2\,000,\ 4\,000,\ 8\,000,\ 16\,000$. The other parameters are $\kappa_{\mathrm{e}}=0.06,\ 0.03,$ 0.015, 0.0075 respectively, $(\delta_{\mathrm{e}},\delta_{\mathrm{i}})=(7,20),\ (\sigma_{\mathrm{e}},\sigma_{\mathrm{i}})=(20,120),\ r=0$.

number of synapses which terminate on neurons which have not fired a single action potential do not contribute to the network activity. It makes thus sense that we have a look at the active subnetwork which we will define as consisting of:

- those neurons which have been pushed over the firing threshold by a sufficient accumulation of postsynaptic potentials at least once within the first 50 time steps[3] and

- those synapses which sprout from active neurons and terminate on active neurons.

Other parts of the network do not influence its dynamics. We denote the number of neurons in the active subnetwork by N^{sub} and the fraction of inhibitory neurons calculated within

---

[3]At the beginning of a simulation run about half of the neurons are initialized as firing an action potential. These neurons do not automatically belong to the active subnetwork. Yet they may be counted when they fire again at some later instant of the simulation.
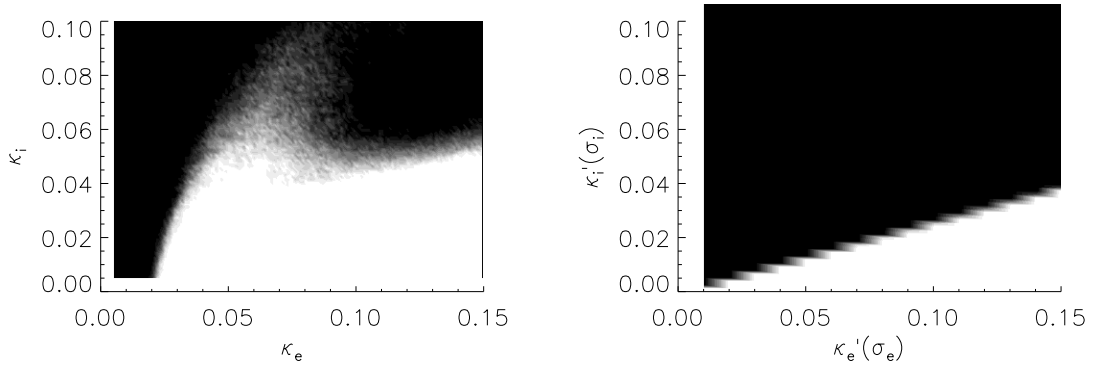
Figure 4.19: Left: the bump in a system of 500 neurons, the greyscale values give the fraction of active networks within 20 experiments with different RNGSs (white=1, black=0). Right: simulation of a completely connected network, i. e. $\kappa_e = \kappa_i = 1$. Pseudo kappa values $\kappa'(\sigma)$ have been calculated according to $\kappa' = \sigma/\sigma_{ref}$, where σ_{ref} is the corresponding fixed σ-value which is used in the left graph. The other parameters are (δ_e, δ_i)=(7,20), $(\sigma_e, \sigma_i) = (20, 120)$, r=0, N=500.

the active subnetwork by p_{inh}^{sub}. In the domain of low connectivity this fraction p_{inh}^{sub} deviates from the prescribed value p_{inh} (cp. figure 4.21). We can see that p_{inh}^{sub} is significantly lower in those networks with sustained autonomous activity, which could explain why the activity is not extinguished.

However, the formation of those low inhibited subnetworks depends on the initialization and on the sequence of the first action potentials. Obviously it turns out that a critical threshold of excitatory synaptic connectivity is needed to ignite a subnetwork which self-organizes in such a way that it is able to maintain autonomous firing of the neurons. When the number of couplings is further increased it becomes less likely that a subnetwork will remain isolated from the rest of the network.

It is difficult to determine the size of such a percolation cluster analytically. Whether a neuron belongs to the active part of the network or not depends not only on the synaptic wiring but also on the durations between incoming PSPs because of their temporal extension. With the parameters used in most of the simulations of this work a neuron requires the addition of nine EPSPs. These must arrive within a period no longer than δ_e to allow temporal summation. Additionally the situation is very sensitive to small details: An IPSP annihilates six EPSPs, thus an additional EPSP might paradoxically decrease the activity in the network when it pushes an inhibitory neuron over the threshold which was not sufficiently excited before. The determination of the size of the active cluster, and the internal (i. e. with respect to this cluster) network parameters was done with computer simulations (see figure 4.21).
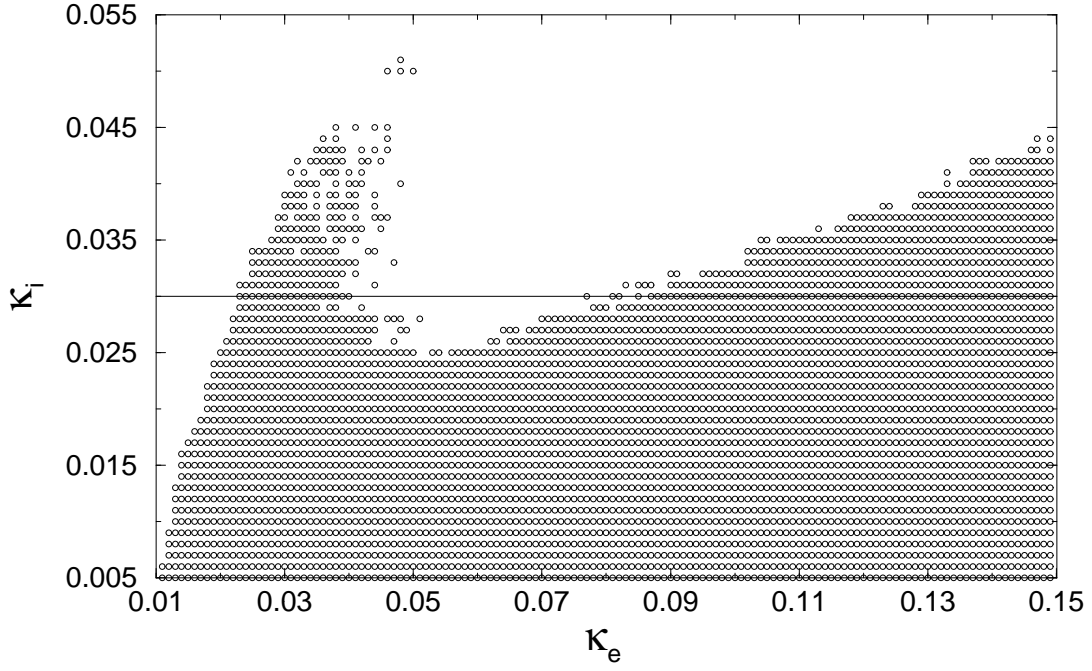
Figure 4.20: Here the RNGS is kept fixed. A symbol is placed at each pair of values (κ_e, κ_i) which showed self-sustained activity after inital firing of one half of the neurons. The line indicates the intersection which is viewed in detail in figure 4.21. The other parameters are (δ_e, δ_i)=(7,20), $(\sigma_e, \sigma_i) = (20, 120)$, r=0, N=1 000.
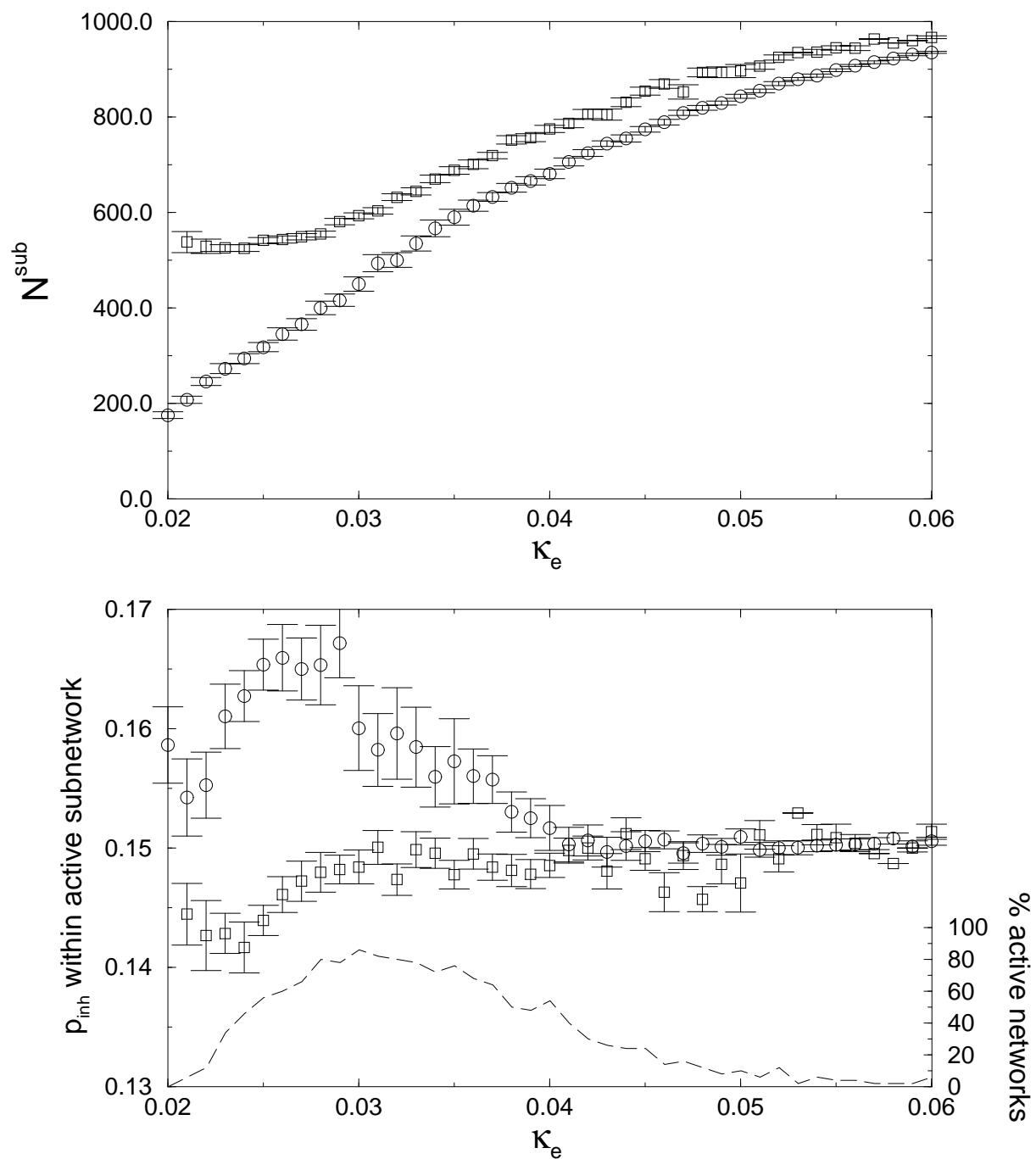
Figure 4.21: Top: The size of the active subnetwork was separately averaged among the "act-ive" cases where autonomous activity persists (squares) and among those cases where the activity ceases (circles). Bottom: The fraction of inhibitory neurons within the active subnetwork is significantly lower in the active cases. The dashed line corresponds to the right scale and gives the fraction of "active" networks among 50 samples with different RNGSs.

4.5   The dependence on synaptic parameters

The reaction of the systems dynamics with respect to changes of the synaptic parameters is especially interesting as this corresponds to the application of drugs to a neural network in vivo or in vitro, where it is not possible to change the connections. Most antiepileptic drugs and, more general, most pharmaceuticals affecting the neural system of an organism act either via activation of postsynaptic receptors, mimicking neurotransmitters and thus increasing the strength or the duration of postsynaptic potentials, or by blocking the receptors without activation of postsynaptic transmembrane currents which decreases the synaptic function (cp. section 1.1.4). The effect of blockade or activation of various excitatory and inhibitory transmitter systems onto the oscillatory behavior of the neural network has been documented in a lot of publications which are compared with the results of our model.

With respect to our results it may appear puzzling that the transition between the regimes occurs at average synapse numbers which are lower than realistic values (see section 3.2). From the data shown in this section we can see that with respect to the position of the critical values the number of synapses scales reciprocally with the amplitude of the single PSPs. Thus that the critical range in our simulations lies at 35 synapses per neuron could be due to unrealistic high PSP amplitudes.

The main results of this section are:

- The transitions from the fluctuating regime to the oscillating regime and further to the flat regime occur when inhibition is increased or when excitation is decreased either by altering the duration or the amplitude of the respective PSPs.

- When other parameters are fixed the three regimes can again be found in different sectors of the δ_e-δ_i-plane.

- Increasing the PSP-durations leads to lower frequency of oscillations which agrees very well with results obtained from in vitro experiments.

- The introduction of the refractory period reduces $\langle a(t)\rangle$ and $D(a(t))$ (cp. section 4.4.2) and the transition borders of the regimes are shifted.

- In the δ_e-κ_i-plane and the κ_e-δ_i-plane the oscillating regime is characterized by a linear relationship of the respective parameters.

- Another regime which has not been mentioned so far has been found for large δ_e and high κ_i. This regime is characterized by oscillatory dynamics and a low average activity.
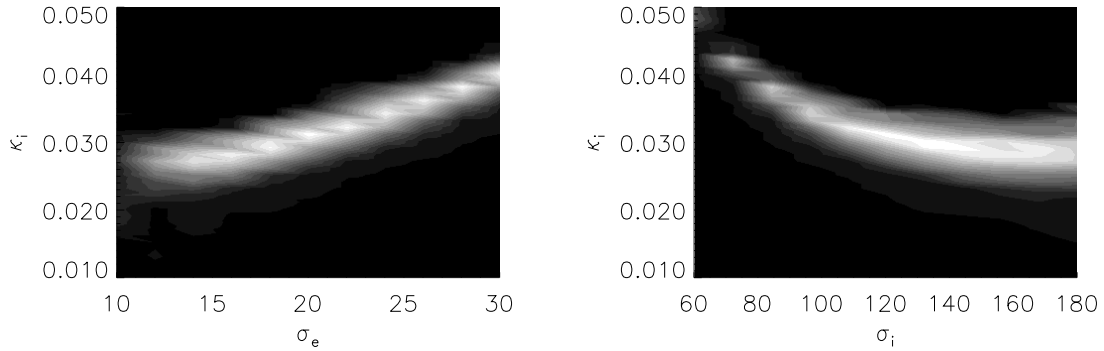
Figure 4.22: The images show the amplitude of population oscillations $D(a(t))$ averaged among ten different network initializations. The white range ($D(a(t))$ high) represents the oscillating regime whereas again we find the flat regime neighboring in the direction of higher κ_i-values and the fluctuating regime at lower κ_i-values. The parameters are $\kappa_e=0.1$, $(\delta_e,\delta_i)=(15,46)$, $r=0$, $N=1\,000$, $\sigma_i=120$ (left) and $\sigma_e=20$ (right).

4.5.1 Dependence on PSP amplitudes

The amplitude of the PSPs shifts the range of the oscillatory regime in the projection onto the κ_i-axis. Within the scanned range the dependence of the κ_i-value corresponding to the maximal oscillation amplitude on σ_e is approximately quadratic (fitting exponent ≈ 2.1) whereas its dependence on σ_i is reciprocal (fitting exponent $\approx$ -2). The data are shown in figure 4.22.

It can bee seen that below certain PSP amplitudes, whether excitatory or inhibitory, no oscillating phase is present, thus the model predicts that blocking either EPSPs or IPSPs abolishes oscillations which is agrees with in vitro experiments [16, 30].

4.5.2 Dependence on PSP durations

Figure 4.23 shows how $\langle a(t)\rangle$ and $D(a(t))$ change with increasing δ_i when δ_e is kept fixed at different values. The fluctuating and oscillating regimes are separated by a sudden increase of the slope $\Delta D(a(t))/\Delta\delta_i$. The border between the oscillating and the flat regime is characterized by the average activity. The transition is not sharp for larger values of δ_e, the δ_i-value at which the network switches off then depends sensitively on the RNGS, i.e. on the details of the synaptic wiring. The discrete steps of the $\langle a(t)\rangle$-values which have been averaged over six different networks indicate that mainly the number of active networks decreases (presumably exponentially). The border of the two regimes is thus best described by two values delimiting the range in which the networks switch off. Phase diagrams for the δ_e-δ_i-plane for networks of
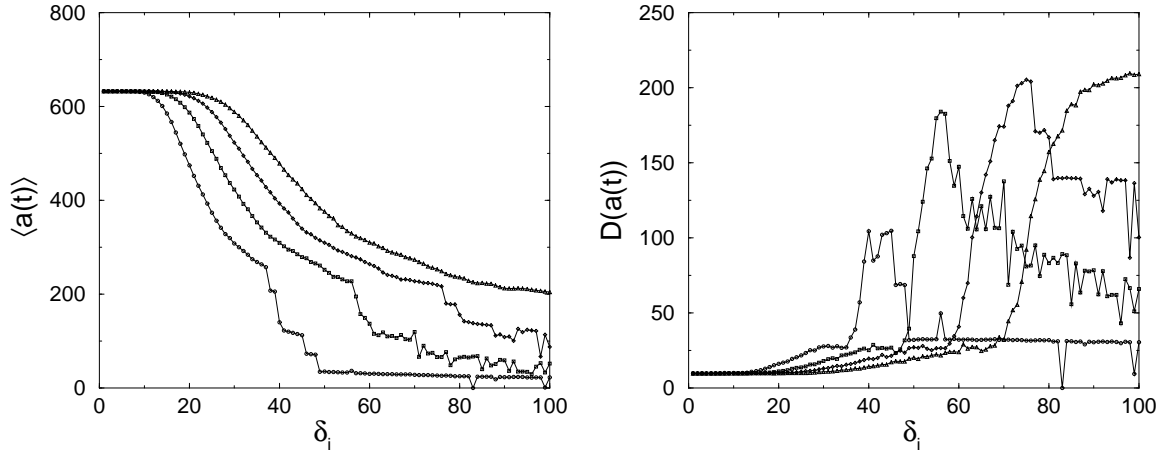
Figure 4.23: Mean activity (left) and amplitude (right) vs. δ_i for δ_e=15, 20, 25, 30 (from left to right). The other parameters are κ_e=0.06, κ_i=0.03, (σ_e, σ_i)=(20,120), r=0 and N=1 000.
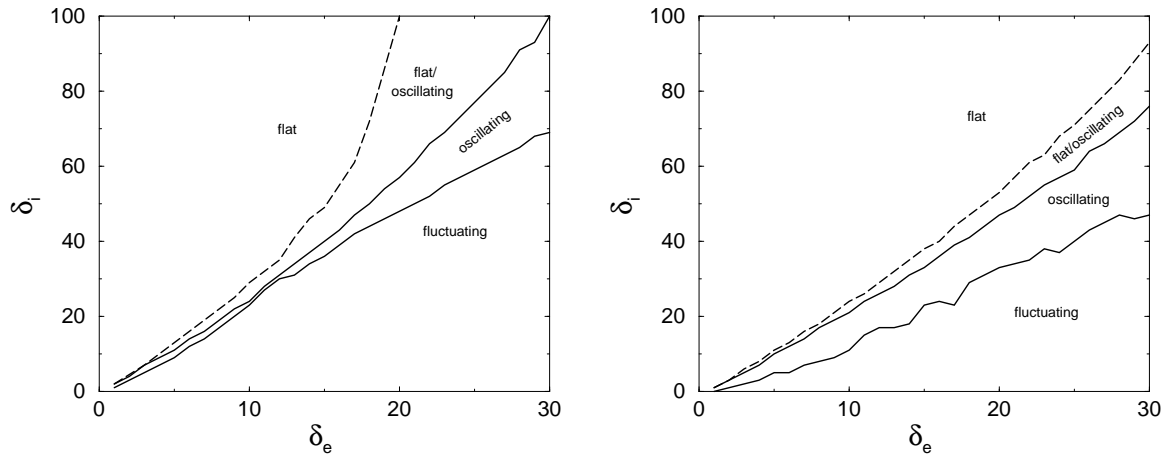

Figure 4.24: Phase diagrams obtained from scanning the δ_e-δ_i-plane for r=0 and r=2 averaged among six different networks. The data correspond to figure 4.23.

1 000 neurons and refractory periods r=0 and r=2 have been estimated with threshold criteria and are shown in figure 4.24.

Here the refractory period shifts the boundaries to lower δ_i-values and decreases the dispersion of the "switch off"-values.

4.5.3   Interdependence of synaptic and network parameters

This section investigates how the location of the regimes in the δ_e-δ_i-plane changes when the connectivities are varied.

For low δ_e-values and high κ_i-values the line which separates the oscillating and the flat regime in the δ_e-δ_i-plane is approximately linear. Analogously to section 4.1 we denote by δ_i^* the value of δ_i at which the transition from the oscillating to the flat regime occurs. The slope $\Delta\delta_i^*/\Delta\delta_e$ of this separating line has been determined in networks where the connectivity of the excitatory neurons has been varied. The results which are shown in figure 4.25 indicate that the slope of the separating line depends linearly on κ_e.

Further, as a more detailed investigation of the parameter dependencies, also the δ_e-κ_i-plane and the κ_e-δ_i-plane have been scanned.

Figure 4.26 shows that also in the δ_e-κ_i-plane the oscillating regime is characterized by a linear relation, here $\kappa_i \approx 0.25\delta_e$. Additionally, another oscillatory regime was found which is characterized by a low average activity. This "low activity, oscillatory" regime is located in the domain of long lasting excitatory PSPs.

Interestingly, the transition from the new regime to the oscillating regime is achieved by decreasing the inhibitory connectivity and further this transition is accompanied by a change of the frequency from 14Hz to 11Hz as shown in figure 4.26. Thus this transition is also a candidate for the transition from normal to epileptiform behavior. Unlike the other transitions mentioned in sections 4.3 and 4.8 this transition further brings along an increase of the average activity.
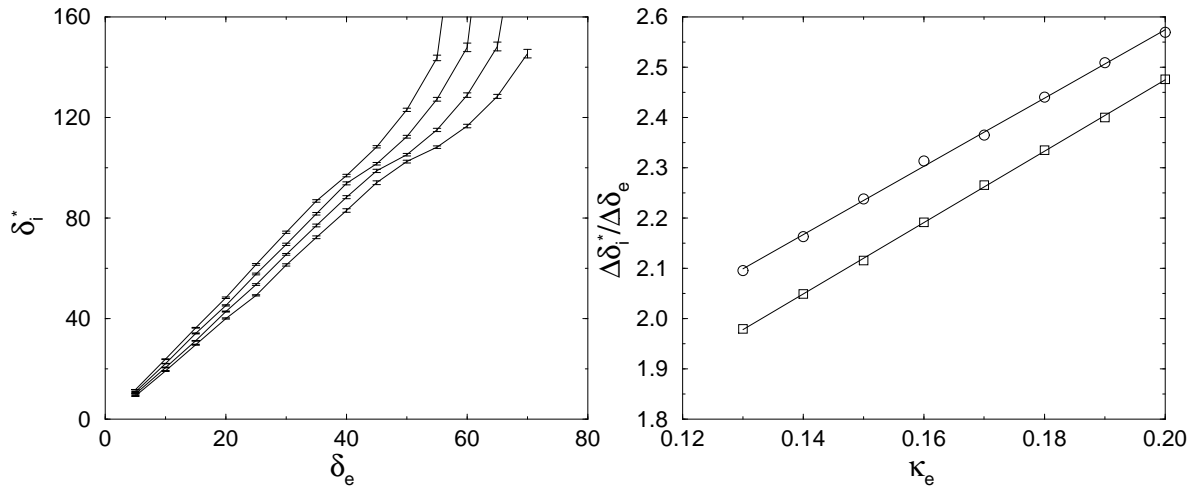
Figure 4.25: Left: For $\delta_e < 40$ δ_i^* increases linearly. κ_e=0.13, 0.15, 0.17, 0.19 (from bottom to top). The other parameters are κ_i=0.064, (σ_e, σ_i)=(20,120), r=0, N=1 000. 20 different RNGSs per δ_e-value. Right: The slope of the lines which separate the oscillating and flat regimes increases linearly with κ_e. Circles correspond to r=0, squares to r=5.
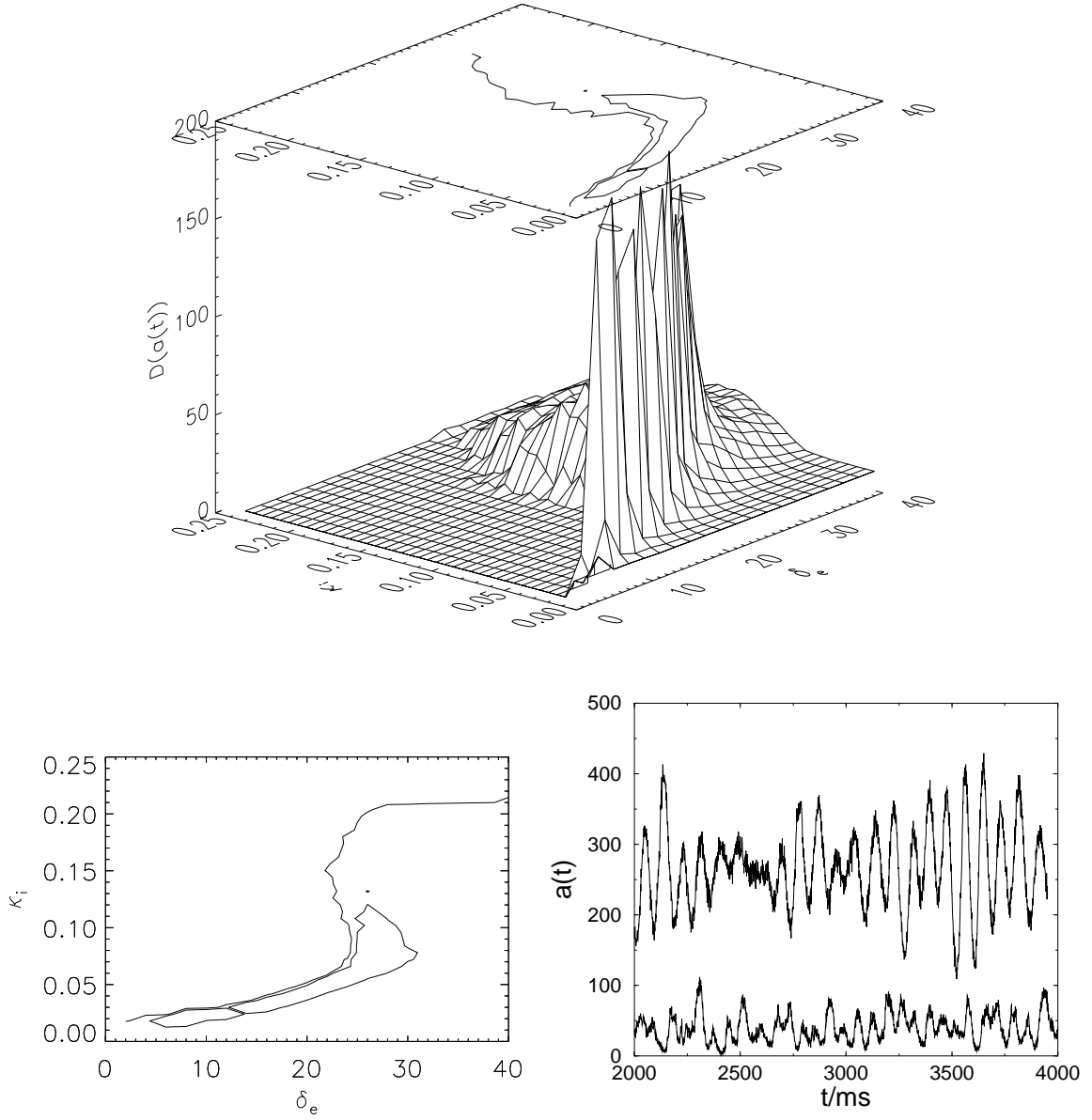
Figure 4.26: Top: For larger values of δ_e also high values of the inhibitory connectivity allow autonomous oscillations with a much lower amplitude. Parameters are κ_e=0.1, δ_i=46, (σ_e, σ_i)=(20,120), r=0, N=1 000. Bottom: The phase diagram on the left shows the location of the regimes. The examples on the right correspond to δ_e=27 and κ_i =0.066 (0.192) in the upper (lower) trace. The oscillation frequency is 11Hz (14Hz). The phase diagram is principally the same when r=2 (data not shown).
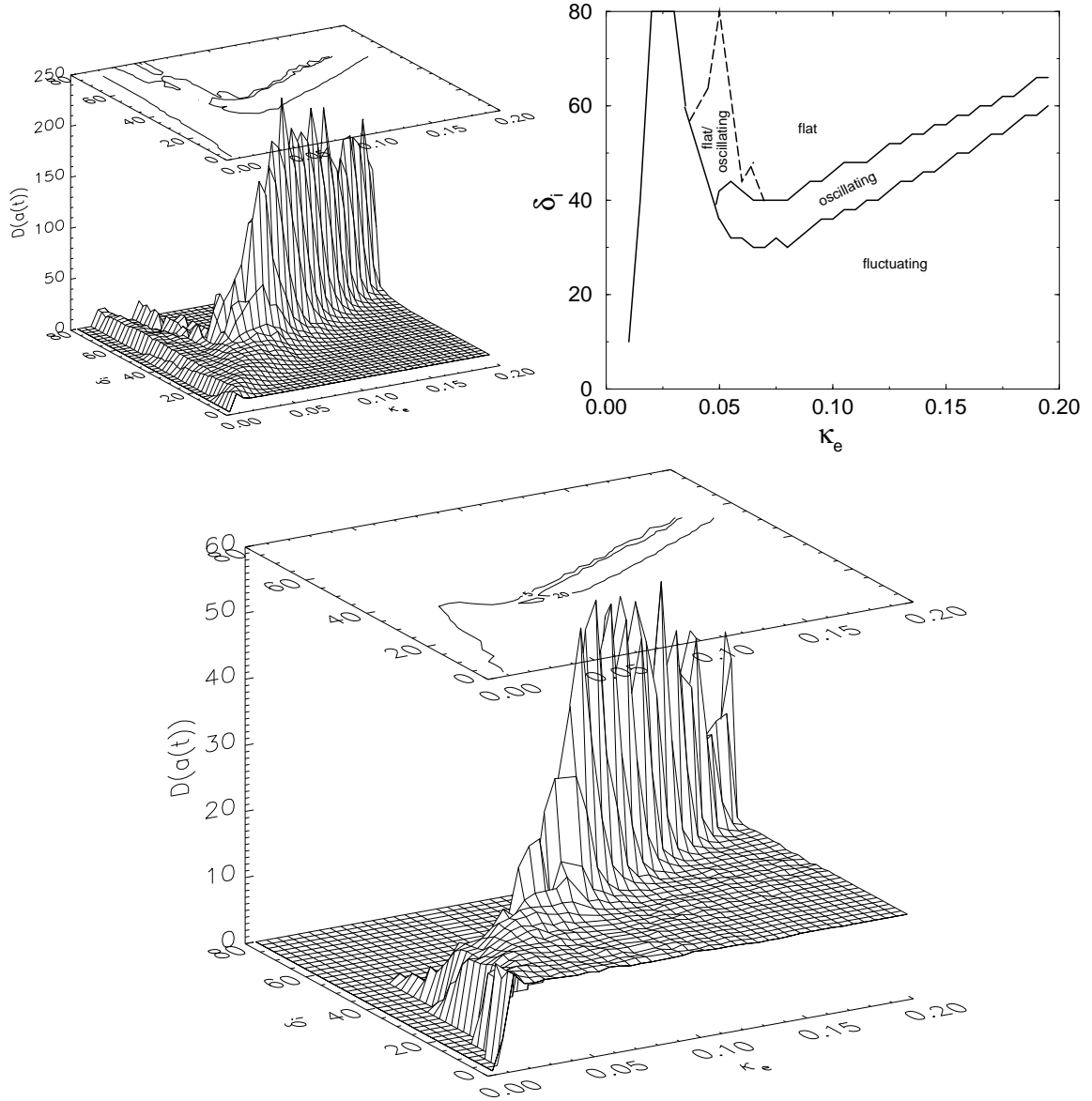
Figure 4.27: Top: The simulation results on the left, $D(a(t))$ is plotted against κ_e and δ_i, yield the phase diagram on the right. Without a refractory period a domain exists where depending on the details of synaptic wiring the networks are either flat or oscillating. Probably this phenomenon relies on the mechanism described in section 4.4.3. Parameters are $\kappa_i=0.035$, $\delta_e=15$, $(\sigma_e, \sigma_i)=(20,120)$, $r=0$, $N=1\,000$. Simulation results using eight different RNGSs have been averaged. Lower: When $r=2$ the bump has nearly vanished.

4.6 Frequency of population oscillations

In section 1.2 we have mentioned that the EEG shows oscillations of various frequencies. The frequencies differ according to the type of the stimulus (in the case that they are event related) and the location within the brain where the oscillation is measured. Further it has been suggested that oscillations of different frequencies have different functions in the cognitive processes. Although there is strong support to the hypothesis that brain waves of different frequencies have these functions described in section 1.2.1 there are many questions open concerning the brain waves. Nevertheless can they be measured and obviously the brain has to be organized in a manner that allows oscillations of different frequencies in different parts of the brain. Further, the change of the frequency of neural oscillations represents a characteristic feature of many epileptic seizures (cp. section 1.2.2).

Thus we are interested in the quantities which determine the population frequency of neural oscillations. In our discrete computer model the frequency of population oscillations is mainly determined by the temporal parameters δ_e and δ_i, their influence on the frequency of the population oscillations is highlighted in this section. Other parameters, i.e. the connectivity, PSP-strength and refractory period do not have a noteworthy influence on the frequency of population oscillations.

4.6.1 Measuring the population frequency

The frequency of population oscillations has been determined via autocorrelation function and Fourier transformation. For each parameter set and random number generator seed a sample of length L=4096ms of the population activity $a(t)$ has been recorded. After initialization and before recording each simulation ran 1000ms without recording in order to let the system equilibrate.

Frequency determination via autocorrelation function

The autocorrelation function of an activity sample of length L has been calculated for values of τ between 0 and 500 according to equations (4.9) and (4.10). Periods larger than 500ms have not been considered.

$$\tilde{C}_\tau = 1/L \sum_{t=1}^{L-\tau} (a(t) - \langle a \rangle)(a(t+\tau) - \langle a \rangle) \quad \tau = 0, 1, \ldots, 500 \tag{4.9}$$

$$C_\tau := \tilde{C}_\tau / \tilde{C}_0 \tag{4.10}$$

The population frequency has been regarded as the position $\tau_{\max}$ of the global maximum of the autocorrelation function beyond the first zero crossing. If the autocorrelation function has no zero crossing, the signal is not oscillating. The maximum value $C_{\max}$ characterizes the

regularity of the oscillation, $\tau_{\max}$ and $C_{\max}$ are characterized by definitions (4.11), (4.12) and (4.13).

$$\tau_{\mathrm{neg}} := \min\{\tau \mid \tau < 0\} \tag{4.11}$$

$$C_{\max} := \max\{C_\tau \mid \tau > \tau_{\mathrm{neg}}\} \tag{4.12}$$

$$\tau_{\max} := \min\{\tau \mid C_\tau = C_{\max}\} \tag{4.13}$$

However, the dynamics of a network does not only depend on the parameters but also on the random number generator seed (RNGS). For many parameter sets there are some networks which fall into the oscillating regime as well as others which do not oscillate. The difference between networks belonging to different RNGSs is the particular wiring of the synaptic connections. If a particular realization of a network is over-inhibited (so that 20ms after initialization the activity in the network has ceased) the autocorrelation function equals zero, if it is fluctuating without a prominent oscillation frequency the algorithmically determined values of $\tau_{\max}$ appear as if they have been picked randomly between 0 and 500. This leads to the "snow" in figure 4.29 in the domain of low δ_{i}-values. These results should not enter averaging the oscillation frequency as the result would be distorted, rather we prefer a preselection of cases which are oscillating and record their percentage. As the unwanted autocorrelation peaks are coupled with small values of $C_{\max}$ they can be sorted out by a threshold criterion $C_{\max} \geq C_{\mathrm{th}}$.

Frequency determination via Fourier transformation

Additionally to the autocorrelation measurement the power spectrum of the simulated network activity has been calculated and analyzed to check the results. The FFT algorithm taken from [74] has been applied to the same epochs of length $L = 4096$ and the absolute value of the Fourier coefficients has been recorded for frequencies between 1/4 and 24 Hz from which the frequency $f_{\max}$ corresponding to the maximal power has been extracted. Again a preselection via a cutoff criterion has been applied before averaging, and for better comparability with the results from the autocorrelation measurement the corresponding period $T = 1/f$ has also been calculated. A comparison has shown that both methods yield the same frequencies or periods respectively. However the resolution of the power spectrum in the frequency domain is limited due to the short epochs and thus the frequency determination is more accurate via autocorrelation.

Of course, the notation of calling a network oscillating if the autocorrelation or the power spectrum of the time course of its oscillation has a high maximum has to be consistent with our earlier synchrony measure. So far we have always measured the amplitude of the oscillation which we defined as the standard deviation of $a(t)$ in a time window of a certain length. In the case of pure noise the standard deviation, which does not take into account any temporal relationship of the data points, might be high whereas the autocorrelation has no first maximum at all. However, if the measurement is limited to the dynamics of our neural networks, the amplitude (standard deviation) of the activity is an equally appropriate measure for synchrony as $C_{\max}$ or $P_{\max}$ respectively (see figure 4.28).
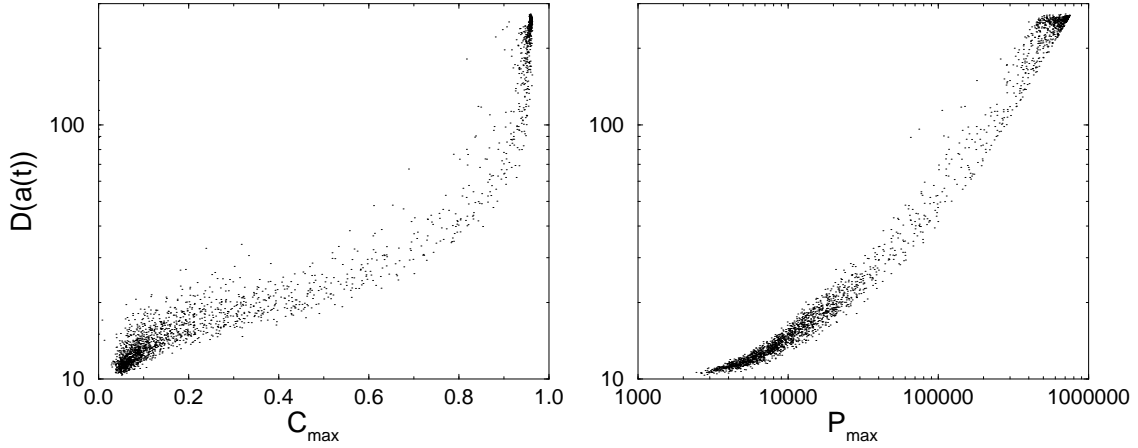
Figure 4.28: Relation between amplitude (standard deviation) and C_{max}(left), P_{max}(right). Parameters are (κ_e, κ_i)=(0.160,0.032), δ_e=20, δ_i=56, 57, ..., 80, (σ_e, σ_i)=(20,120), r=0, N=1 000.

4.6.2 The influence of δ_i on the population frequency

Looking at the projection of the parameter-space onto the δ_i-axis the transition between the regimes occurs at some critical value δ_i^c which is of course dependent on the other parameters. Figure 4.29 shows autocorrelation maxima determined from simulations with r=0 as an example. In the upper graph where C_{max} is plotted, we can see clearly the transition from the fluctuating to the oscillating regime. The critical value δ_i^c at which the transition occurs is linearly shifted to higher δ_i-values when δ_e is raised. The extension of the domain of the oscillating regime in the δ_i-projection grows faster than linearly with δ_e (cp. section 4.5). Looking at the frequencies in the oscillating regime one observes that when minor shifts, which are due to different values of δ_e, are neglected a linear approximation yields $T \approx 2\delta_i$.

In order to measure the population frequency in the oscillating regime and its dependency on the synaptic parameters we collect the values of τ_{max} for a hundred different RNGSs. Those cases where the corresponding value of C_{max} is low are classified as "not oscillating" and do not enter averaging. Figure 4.30 shows the resulting average period as well as the fraction of networks that yield oscillations with $C_{max} \geq 0.9$. The fraction of networks fulfilling this condition peaks at $\delta_i = 79$. When we move from this peak to lower δ_i-values more and more networks are lost to the fraction with lower C_{max}-values, i.e. they have a more distorted oscillation which means a transition to the fluctuating regime. Moving to higher δ_i-values we find that an increasing number of networks is lost to the flat regime. Whereas the dependency of T on δ_i is linear on the right side of the peak value ($\Delta T = \Delta\delta_i$), the slope is higher on the left side of the peak, a linear fit yields 2.6. This interesting feature is due to the relation between frequency and stability of population oscillations which is described in the next section.
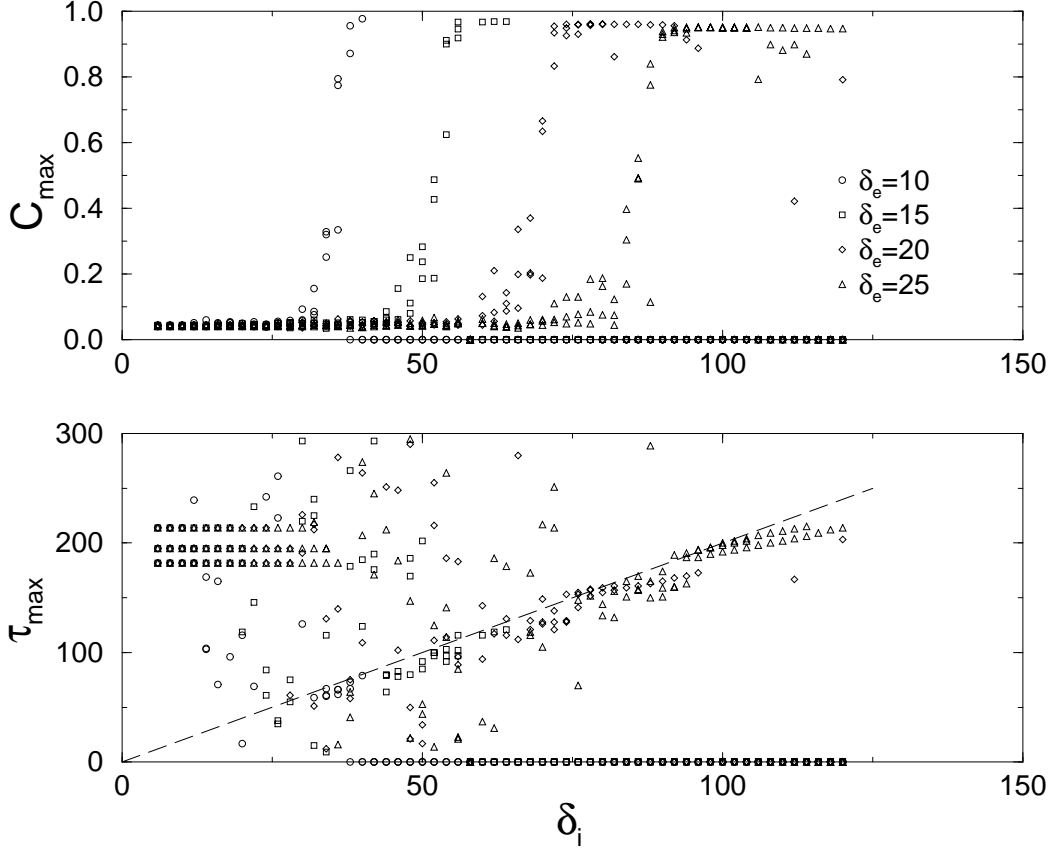
Figure 4.29: Here we show all resulting values of the frequency determination via the auto-correlation method. For each pair (δ_e, δ_i) three simulations with different RNGSs have been run. The upper graph shows the transition from the fluctuating to the oscillating regime which is characterized by a significant increase of C_{max}. The critical δ_i-value at which this transition occurs shifts linearly when δ_e is raised (here $\delta_i^c \approx 3.4\delta_e$). The lower graph shows τ_{max} which estimates the period of the population oscillations. At very low levels of δ_i the network dynamics are insensitive to changes of δ_e and δ_i, thus the three horizontal lines in the very left half represent simulation runs which are exactly identical. The "snow" that appears when $\delta_i < \delta_i^c$ is due to spurious periods which are found by the C_{max}-detection algorithm and correspond to very low maxima of auto-correlation functions in the fluctuating regime. In the oscillating regime the duration of the period clusters around the approximation $T \approx 2\delta_i$ (dashed line). Parameters are (κ_e, κ_i)=(0.160,0.032), (σ_e, σ_i)=(20,120), r=0, N=1 000.
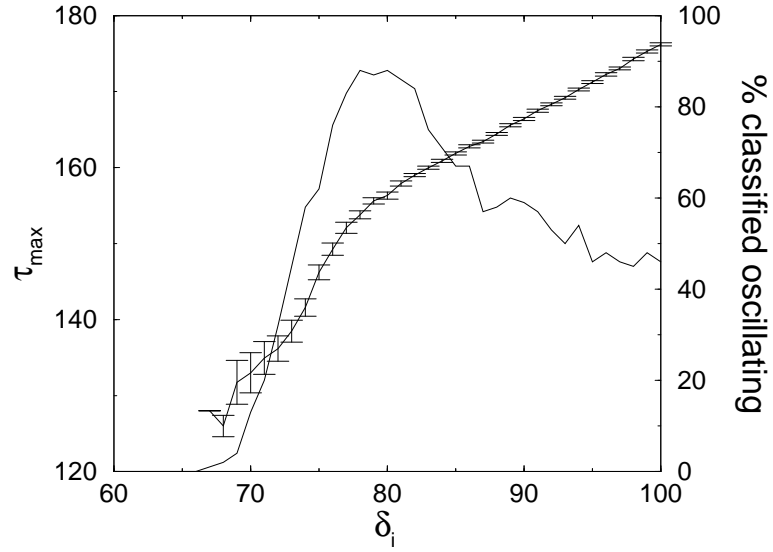
Figure 4.30: The average period of the population oscillations determined via autocorrelation is plotted versus δ_i. The dashed line corresponds to the right scale and gives the percentage of oscillating networks. Parameters are $(\kappa_e, \kappa_i) = (0.160, 0.032)$, $\delta_e = 20$, $(\sigma_e, \sigma_i) = (20, 120)$, $r = 0$, $N = 1\,000$. A hundred simulations with different RNGS have been made for each value of δ_i.
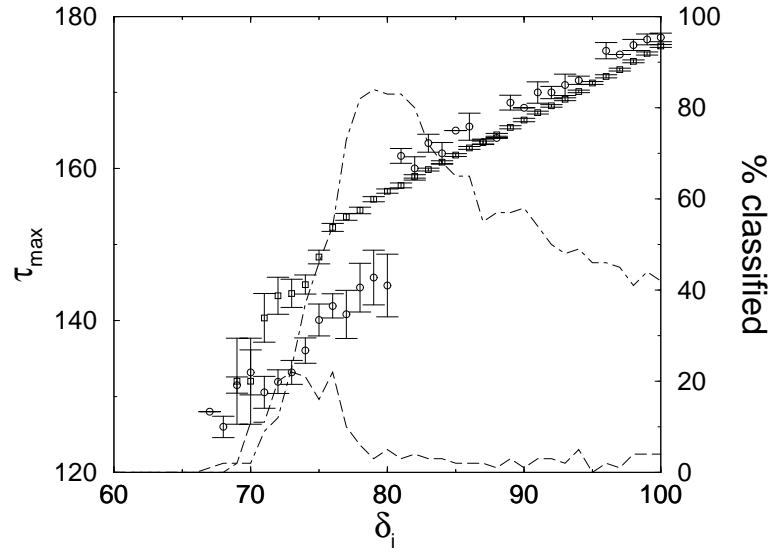

Figure 4.31: The data of figure 4.30 have been classified into two bins. Circles and squares correspond to the left ordinate scale and give the average value of τ_{max} for $C_{max} \in [0.9, 0.95]$ and $C_{max} \in [0.95, 1.0]$ respectively. The dashed and dot-dashed lines correspond to the right ordinate scale and give the relative fraction of simulation runs classified into the corresponding bin.

4.6.3 Frequency-shift with increasing synchrony

In many cases EEG recordings of epileptic seizures show a characteristic frequency shift: the oscillation of the signal is decelerated to a frequency of 3 Hz just with the onset of the epileptic seizure (cp. section 1.2.2). Which mechanism is responsible for this phenomenon? Although it is likely that there are additional mechanisms which contribute to the frequency shift of epileptic seizures (cp. section 4.8), the results obtained in the previous section indicate that, even without further ingredients to our network model, synchrony of network oscillations is accompanied by a deceleration of their rhythm. Also experiments show this relation between the power of an oscillation (highest peak in the power spectrum) and its frequency [30]. Figure 4.32 shows this relation for data obtained from different simulations with the same parameters.

Taking up the simple model which was introduced in section 4.2.1 this section will provide a rough explanation of the mechanism which is supposed to underlie this implicit frequency change. Additionally the change of the slope in graph 4.30 can be explained with the same model.

The results of the previous section exhibit at least two interesting phenomena which we want to explain qualitatively by the following considerations:

- The slope $\Delta\tau_{\mathrm{max}}/\Delta\delta_{\mathrm{i}}$ changes at $\delta_{\mathrm{i}} \approx 78$ (see figure 4.30).

- Within a set of simulations with the same parameter values, especially δ_{i} is kept fixed, the frequency decreases with increasing amplitude (see figures 4.31 and 4.32).

In section 4.2.1 we assumed that there exists a threshold I_{min}, such that with some exclusions firing activity is suppressed when $I(t) > I_{\mathrm{min}}$. Let us now accept another refinement of our assumed mechanism of the population oscillations from sections 4.2 and 4.2.1:

> We call the duration of the suppression period T_{supp} and assume that it yields an additive contribution to the period of the population oscillation.

Now we can qualitatively derive the two phenomena which have been observed in the last section. The time T_{supp} during which firing is suppressed is given by the time during which $I(t)$ exceeds I_{min}. Figure 4.33 shows how T_{supp} changes when δ_{i} is increased. The resulting curve bends apparently similar to the measured curve describing the dependency of the period on δ_{i} (cp. figure 4.30). $\Delta T_{\mathrm{supp}}/\Delta\delta_{\mathrm{i}} > 1$ holds when the tip of $I(t)$ has just crossed the threshold. When the shape of the convolution is close to the square pulse because $\delta_{\mathrm{i}} \gg \phi$, $\Delta T_{\mathrm{supp}}/\Delta\delta_{\mathrm{i}} \approx 1$ (cp. figure 4.33).
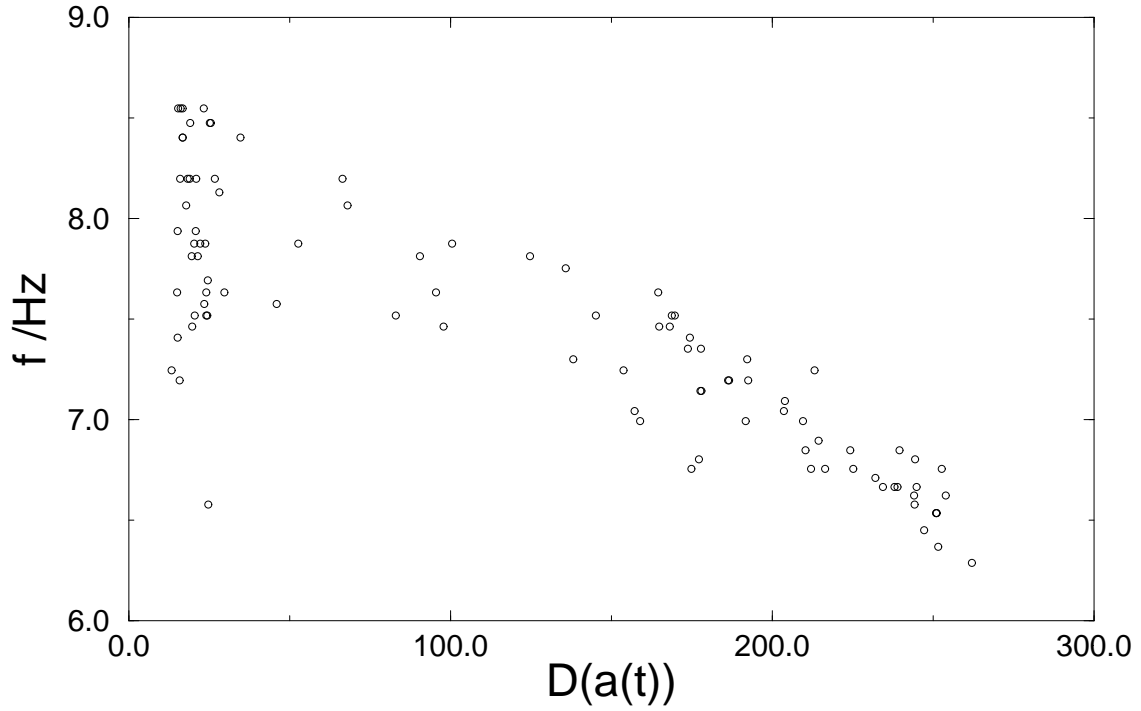
Figure 4.32: A hundred simulations of networks with the same parameters and different RNGSs yield different oscillations with different amplitudes. We can see that the frequency of the oscillation is related to the amplitude. The data correspond to the data shown in figure 4.30, here the case δ_i=74 has been extracted.

4.7   Propagation of oscillatory activity

So far the model explains that a tiny piece of cortex tissue can become critical in the sense that it may spontaneously flip to synchronous oscillations of the neural population. However, an epileptic seizure is a phenomenon that involves a larger part of the brain and eventually the whole organism. Whereas generalized epileptic seizures arouse from central parts of the brain in the case of focal epilepsy the seizure is ignited in a very localized part of the cortex. In this case excision of that so called epileptic focus may help the patient. This operation is risky but it is sometimes done when treatment with drugs does not apply.

Usually a piece of cortex tissue becomes an epileptic focus through a physiological change of the neural network in that particular region of the focus, in many cases epilepsy is due to an injury of the head. In a recent paper [75] it is shown that in the case of post-traumatic epilepsy, the cortex tissue of rats has changed such that inhibition is stronger than usual. This is due to larger amplitude of IPSPs as well as to a higher number of inhibitory synapses. It is presumed that after injury axons of inhibitory neurons sprout to establish additional synapses and thus lead to stronger inhibition.
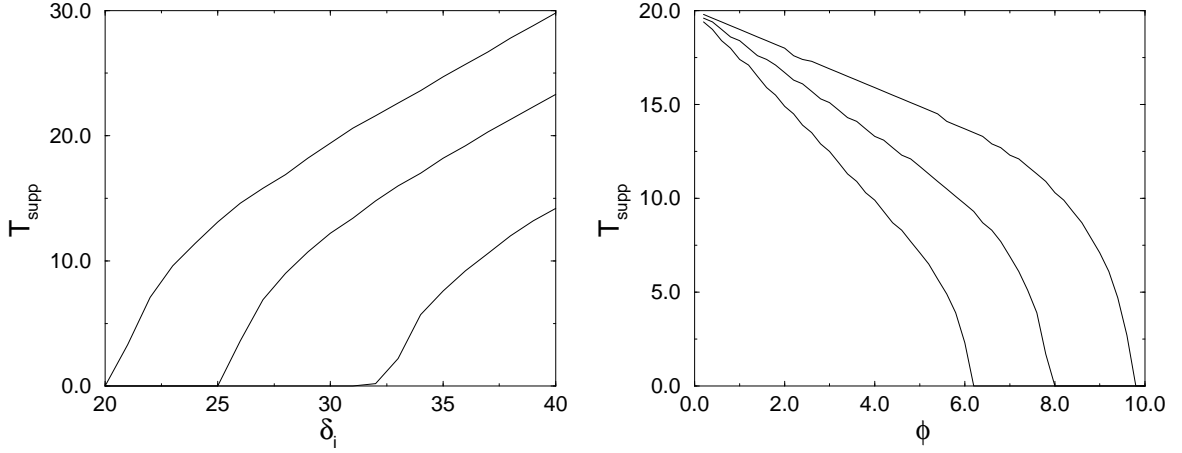
Figure 4.33: Left: T_{supp} vs. δ_{i} for θ=0.7, 0.8, 0.9 and $\phi = 10$. The graph bends similar to the measured dependency of the period on δ_{i} shown in figure 4.33. Right: T_{supp} vs. ϕ for θ=0.7, 0.8, 0.9 (from top to bottom) and $\delta = 20$.

We note that in this observations the direction of change the neural network has undergone, i. e. stronger inhibition (either by strength or by number of synapses), is the same as in our discrete computer model. Simulating a small cube of cortex tissue may thus be a suitable model of post-traumatic focal epilepsy. It remains to explain how the synchronous oscillations of the neural tissue spread over the cortex after they are ignited in the focus which has changed due to an external impact. Thus we take a look at how stimulation of the model neural network influences its dynamics. The stimulation may be thought of coming from the nearby neural tissue which is already ignited. If periodic stimulation of neural tissue lowers the borders of the oscillating regime, epileptiform activity may spread over the cortex similar to a forest fire.

To investigate this assumption we will recall the transition from oscillating to epileptiform regimes due to increasing the inhibitory synaptic density which is shown in figures 4.2 and 4.13 respectively. Say that $\kappa_{\mathrm{i}}^{\mathrm{c}}$ is a critical value for the inhibitory connectivity such that synchronous oscillations occurred when $\kappa_{\mathrm{i}} \geq \kappa_{\mathrm{i}}^{\mathrm{c}}$. We now expect that the value of $\kappa_{\mathrm{i}}^{\mathrm{c}}$ which separates the oscillating regime from the epileptiform regime decreases when stimulation of the form 4.14 is simultaneously added to the membrane potential of every neuron.

$$e_i = \sigma_{\mathrm{stim}} \sin(2\pi t / T_{\mathrm{stim}}) \tag{4.14}$$

Figure 4.34 shows how this transition shifts when we impose periodic stimulation of different strength σ_{stim} and period T_{stim} on the simulated network. We can see that with increasing σ_{stim} the value of $\kappa_{\mathrm{i}}^{\mathrm{c}}$ decreases. Further, there seems to be some resonance phenomenon, i. e. we see a maximal decrease of $\kappa_{\mathrm{i}}^{\mathrm{c}}$ when the period of the stimulation matches that of the autonomous network, which in this case is $T_{\mathrm{auto}} = 86\mathrm{ms}$.

It has also been observed that stimulation raises $\kappa_{\mathrm{i}}^{\mathrm{c}}$ when the period of the stimulating signal is somewhat smaller than T_{auto}. Further it has been observed that stimulation with a
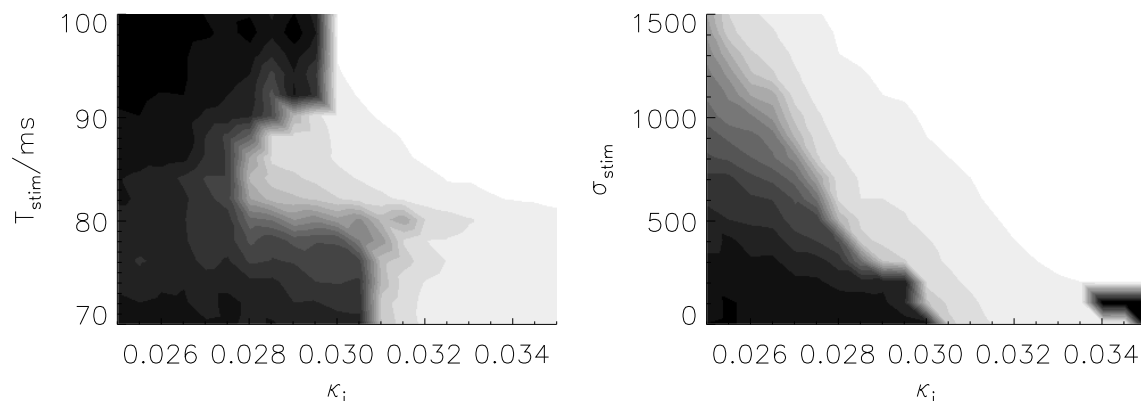
Figure 4.34: The greyscales code the value of $D(a(t))$. Increasing κ_i leads to a transition from the fluctuating regime (dark, $D(a(t))$ small) to the oscillating regime (light, $D(a(t))$ large). Left: κ_i^c is lowered most when $T_{stim}{=}86$, here $\sigma_{stim}{=}500$ is fixed. Right: The strength of the stimulation is varied whereas $T_{stim}{=}86$ is fixed.

sinusoidal shape was more facilitating than stimulation with a truncated sine wave leaving only the positive part which again shows the importance of inhibition in synchronous population oscillations.

4.8 Introduction of slow inhibitory PSPs

Although not all epileptic seizures which arise in the cortex show this feature one prominent attribute of many EEG recordings of epileptic seizures is a significantly decreased frequency of the dominant oscillation (cp. section 1.2.2). However, the conclusion of section 4.6 has been that the frequency of the oscillation is, except for a minor frequency deviation at the onset of the oscillating regime, mainly determined by the PSP durations. A frequency shift did not occur together with the transition to epileptiform activity shown in section 4.3. Thus modeling the frequency shift during an epileptic seizure requires a refinement of the model.

From the physiological point of view there are at least two features that have been neglected in the basic model and which are good candidates to bring along a change of the frequency accompanying the onset of synchronized activity.

- The simplification of the PSP shapes to square pulses may change the dependence of the frequency on the synchrony (cp. section 4.6.3). Thus the shape of the PSPs could be modified so that it looks more like an exponentially decaying potential.

- Most inhibitory gabaergic neurons activate two kinds of inhibitory GABA receptors, the GABA$_A$ receptor which induces a fast Cl$^-$ mediated IPSP with a time constant of about

40ms and the $GABA_B$ receptor which induces K^+ mediated IPSPs of a much longer time constant of 150-200ms [61].

Another point that suggests a refinement of the model is that our results of the basic model indicate that more inhibition instead of less induces oscillations in neural tissue whereas physiological findings at first view suggest the opposite. Dysfunctions of the $GABA_A$ receptor mediated inhibition have been found in many cases of epilepsy [50] and $GABA_A$ antagonists like penicillin for instance are known to induce seizures in slice preparations. On the other hand many anti-epileptic drugs in clinical practice strengthen GABA mediated inhibition in order to stop seizures [62].

This indeed seems to contradict our simulation results, but the matter is more complex. It has also been observed that the number of inhibitory synapses is increased in the tissue of epileptic foci which have been excised in epilepsy surgery [75]. Further, there are cases where activation of gabaergic inhibition aggravates the seizures. The clue might be that the neurotransmitter GABA affects two receptors which induce different IPSPs. Blocking the $GABA_A$ receptor does not mean that there is no inhibition in the neural network. It also has been found that $GABA_B$, the slow inhibitory receptor plays a crucial role in the mechanism of epileptiform 3Hz spike-and-wave discharges which are related to absence seizures [56]. Further, activation of $GABA_B$ receptors leads to seizures in rats [69].

Now the second suggestion appears to be a promising modification. We thus introduce a third type of postsynaptic potential with duration δ_s and strength σ_s. The number of synaptic sites is not changed: this slow IPSP will be triggered together with the fast IPSP by action potential firing of inhibitory neurons. Like in reality an inhibitory postsynaptic potential is thus composed of a fast and a slow component [61]. However, as we do not care about the detailed curvature of the PSPs, the modification can be interpreted either as introduction of another neurotransmitter with a long characteristic time or the introduction of a two step prolonged IPSP as a discrete approximation of the exponentially decaying PSP. Figure 4.35 illustrates the compound synaptic PSP consisting of the fast and the slow part.
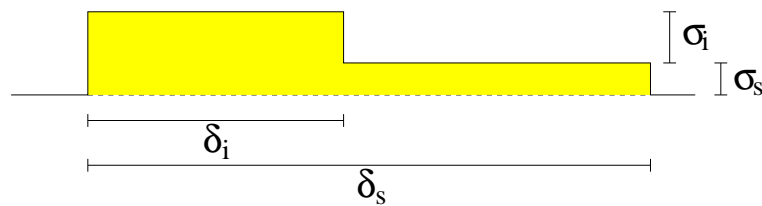

Figure 4.35: The compound inhibitory PSP.

Simulation results with slow IPSP: spiking regime

An interesting change that comes along with the introduction of the new inhibitory potential is that another regime is inserted between the fluctuating and the oscillating regime which

have already been described in section 4.1. Figures 4.36 and 4.38 (without and with refractory period respectively) show how the amplitude and the average activity change in the sequence of the now four regimes (fluctuating, spiking, oscillating, flat) of the extended model.
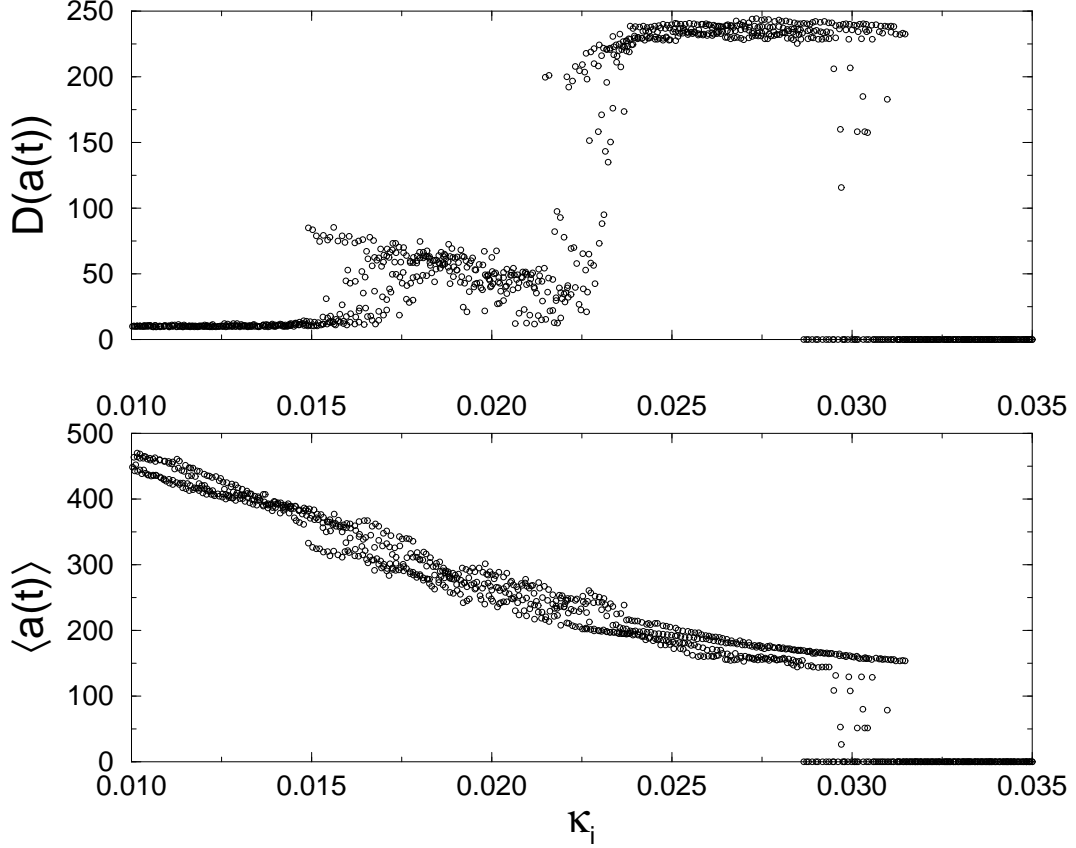

Figure 4.36: $D(a(t))$ and $\langle a(t)\rangle$ have been calculated for different values of κ_i and four different RNGSs. The other parameters are $\kappa_e{=}0.1$, $(\delta_e,\delta_i,\delta_s){=}(15,62,140)$, $(\sigma_e,\sigma_i,\sigma_s){=}(20,60,60)$, $r{=}0$, $N{=}1000$.

The network activity in the spiking regime is characterized by fluctuating activity of a high frequency and intermittently occurring spikes of a low frequency. An example is presented in figure 4.37. The number of occurrences of high amplitude spikes increases with higher values of κ_i. Eventually the network is continuously spiking with a rather steady frequency, but the transition to the oscillating regime brings along another kind of oscillation (see figure 4.39). The increase of the spike frequency within the range of the intermediate regime is shown in figure 4.41.

Introducing the refractory period does not change the situation very much: the κ_i-values where transitions occur are lowered and of course the average activity and the amplitude are decreased.
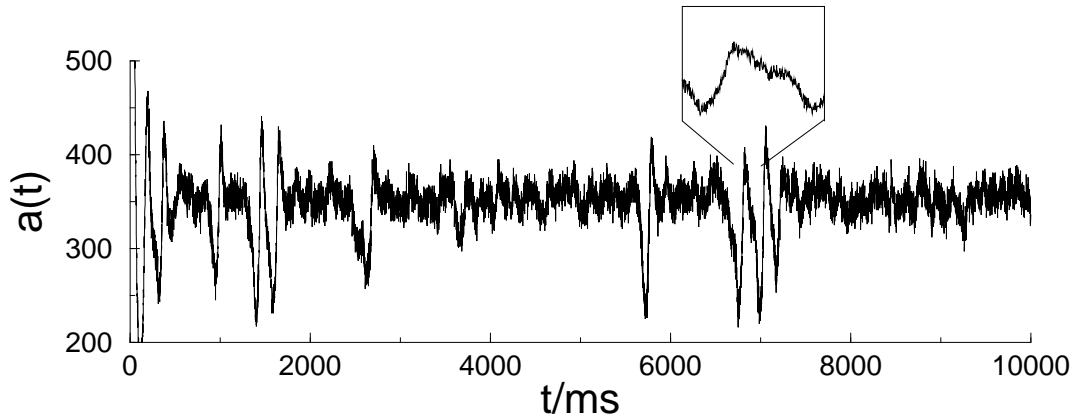
Figure 4.37: The spontaneously occurring spikes correspond to a frequency of 4.3 Hz, whereas the frequency of the fluctuating activity varies between 5 and 12Hz. Here κ_i=0.0160, the other parameters are the same as in figure 4.36.

The isolated spikes are spontaneously arising events of hypersynchrony which are observed in the EEG of epileptic patients during interictal periods. It thus remains to examine if the mechanism which underlies these spikes is similar to the mechanism of interictal spikes in the EEG of epileptic persons.

Many experiments in vitro show that either activation of excitatory synapses or blocking the $GABA_A$ receptors which induce the fast IPSP lead to oscillation whereas activation of the gabaergic inhibitory synapses abolishes oscillations. Further do many antiepileptic drugs activate the GABA receptors. Thus it may appear puzzling that in the basic model which does not include the slow inhibitory potentials increasing inhibition leads to oscillations and increasing excitation leads to fluctuations as it has been shown in section 4.4.

Now that a second slow IPSP has been added to the model the situation is different. As shown in figure 4.42 simultaneously increasing the strength of both types of IPSPs diminishes the amplitude of the oscillations which corresponds to the application of AEDs. Further, when the $GABA_B$ receptors are active, increasing the amplitude of fast IPSPs stops oscillations whereas increasing the amplitude of EPSPs induces oscillations.
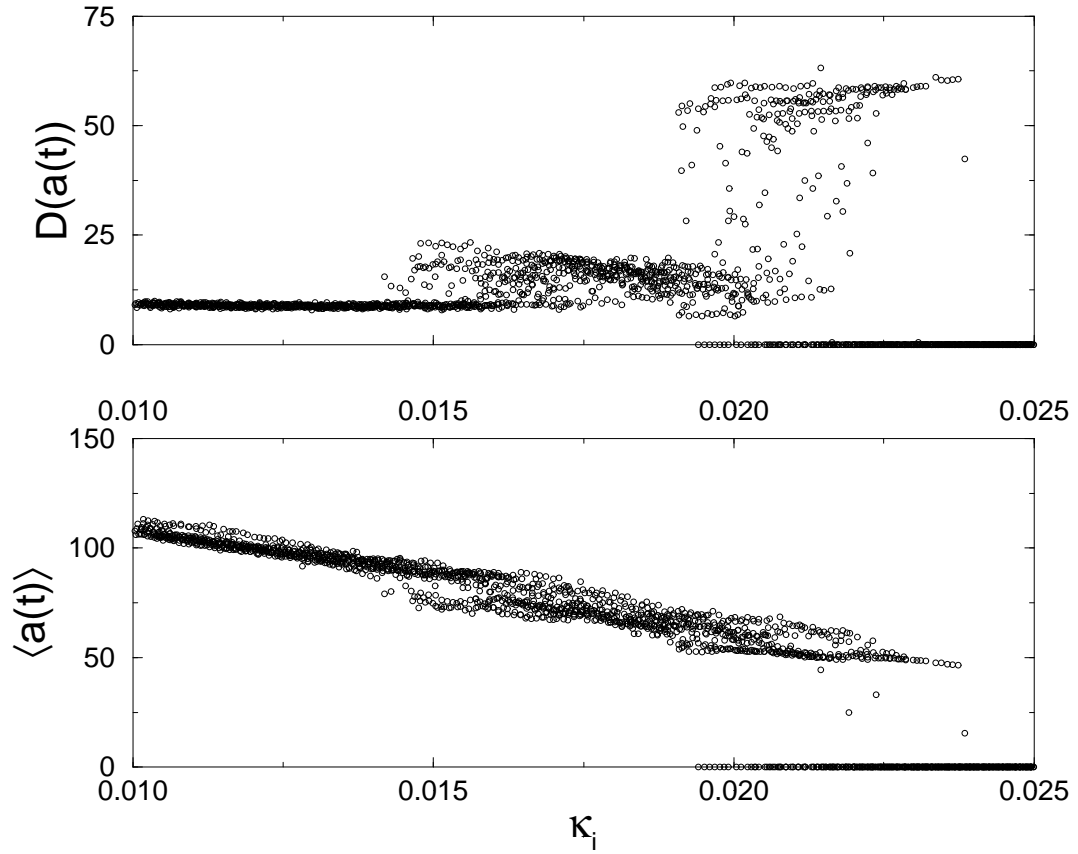
Figure 4.38: With refractory period $r{=}5$ the transitions between the regimes are shifted to lower κ_i-values, the other parameters are the same as in figure 4.36.
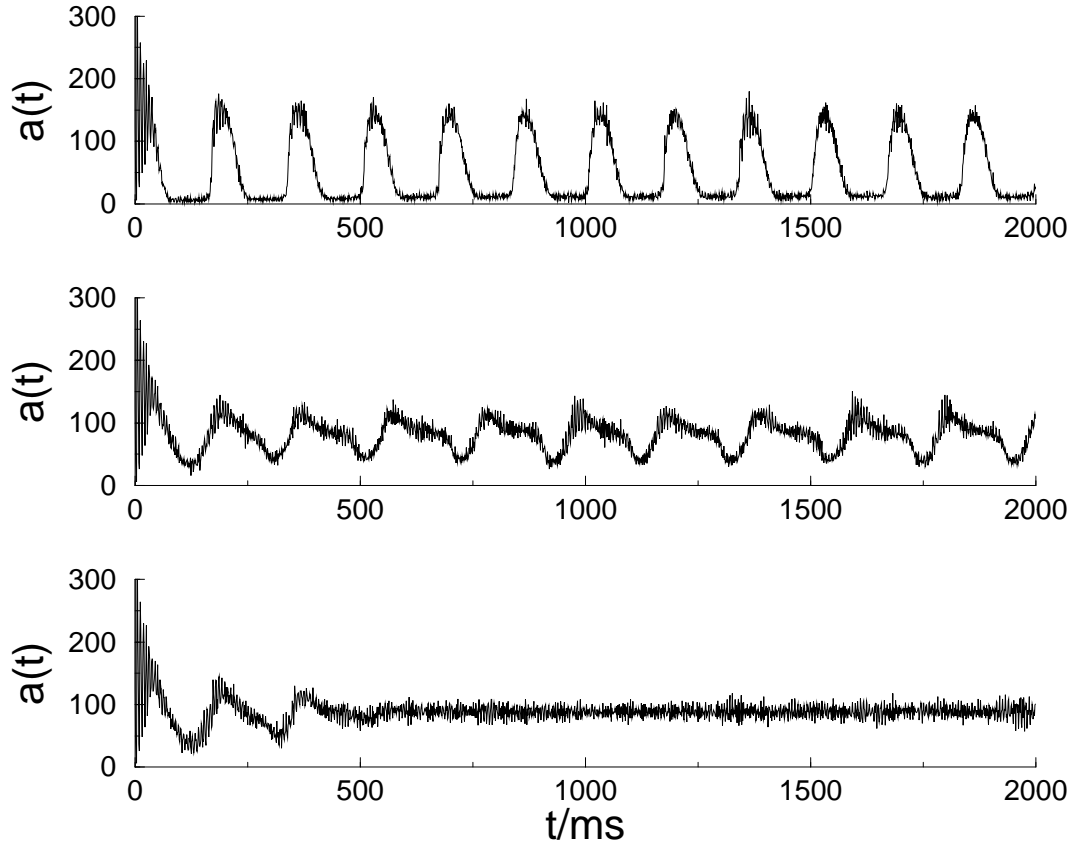
Figure 4.39: Example epochs of the activity in the three active regimes shown in figure 4.38. The connectivities are κ_i= 205, 146, 145 from top to bottom.
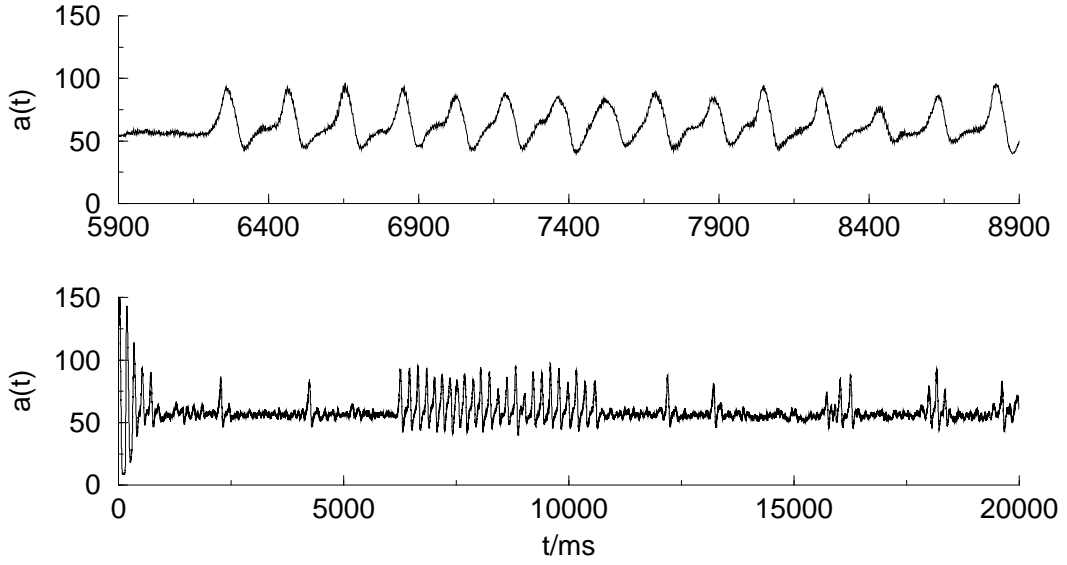
Figure 4.40: Intermittently occurring spikes are characteristic for the intermediate regime. A spontaneously occurring oscillatory period exhibits an average frequency of 5.6Hz. $\kappa_i= 194$, the other parameters are as in figure 4.38, high frequencies have been filtered by averaging over a moving time window of 15 ms. The upper trace gives a detailed view at the onset of the spiking period.

Figure 4.41: The frequency of occurrence of spikes increases with κ_i. The number of spikes has been counted in four differently initialized simulations of 40 000 ms each. The parameters are the same as n figure 4.36
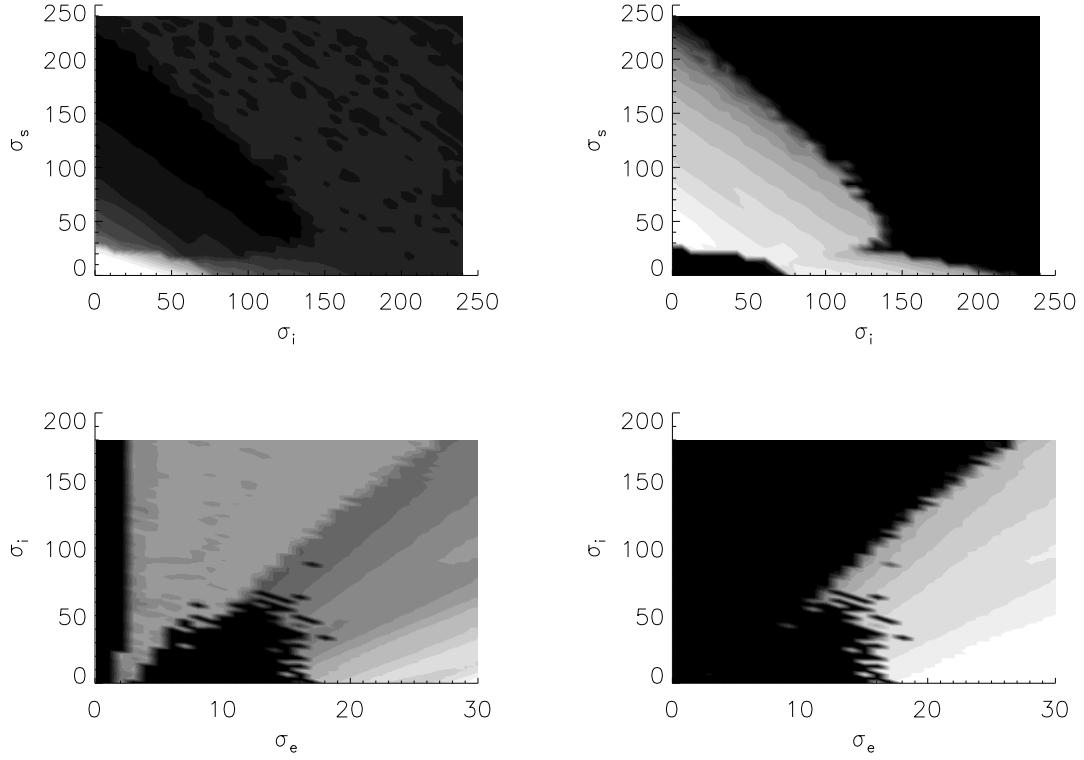
Figure 4.42: The upper graphs show the dependence of the average activity $a(t)$ (left) and the amplitude $D(a(t))$ (right) on σ_i 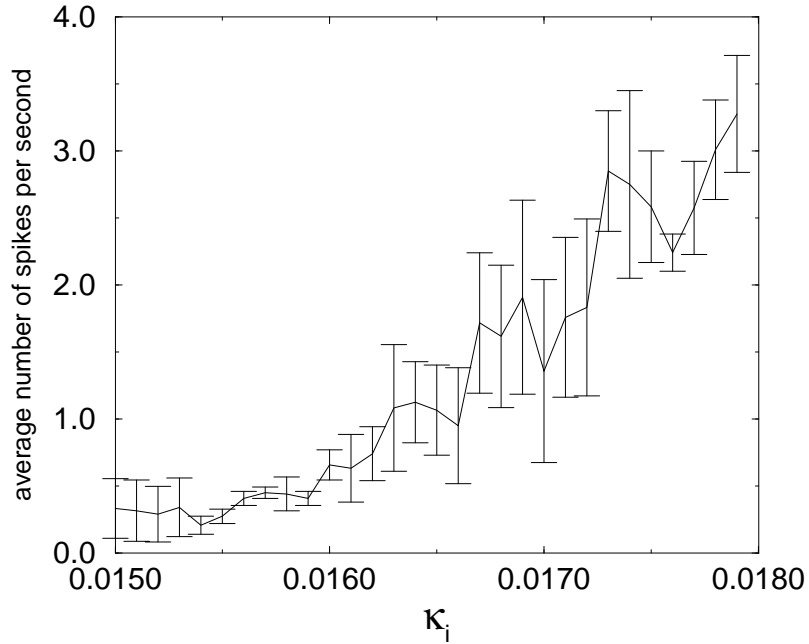and σ_s as greyscale plots. σ_e=20 is fixed. The light region in the upper right graph corresponds to oscillations with a high amplitude. Simultaneously increasing both types of IPSPs diminishes the amplitude and finally abolishes the oscillations. The lower graphs show the dependency of $a(t)$ (left) and $D(a(t))$ (right) on σ_e and σ_i when σ_s=60 is fixed. When slow inhibition persists, increasing σ_e leads to oscillations (light region in the right graph), whereas increasing σ_i abolishes oscillations. The other parameters are (κ_e, κ_i)=(0.1,0.03), $(\delta_e, \delta_i, \delta_s)$=(15,62,140), r=0, N=1000.

5 Discussion

All neural network models of the brain are rather approximative and simplifications are a natural feature of any model. The physiological knowledge of the structure of the brain, the measured details of electric potentials and the biochemical processes in neurons provide more information than is contained in any single model. For that reason the crucial point is the selection of the right features which should enter the model.

Neural networks of the cortex exhibit a very complex structure, the input to a cortical neuron is the superposition of postsynaptic potentials from 10^4 synaptic terminals. The shape of a neuron with its long and ramified neurites yet indicates that the connections reach many other neurons which are located far away. It is thus likely that the mechanism which leads to the synchronization of neural firing at the onset of an epileptic seizure is determined to a great extent by the compound action of a large number of postsynaptic potentials. On the other hand the single unit itself underlies complex mechanisms which are hardly understood and the precise timing of action potential firing and the phase relations of interacting neurons might also be crucial for the emergence of synchronized population activity.

In order to investigate epilepsy one now has to decide whether to use a reduced unit model in combination with a detailed network or a reduced network in combination with a detailed unit. These alternatives are imposed by the limited computational possibilities. The dilemma is similar to problems of modeling and simulating other types of complex systems like earthquakes, granular media, proteins, spin glasses, stock markets, traffic, weather etc. Concerning epilepsy in neural networks we believe that a competitive comparison of both approaches which are characterized above is needed to get maximal insight into the matter.

In addition to a summary of the simulation results obtained with the newly developed discrete model this discussion also includes a comparison with a differential equation model which has simultaneously been applied to epilepsy by Christian Hauptmann [40]. During the whole process of the investigation both points of view have frequently been compared.

The essential aspects of this thesis as the applied simplifications, the influence of randomness, the dependence on the parameters, spontaneous occurrence of epileptiform activity, the proposed mechanism of oscillations and a comparison with physiological results are summarized and discussed in the following:

Simplifications and computational cost

The concept of the discrete model aims at a reduction of the complexity of the original dynamical system and a reduction of the computational cost. It is based on the two following simplifications:

- Introduction of a discrete time step of one millisecond which resembles the duration of an action potential.

- Reduction of the postsynaptic potentials to square pulses.

The first simplification eliminates the influences of the detailed dynamics of an action potential on the network behavior. In real neural networks small differences in the firing times of two neurons can grow or decrease with the temporal evolution of the network. Thus temporal rejection of action potential firing in two neurons is thinkable as well as attractive mechanisms which lead to synchrony. These effects have been found to play a part in the synchronization of neurons in microcircuits of a few neurons [40].

An implication of the discrete time step is that action potential firing is always quantized in the discrete model. As a consequence the use of parallel update of all neurons in one time step implies some artificial synchrony on this millisecond raster and leads to unnatural limit cycles. Now the simulation of epilepsy aims at regular firing which spontaneously emerges out of chaotic behavior. Thus a discrete model with parallel update which is generally prone to exhibit regular dynamics is not suitable. In order to obtain irregular network dynamics the application of random sequential update is an appropriate method to insert fluctuations.

In a large network a single PSP represents only a very small fraction of the total synaptic input to a neuron. For that reason it is justified to reduce the shapes of action potentials and postsynaptic potentials to square pulses. The characteristics of a PSP can be reduced to a single time constant and an amplitude. Nevertheless, the influence of a more detailed PSP shape and the increased complexity which results from that refinement can partly be seen in section 4.8.

The computing time that is saved by the above simplifications allows to simulate more complex structures of the network, i.e. more neurons and first of all more synapses. Further, the simulation speed makes it possible to run many simulations and to vary different parameters in order to obtain phase diagrams.

The computer simulations of the discrete model run about 500 times faster than computer simulations of the differential equation model described in [40]. The comparison is based on simulations with 800 neurons and about 20 synapses per neuron. A general comparison is difficult as the computing time in the discrete model is proportional to the activity and the number of synapses, whereas the computing time of the differential equation model depends on the number of units and the number of synapses.

Randomness

Random influences in computational models are introduced in order to represent those influences in the real system which are not explicitly modeled. Here two sources of randomness enter the model:

- The synaptic connections of the neurons are randomly set.

- Random sequential update represents a permanent source of jitter in the firing of action potentials.

Random synaptic connections correspond very well to the structure of small parts of the cortex. On the other hand directed neuronal connections like circular connections of excitatory and inhibitory neurons can be found in the thalamus [58] and the olfactory system [27] and have been suggested to induce oscillations.

As discussed before jitter has been introduced into the model by using random sequential update in order to distort the artificial regularity which is imposed by the discrete time step. The use of random sequential update can be justified as substituting the missing signal propagation times and the various sources of noise in the cortical network.

Parameter dependence

Due to the multitude of parameters, scanning the entire parameter space is very time consuming even if the model allows comparably fast computer simulations. We investigated a couple of planar intersections of the parameter space in order to give a qualitative overview of the dependence of the network dynamics on the parameters.

The result was that in large systems with many synapses the linear ratio of the synaptic connectivities roughly characterizes the regime. Low values of the ratio κ_i/κ_e correspond to fluctuating dynamics whereas high values induce too much inhibition in the network and abolish autonomous activity. Intermediate values lead to oscillations of the population activity.

In a similar manner the ratios δ_i/δ_e, δ_i/κ_e, κ_i/δ_e determine the network dynamics.

These are rough approximations which are valid only in a certain domain of the parameter space. At least two further interesting phenomena have been observed in sections 4.4.3 and 4.5.3:

- For low numbers of excitatory synapses the regime borders deviate substantially from the above estimation due to the self-organized formation of active subnetworks which have different network parameters.

- Long lasting EPSPs induce another interesting regime presented in section 4.5.3 which might be interesting with regard to epilepsy but has not been observed in detail.

Spontaneous occurrence of epileptiform activity

Not only variation of the parameters leads to strong oscillatory dynamics in the dynamics of the model. Spontaneous switching to hypersynchronous activity was found when the parameters of the model were located at the border of the oscillating and the fluctuating domains.

In agreement with physiological findings the transition from normal to hypersynchronous network behavior is accompanied by a transition to bursting behavior on the single neuron level. The observed burst discharges are evoked by a compound long lasting network EPSP.

Many epileptiform patterns in real EEG data are accompanied by a decrease of the frequency to about 3Hz with the onset of the regular hypersynchronous oscillations. Whereas the spontaneous transitions in simulations of the basic model which have been shown in section 4.3 did not exhibit such a frequency shift, the extended model, which in comparison to the basic model further included a slow IPSP, could produce this frequency shift. The simulation results shown in section 4.8 exhibit spontaneous synchronization whereby the frequency of the hypersynchronous oscillations was significantly reduced.

The mechanism of the oscillations

Today the mechanism of brain waves is still not understood. Some hypothetical mechanisms have been described in section 1.2.1. The hypothesis that brain waves are an emergent phenomenon of a population of neurons rather than synchronized activity of individually oscillating units is strongly supported by computer simulations and physiological experiments. It has been shown that excitatory *and* inhibitory synaptic coupling is needed for population oscillations. Further it has been observed that single neurons do not fire action potentials in all oscillation cycles and occasionally spike in the valleys of population activity. Rather the firing of action potentials is a stochastic process whereby the probability of AP firing oscillates. The importance of inhibitory neurons in neural population oscillations is widely accepted, but different network architectures imply minor differences in the mechanisms of synchronization.

- The oscillations of the discrete model do not show a phase shift between inhibitory and excitatory firing events. Nevertheless the cumulative postsynaptic potentials peak at different times because of the different synaptic time constants. That excitatory and inhibitory neurons are in phase is clearly a consequence of the network architecture: as the synaptic connections are set without regarding the type the of the target neuron the membrane potentials of both types of neurons follow the same probability distributions.

- Oscillations in the differential equation model studied by Hauptmann [40] exhibit a phase shift between excitatory and inhibitory neurons which is also induced by the architecture of the network. To fire an action potential an inhibitory neuron requires the accumulation of several EPSPs evoked by previously fired action potentials of its local excitatory neighbor.

In both models the restorative action of the inhibitory neurons has been identified as being essential for synchronization of neuronal firing. The characteristic sequence of the peak of population activity being followed by the peak of the cumulative EPSPs and thereafter by the peak of the cumulative population IPSPs can be found in simulations of both models during population oscillations. This sequence agrees with experimental findings [30].

A schematical description of the mechanism of synchronization has been suggested in section 4.2.1. In section 4.6.3 this description could be used to explain other phenomena concerning the dependence of the frequency on the duration of the IPSPs.

Comparison with physiological results

Many anti-epileptic drugs (AEDs) effect an enhancement of the gabaergic system, i.e. a strengthening of inhibition, in order to suppress oscillations. Further, blocking the inhibitory $GABA_A$ receptor in experiments with slice preparations in vitro is known to result in epileptiform discharges. In this context it may appear puzzling that *increasing* the number of inhibitory synapses in the *basic* model leads to oscillations whereas a reduction of inhibition leads to fluctuations.

The putative discrepancy between the experimental findings and the results obtained from the basic model is due to the fact that there are two different inhibitory receptors in real brains whereas the basic model has only one. Blocking $GABA_A$ receptors in experiments with slice preparations often induces epileptiform oscillations. However, this can not be compared with decreasing inhibition in the *basic* model because in the slice preparation the slow inhibitory $GABA_B$ receptors persist to be active and contribute to oscillatory activity. For that reason and also, as mentioned above, in order to obtain a reduced frequency of oscillations during hypersynchronous activity the basic model has been extended so that two inhibitory PSPs, a fast and a slow IPSP, appear in the model.

As section 4.8 shows, the clinical practice agrees with the simulation results of the *extended* model where two inhibitory receptors are present: many AEDs increase the concentration of the inhibitory neurotransmitter GABA in the extracellular medium and thus activate slow as well as fast inhibitory receptors. In agreement with the clinical experience the simulation results indicate that simultaneously increasing the synaptic strength of both types of IPSPs abolishes regular oscillations.

Experimental results yield that an increased number of inhibitory synapses occurs in epileptic foci [75]. This has been interpreted in two ways: as part of the epileptogenic process

and as counter-reaction of the organ to suppress the excessive firing. A classic opinion which is based on the observation that disinhibition produces epileptogenesis follows the simple rule that more inhibition decreases oscillations. According to this rule one would rather believe the second interpretation. The simulation results support the first interpretation.

Finally, the period of population oscillations increases linearly with the time constant of the IPSPs which has also been observed in experiments.

Conclusion

It could be shown that the simplified discrete model which is presented in this thesis is able to reproduce epileptiform behavior according to the criteria mentioned in the introduction. Computer simulations of the discrete model are significantly faster than computer simulations of differential equation models which include a more detailed description of the dynamics of single action potentials and single postsynaptic potentials. Therefore the new model can be employed in large scale computer simulations of neural networks and scanning of the parameter space.

The simulation results are similar to results obtained from a model which is based on differential equations. Nevertheless there are differences in some details. We hypothesize that different network architectures rather than the different modeling approaches account for that minor differences in the simulation results.

The dependence of the systems dynamics on the parameters qualitatively agrees with physiological findings. Dependent on the chosen parameters fluctuating and oscillating dynamics occurred in simulations of the model as well as spontaneous transitions from fluctuating to regularly oscillating behavior similar to epileptiform events in vivo. A significantly reduced frequency of the oscillations which appears during many epileptic seizures could be simulated when slow IPSPs have been introduced into the model.

List of abbreviations and symbols

AP	action potential
$a(t)$	number of action potentials fired within time step t
ACSF	artificial cerebrospinal fluid
AED	antiepileptic drug
AHP	afterhyperpolarization
AMPA	amino-3-hydroxy-5-methyl-4-isoxazole-propionic acid, excitatory neurotrnsmitter
C_{max}	first maximum of autocorrelation function
$D(a(t))$	temporal standard deviation of $a(t)$
δ_{e}	duration of excitatory PSPs
δ_{i}	duration of GABA$_{\mathrm{A}}$ mediated inhibitory PSPs
δ_{s}	duration of slow GABA$_{\mathrm{B}}$ mediated inhibitory PSPs
$E(t)$	global and temporal sum of EPSPs in the network
EEG	electroencephalogram
EPSP	excitatory postsynaptic potential
GABA	γ-aminobutyric acid, inhibitory neurotransmitter
$I(t)$	global and temporal sum of IPSPs in the network
IPSP	inhibitory postsynaptic potential
κ_{e}	average number of synapses per neuron divided by N
κ_{i}	average number of synapses per neuron divided by N
LTP	long term potentiation
N	number of neurons in the neural network model
NMDA	N-methyl-D-aspartate, excitatory neurotransmitter
PDS	paroxysmal depolarization shift
PSC	postsynaptic current
PSP	postsynaptic potential
p_{inh}	fraction of inhibitory neurons in neural network model
RNGS	random number generator seed
σ_{e}	amplitude of excitatory PSPs
σ_{i}	amplitude of GABA$_{\mathrm{A}}$ mediated inhibitory PSPs
σ_{s}	amplitude of slow GABA$_{\mathrm{B}}$ mediated inhibitory PSPs
τ_{max}	position of first maximum of autocorrelation function
θ	firing threshold of a neuron

List of abbreviations and symbols

Bibliography

[1] M. Abeles, *Corticonics: Neural circuits of the neocortex* (Cambridge University Press, Cambridge, 1991).

[2] D. J. Amit, H. Gutfreund, H. Sompolinsky, *Phys. Rev. Lett.*, 1530 (1985).

[3] D. J. Amit, *Modeling Brain Function - The world of attractor neural networks* (Cambridge University Press, Cambridge, 1989).

[4] J. Arnhold, P. Grassberger, K. Lehnertz, *Physikalische Blätter*, **56**, 4/27, (2000).

[5] A. Babloyantz, A. Destexhe, *Proc. Natl. Acad. Sci. USA*, **83**, 3513 (1986).

[6] E. Başar, *Brain Function and Oscillations, Volume I* (Springer, Berlin, 1998).

[7] H. H. Bauer, K. Pawelzik, *Physica D*, **69**, 380 (1993).

[8] H. Berger, *J. Psychol. Neurol.*, **40**, 160 (1930).

[9] S. M. Blinkov, I. I. Glezer, *The human brain in figures and tables - A quantitative handbook*, (Basic Books, New York, 1968).

[10] T. V. P. Bliss, G. L. Collingridge, *Nature*, **361**, 31 (1993).

[11] E. Bracci, M. Vreugdenhil, S. P. Hack, J. G. R. Jefferys, *J. Neurosci.*, **19**, 8104, (1999).

[12] A. Bragin, G. Jando, Z. Nadasdy, J. Hetke, K. Wise, G. Buzsáki, *J. Neuroscience*, **15**, 47 (1995).

[13] A. Bragin, J. Engel, Jr., C. L. Wilson, I. Fried, G. W. Mathern, *Epilepsia*, **40**, 127 (1999).

[14] V. Braitenberg, A. Schüz, *Anatomy of the cortex* (Springer, Berlin, 1991).

[15] E. H. Buhl, K. Halasy, P. Somogyi, *Nature*, **368**, 823 (1994).

[16] E. H. Buhl, G. Tamás, A. Fisahn, *J. Physiol.*, **513.1**, 117 (1998).

[17] P. B. Cipollini, *Somatosensory & Motor Research*, **15**, 276 (1998).

[18] S. R. Cobb, E. H. Buhl, K. Halasy, O. Paulsen, P. Somogyi, *Nature*, **378**, 75 (1995).

Bibliography

[19] B. W. Connors, M. J. Gutnick, D. A. Prince, *J. Neurophysiol.*, **48**, 1302 (1982).

[20] B. W. Connors, M. J. Gutnick, *Trends Neurosci.*, **13**, 99 (1990).

[21] T. C. Cope, L. M. Mendell, *J. Neurophysiol.*, **47**, 455 (1982).

[22] H. H. Dale, *Proc. R. Soc. Med.*, **28**, 319 (1935).

[23] A. Draguhn, R. D. Traub, D. Schmitz, J. G. R. Jefferys, *Nature*, **394**, 189 (1998).

[24] J. S. Duncan, in *The treatment of epilepsy*, ed. by S. Shorvon, F. Dreifuss, D. Fisch, D. Thomas (Blackwell, Oxford, 1996).

[25] M. Ebe, I. Homma, *Leitfaden für die EEG-Praxis, ein Bildkompendium* (Gustav Fischer Verlag, Stuttgart, 1992).

[26] S. F. Edwards, P. W. Anderson, *J. Physics*, **F 5**, 965 (1975).

[27] F. H. Eeckman, W. J. Freeman, *Brain Res.*, **528**, 238 (1990).

[28] J. Engel, *Seizures and Epilepsy*, (F. A. Davis Company, Philadelphia, 1989).

[29] A. K. Engel, P. König, W. Singer, *Proc. Natl. Acad. Sci. USA*, **88**, 9136 (1991).

[30] A. Fisahn, F. G. Pike, E. H. Buhl, O. Paulsen, *Nature*, **394**, 186 (1998).

[31] R. FitzHugh, *Biophys. J.*, **1**, 445 (1961).

[32] W. J. Freeman, *Scientific American*, **264/2**, 34 (1991).

[33] W. Gerstner, *Phys. Rev. E*, **51**, 738 (1995).

[34] F. Giannakopoulos, C. Hauptmann, A. Zapp, *Fields Institute Communications, accepted* (2000).

[35] F. Giannakopoulos, U. Bihler, C. Hauptmann, H. J. Luhmann, *to be published.*

[36] R. Glaser, *Biophysik, 4. Aufl.* (Gustav Fischer Verlag, Jena, 1996).

[37] P. Grassberger, I. Procaccia, *Phys. Rev. Lett.*, **50**, 346 (1983).

[38] C. M. Gray, *J. Comp.Neurosci.*, **1**, 11 (1994).

[39] A. Gupta, Y. Wang, H. Markram, *Science*, **287**, 273 (2000).

[40] C. Hauptmann, Ph. D. Thesis, Universität zu Köln (2000).

[41] D. O. Hebb, *The organization of behavior* (Wiley, New York, 1949).

[42] R. Hegger, H. Kantz, T. Schreiber, CHAOS, **9**, 413 (1999).

[43] A. L. Hodgkin, A. Huxley, *J. Physiol. (London)*, **117**, 500 (1952).

[44] J. J. Hopfield, *Proc. Natl. Acad. Sci.*, **79**, 2554 (1982).

[45] D. Johnston, T. H. Brown, in *Electrophysiology of Epilepsy*, ed. by P. A. Schwartzkroin, H. Wheal (Academic Press, London, 1984).

[46] D. Johnston, S. M. Wu, *Foundations of cellular neurophysiology* (MIT Press, Cambridge, 1995).

[47] S. A. Kauffman, *At Home in the Universe - The Search for Laws of Self-Organization and Complexity* (Oxford University Press, New York, 1995).

[48] S. S. Kety, *Sci. Am.*, **241**, 202 (1979).

[49] C. Koch, J. L. Davis (eds.), *Large-Scale Neuronal Theories of the Brain* (MIT Press, Cambridge, 1994).

[50] K. Krnjević, in *GABA Mechanisms in Epilepsy*, ed. by G. Tunnicliff, B. U. Raess (Wiley-Liss, New York, 1991).

[51] K. Lehnertz, C. E. Elger, *Phys. Rev. Lett.*, **80**, 5019 (1998).

[52] K. Lehnertz, R. G. Andrzejak, J. Arnhold, G. Widman, W. Burr, P. David, C. E. Elger, in *Chaos in Brain?*, ed. by K. Lehnertz, J. Arnhold, P. Grassberger, C. E. Elger, (World Scientific, Singapore, 2000).

[53] H. Liljenström, in *Matter matters? - On the material basis of the cognitive activity of mind*, ed. by P. Århem, H. Liljenström, U. Svedin (Springer, Heidelberg, 1997).

[54] J. E. Lisman, M. A. P. Idiart, *Science*, **267**, 1512 (1995).

[55] J. E. Lisman, *Nature*, **394**, 132 (1998).

[56] Z. Liu, M. Vergnes, A. Depaulis, C. Marescaux, *Neuroscience*, **48**, 87 (1992).

[57] R. R. Llinás, *Science*, **242**, 1654 (1988).

[58] R. R. Llinás, U. Ribary, *Proc. Acad. Natl. Sci*, **90**, 2078 (1993).

[59] W. W. Lytton, T. J. Sejnowski, *J. Neurophysiol.*, **66**, 1059 (1991).

[60] H. Markram, J. Lübke, M. Frotscher, B. Sakmann, *Science*, **275**, 213 (1997).

[61] D. A. McCormick, *J. Neurophysiol.*, **62**, 1018 (1989).

[62] Medical Sciences Bulletin, **20(5)** (1997).

[63] M. R. Mehta, C. Dasgupta, G. R. Ullal, *Biol. Cybern.*, **68**, 335 (1993).

[64] R. Miles, K. Tóth, A. I. Gulyás, N. Hájos, T. F. Freund, *Neuron*, **16**, 815 (1996).

[65] R. Miles, *Science*, **287**, 244 (2000).

Bibliography

[66] G. A. Miller, *Psychol. Rev.*, **63**, 81 (1956).

[67] G. Moran, *Trans. Am. Math. Soc.*, **347**, 1649 (1995).

[68] C. Morris, H. Lecar, *Biophys. J.*, **35**, 193 (1981).

[69] R. Motalli, J. Louvel, V. Tancredi, I. Kurcewicz, D. Wan-Chow-Wah, R. Pumain, M. Avoli, *J. Neurophysiol.*, **82**, 638 (1999).

[70] J. Nagumo, S. Arimoto, S. Yoshizawa, *Proc. IRE*, **50**, 2061 (1962).

[71] M. M. Patil, C. Linster, E. Lubenov, M. E. Hasselmo, *J. Neurophysiol.*, **80**, 2467 (1998).

[72] J. Pham, K. Pakdaman, J.-F. Vibert, *Bio Systems*, **48**, 179 (1998).

[73] J. P. Pijn, Ph. D. Thesis, University of Amsterdam (1990).

[74] W. H. Press, S. A. Teukolsky, W. T. Vetterling und B. P. Flannery, *Numerical Recipes in C: The Art of Scientific Computing*, 2. Aufl. (Cambridge University Press, Cambridge, New York, 1992).

[75] D. A. Prince, K. Jacobs, *Epilepsy Research*, **32**, 83 (1998).

[76] J. Rinzel, G. B. Ermentrout, in *Methods in Neuronal Modelling*, ed. by C. Koch, I. Segev (MIT Press, Cambridge, 1989).

[77] E. Rodriguez, N. George, J.-P. Lachaux, J. Martinerie, B. Renault, F. J. Varela, *Nature*, **397**, 430 (1999).

[78] G. Roth, *Naturwiss. Rundschau*, **52**, 231 (1999).

[79] G. M. Shepherd, *Neurobiology* (Oxford University Press, New York, 1988).

[80] W. Singer, *Nature*, **397**, 391 (1999).

[81] Y. Soen, N. Cohen, D. Lipson, E. Braun, *Phys. Rev. Lett.*, **82**, 3556 (1999).

[82] H. Sompolinsky, I. Kanter, *Phys. Rev. Lett.*, **57**, 2861 (1986).

[83] M. Steriade, D. A. McCormick, T. J. Sejnowski, *Science*, **262**, 679 (1993).

[84] R. D. Traub, R. Miles, R. K. S. Wong, *Science*, **243**, 1319 (1989).

[85] R. D. Traub, R. Miles, *Neural networks of the hippocampus* (Cambridge University Press, Cambridge, 1991).

[86] D. Volk, *Int. J. Mod. Phys. C*, **9**, 693 (1998).

[87] D. Volk, *Int. J. Mod. Phys. C*, **10**, 815 (1999).

[88] D. Volk, in *"Chaos in Brain?"*, ed. by K. Lehnertz, J. Arnhold, P. Grassberger, C. E. El-ger, (World Scientific, Singapore, 2000).

[89] M. A. Whittington, R. D. Traub, J. G. R. Jefferys, *Nature*, **373**, 612 (1995).

[90] J. B. Willis, Y. C. Ge, H. V. Wheal, *J. Neurosci. Meth.*, **47**, 205 (1993).

[91] M. Wilson, J. M. Bower, *J. Neurophysiol.*, **67**, 981 (1992).

Bibliography

Acknowledgements

Acknowledgements

100

Zusammenfassung

Die vorliegende Arbeit beschäftigt sich mit der Modellierung und der Simulation biologischer neuronaler Netzwerke, insbesondere mit dem Ziel ein dynamisches Verhalten zu reproduzieren, das epileptischen Anfällen zugrundeliegt.

Die Nervenaktivität während epileptischer Anfälle wird als Elektroenzephalogramm (EEG) gemessen und ist durch die folgenden Punkte charakterisiert.

- Regelmäßige Oszillation

- Hohe Amplitude im Vergleich zur Zeit vor dem Anfall

- Niedrige Frequenz von etwa 3Hz (oftmals, nicht immer)

Weiter ist das *spontane* Auftreten dieser sogenannten epileptiformen Aktivität wesentlich. Die hohe Amplitude des EEG-Signals während epileptischer Anfälle wird auf ein übermäßig synchrones Feuern der Neuronen in einem Gehirnareal zurückgeführt. Betrachtet man einzelne Neuronen, so beobachtet man mit dem Einsetzen der synchronen Netzwerkaktivität einen Wechsel vom unregelmäßigen Feuern isolierter Aktionspotenziale zum Feuern rascher Abfolgen von jeweils mehreren Aktionspotenzialen, denen eine längere Pause folgt. Diese sogenannten „bursts" sind auf zellulärer Ebene charakteristisch für epileptiforme Aktivität.

Während zur Untersuchung der Dynamik neuronaler Systeme häufig kontinuierliche mathematische Modelle benutzt werden, die durch Differentialgleichungen beschrieben werden, ist das Ziel dieser Arbeit die Entwicklung eines diskreten, möglichst einfachen Modells, das epileptiforme Aktivität mit den oben genannten Charakteristika reproduziert. Ein einfaches diskretes Modell hat vor allem zwei Vorteile: Zum einen wird eine wesentlich geringere Rechenzeit bei Computersimulationen erwartet. Dadurch werden Simulationen größerer Systeme und das Abtasten größerer Parameterbereiche möglich. Weiter lässt das Weglassen von Details die wesentlichen Mechanismen, die neuronaler Dynamik zugrundeliegen, stärker hervortreten.

Der Ausgangspunkt des in dieser Arbeit dargestellten neu entwickelten Modells ist das Hopfield-Modell. Dieses Modell des assoziativen Gedächtnisses wurde von diskreten physikalischen Modellen für Spin-Gläser inspiriert und begründet eine Klasse von Modellen neuronaler Netzwerke, die als sogenannte Attraktornetzwerke zusammengefasst werden. Das Hopfield-

Modell zeichnet sich durch diskrete Zustände und eine zeitliche Entwicklung in diskreten Zeitschritten aus.

Das dynamische Verhalten des Hopfield-Modells beschränkt sich auf die Konvergenz zu lokalen Energieminima. Verwendung einer Hebbschen Lernregel ermöglicht es, verschiedene Zustände einzuspeichern, so dass diese lokale Energieminima und somit stabile Fixpunkte der Netzwerkdynamik sind. Sofern die Speicherkapazität, d. h. das Verhältnis der Zahl der eingespeicherten Muster zur Zahl der Neuronen nicht zu groß ist, besteht Ähnlichkeit der stabilen Zustände mit den Zuständen ihres jeweiligen Attraktionsbereichs im Sinne eines geringen Hamming-Abstandes. Das Hopfield-Modell kann somit zur Erkennung von zuvor eingespeicherten Mustern aus verrauschten Vorlagen verwandt werden.

Den Anfang dieser Doktorarbeit bildeten Computersimulationen des Hopfield-Modells mit dem Ziel der Bestimmung der kritischen Speicherkapazität. Die einfachen dynamischen Eigenschaften des Hopfield-Modells gestatten allerdings keine Oszillationen in der Art wie sie in Aufzeichnungen des EEGs auftreten. In Hinblick auf die Simulation von Epilepsie wurde das Modell daher modifiziert, indem Eigenschaften von anderen Modellen integriert wurden. Weiter wurde die Funktion des Hopfield-Modells als Gedächtnis aufgegeben.

Die wesentlichen Merkmale des so erhaltenen Modells sind

- Diskrete Zustände

- Diskreter Zeitschritt

- Unterscheidung exzitatorischer und inhibitorischer Neuronen

- Zufällig vernetzter, gerichteter Graph als Modell des Netzwerks

- Zeitlich ausgedehnte postsynaptische Potenziale

- Refraktärzeit nach dem Feuern eines Neurons

- Zufällig sequentieller Update der einzelnen Neuronen

Die Verwendung zufällig sequentiellen Updates hat sich im Vergleich mit parallelem Update als geeigneter für die Simulation des diskreten Modells herausgestellt. Die Verwendung parallelen Updates führte grundsätzlich zu unnatürlich regelmäßigen Oszillationen. Zufällig sequentieller Update bringt zufällige zeitliche Verzögerungen beim Feuern eines Aktionspotenzials (jitter) von der Größenordnung einer Millisekunde in das Modell ein. Diese entsprechen Fluktuationen verschiedener Ursachen im biologischen Gehirn, die das Feuern von Aktionspotenzialen zeitlich verzerren.

Die wesentlichen Vereinfachungen gegenüber anderen, kontinuierlichen Modellen sind

- Einführung eines diskreten Zeitschritts entsprechend einer Millisekunde.

- Vereinfachung der postsynaptischen Potenziale zu Rechteck-Impulsen.

Die Dauer eines Aktionspotenzials ist etwa eine Millisekunde. Daher ist mit der ersten Vereinfachung das Aktionspotenzial auf eine binäre Information reduziert. Von der detaillierten Dynamik der Membranprozesse, die einem Aktionspotenzial unterliegt, wird im diskreten Modell also abstrahiert. Die zweite Vereinfachung rechtfertigt sich durch die große Zahl postsynaptischer Potenziale, die zusammen auf ein Neuron wirken. Im Cortex existieren etwa 10^4 synaptische Verbindungen pro Neuron. Aufgrund ihrer zeitlichen Ausdehnung addieren sich weiterhin postsynaptische Potenziale, die zu verschiedenen Zeiten im Dendritenbaum eines Neurons erzeugt werden.

Der relative Anteil der inhibitorischen Neuronen in den Neuronennetzen wurde konstant auf dem physiologisch gerechtfertigten Wert von 15% gehalten. Um verschiedene Dynamiken des Modells zu finden, wurden die acht anderen Parameter variiert: Die Anzahl der Neuronen, die Dauer der Refraktärperiode und, jeweils separat für exzitatorische und inhibitorische Neuronen, die Anzahl der Synapsen pro Neuron sowie die Dauer und die Amplitude postsynaptischer Potenziale.

Bei der Untersuchung der Simulationsergebnisse wurden vor allem die mittlere Aktivität, d. h. die mittlere Anzahl der Aktionspotenziale pro Zeitschritt, und die Amplitude gemessen, die als Standardabweichung der zeitlichen Entwicklung definiert wurde.

In Abhängigkeit von unterschiedlich eingestellten Parameterwerten fällt die Dynamik des Modells nach einer Initialisierung mit zufälliger Aktivität in eines von drei verschiedenen Regimes. Die Dynamik im fluktuierenden Regime ist charakterisiert durch eine geringe Amplitude und allenfalls gelegentlich auftretenden Oszillationen mit kurzer Kohärenzlänge. Die Dynamik im oszillierenden Regime ist charakterisiert durch eine regelmäßige Oszillation mit einer hohen Amplitude. Ein drittes Regime ist dadurch gekennzeichnet, dass die Inhibition im Netzwerk so stark ist, dass eine anfänglich gesetzte Aktivität nach einer kurzen Zeit erlischt.

Ein Übergang von fluktuierender zu oszillierender Dynamik erfolgt durch Verstärkung der Inhibition im Netzwerk. Dies kann entweder durch Verändern der Netzwerkparameter, d. h. durch Erhöhen der Synapsenzahl inhibitorischer Neuronen, oder durch Verändern synaptischer Parameter, d. h. Erhöhung der Amplitude oder der Dauer inhibitorischer postsynaptischer Potenziale, geschehen.

Entsprechende Variation der Exzitation zeigt, dass in vielen Fällen das Verhältnis von Inhibition zu Exzitation maßgeblich ist. Vergleichsweise geringe Inhibition führt zu fluktuierender Dynamik, während bei zu starker Inhibition keine autonome Aktivität im Netzwerk möglich ist und die Aktivität sehr bald nach der Initialisierung erlischt. In einem dazwischenliegenden Parameterbereich treten regelmäßige Oszillationen mit hoher Amplitude auf.

Allgemein ist der Mechanismus der „brain waves" noch nicht geklärt. Diesbezüglich existieren jedoch verschiedene Hypothesen, die in Kapitel zwei vorgestellt wurden. Die Rolle inhibitorischer Neuronen bei der Synchronisation wird von vielen Experimenten belegt. In

den Computersimulationen wird Synchronisation durch langsame inhibitorische postsynaptische Potenziale bewirkt. Diese unterdrücken das Feuern von Aktionspotenzialen durch die starke axonale Verzweigung gleichzeitig in vielen Neuronen bis exzitatorische postsynaptische Potenziale weitgehend abgeklungen sind. Das gleichzeitige Abklingen inhibitorischer postsynaptischer Potenziale funktioniert dann als Startschuss für neuronales Feuern. Bei hinreichender exzitatorischer Koppelung des Netzwerks wird durch wechselseitige Erregung vieler exzitatorischer Neuronen eine rasche Kettenreaktion ausgelöst, die somit zum synchronen Feuern der Population führt.

Die Untersuchung des Mechanismus in den Computersimulationen des Modells inspirierte ein stark vereinfachtes mathematisches Modell der Synchronisation durch Populationssummen inhibitorischer postsynaptischer Potenziale. In Übereinstimmung mit den Ergebnissen aus Computersimulationen erklärt dieses Modell, weshalb eine Stärkung der Inhibition zur Synchronisation der Neuronen und damit zum Oszillieren der Populationsaktivität führt.

Spontanes Wechseln der Dynamik vom fluktuierenden zum oszillierenden Regime tritt im diskreten Modell auf, wenn die Parameter gerade im Grenzbereich zwischen den beiden Regimes sind. In Übereinstimmung mit physiologischen Messungen ist der Wechsel zu Oszillationen der Populationsaktivität verbunden mit dem Übergang des Verhaltens einzelner Neuronen von unregelmäßigem Feuern isolierter Aktionspotenziale zum Feuern von „bursts".

Die bei vielen epileptischen Anfällen auftretende Änderung der Frequenz kann allerdings bei Simulationen dieses Modells nicht beobachtet werden. Um auch dieses Phänomen zu modellieren, wurde ein zweites inhibitorisches postsynaptisches Potenzial in das Modell integriert. Entsprechend der realen Situation gibt es im so erweiterten Modell langsame und schnelle inhibitorische postsynaptische Potenziale.

Im erweiterten Modell konnte ein viertes Regime beobachtet werden, das durch gelegentlich auftretende Spikes gekennzeichnet ist. In diesem Regime treten auch längere Perioden von regelmäßigen Oszillationen mit geringerer Frequenz auf.

Schließlich stimmen die Resultate der Computersimulationen qualitativ mit physiologischen Resultaten überein.

- Die gleichzeitige Erhöhung der Amplituden langsamer und schneller inhibitorischer postsynaptischer Potenziale, entsprechend einer Aktivierung der durch den Neurotransmitter GABA vermittelten Inhibition, unterdrückt die Amplitude der Oszillationen. Dies entspricht der Wirkung vieler Medikamente zur Behandlung von Krampfanfällen.

- Die Periodendauer der Aktivität im oszillierenden Regime ist linear abhängig von der Dauer der inhibitorischen postsynaptischen Potenziale.

- Eine Erhöhung der Konnektivität der inhibitorischen Neuronen induziert Oszillationen. Dies entspricht der Beobachtung, dass in verletzungsbedingten cortikalen Epilepsieherden bei Ratten die Anzahl inhibitorischer Synapsen höher ist [72].

Insgesamt konnte gezeigt werden, dass das in dieser Arbeit neu entwickelte diskrete Modell biologischer neuronaler Netze epileptiforme Aktivität mit den anfangs erwähnten Merkmalen reproduzieren kann. Die Abhängigkeit der Dynamik von den Modellparametern stimmt qualitativ mit den Ergebnissen physiologischer Experimente überein. Weiter konnten Details wie das Feuern von „bursts" während der stark synchronen Populationsaktivität beobachtet werden. Computersimulationen des neuen Modells sind erheblich schneller als Simulationen von Modellen, die auf Differentialgleichungen beruhen und die detaillierte Dynamik von Aktionspotenzialen und postsynaptischen Potenzialen modellieren. Daher eignet sich das Modell besonders gut, um den Einfluß verschiedener Parameterkonfigurationen auf die Netzwerk Dynamik zu untersuchen.

Zusammenfassung

Erklärung

Ich versichere, dass ich die von mir vorgelegte Dissertation selbständig angefertigt, die benutzten Quellen und Hilfsmittel vollständig angegeben und die Stellen der Arbeit - einschließlich Tabellen, Karten und Abbildungen -, die anderen Werken im Wortlaut oder dem Sinn nach entnommen sind, in jedem Einzelfall als Entlehnung kenntlich gemacht habe; dass diese Dissertation noch keiner anderen Fakultät oder Universität zur Prüfung vorgelegen hat; dass sie - abgesehen von unten angegebenen Teilpublikationen - noch nicht veröffentlicht worden ist sowie, dass ich eine solche Veröffentlichung vor Abschluss des Promotionsverfahrens nicht vornehmen werde. Die Bestimmungen dieser Promotionsordnung sind mir bekannt. Die von mir vorgelegte Dissertation ist von Prof. Dr. T. Küpper und Prof. Dr. D. Stauffer betreut worden.

Köln, 9. Mai 2000

Teilpublikationen:

Volk, D. On the phase transition of Hopfield networks - another Monte Carlo study. *Int. J. Mod. Phys. C*, **9**, 693 (1998).

Volk, D. Epileptic seizures in a discrete model of neural networks of the brain. *Int. J. Mod. Phys. C*, **10**, 815 (1999).

Volk, D. Spontaneous synchronization in a discrete neural network model. In *"Chaos in Brain?"*, ed. by K. Lehnertz, J. Arnhold, P. Grassberger, C. E. Elger, (World Scientific, Singapore, 2000).

Volk, D. Population oscillations in a discrete model of neural networks of the brain. Submitted to Bio Systems, February 2000.

Volk, D. Spiking behavior and epileptiform 3Hz oscillations in a discrete model of neural networks, in preparation.

Lebenslauf

Daniel Volk
Krieler Str. 19
50935 Köln

Persönliche Angaben

Geburtstag:	13.03.1971
Geburtsort:	Essen
Familienstand:	ledig
Staatsangehörigkeit:	deutsch

Schulbildung

1977 bis 1981	Grundschule in Duisburg-Großenbaum
1981 bis 1990	Mannesmann-Gymnasium in Duisburg-Huckingen
23.05.1990	Allgemeine Hochschulreife

Zivildienst

Sept. 1990 bis Nov. 1991	Duisburger Werkstatt für Behinderte

Studium

Okt. 91 bis Sept. 92	Studium der Informatik an der Universität Dortmund
Okt. 92 bis Feb. 98	Studium der Mathematik an der Universität-GHS Duisburg
07.02.1998	Studienabschluss: Diplom-Mathematiker
Seit 01.03.1998	Stipendiat des Graduiertenkollegs *Scientific Computing*